

1-1-2010

Optimal Precipitation Of Zn^{+2} and Ni^{+2} From Aqueous Solution: Influence Of Rapid Mixing Parameters

Ayad Hmood
Ryerson University

Follow this and additional works at: <http://digitalcommons.ryerson.ca/dissertations>

 Part of the [Chemical Engineering Commons](#)

Recommended Citation

Hmood, Ayad, "Optimal Precipitation Of Zn^{+2} and Ni^{+2} From Aqueous Solution: Influence Of Rapid Mixing Parameters" (2010). *Theses and dissertations*. Paper 1397.

This Thesis is brought to you for free and open access by Digital Commons @ Ryerson. It has been accepted for inclusion in Theses and dissertations by an authorized administrator of Digital Commons @ Ryerson. For more information, please contact bcameron@ryerson.ca.

**OPTIMAL PRECIPITATION
OF Zn^{+2} AND Ni^{+2} FROM AQUEOUS SOLUTION:
INFLUENCE OF RAPID MIXING PARAMETERS**

By

Ayad Hmood

Bachelor of Chemical Engineering,
University of Baghdad, Baghdad, Iraq, 1992

A Thesis

presented to Ryerson University

in partial fulfillment of the

requirements for the degree of

Master of Applied Science

in the program of

Chemical Engineering

Toronto, Ontario, Canada, 2010

© 2010 by Ayad Hmood

Author Declaration

I hereby declare that I am the sole author of this thesis. I authorize Ryerson University to lend this thesis to other institutions or individuals for the purpose of scholarly research.

.....
Ayad Hmood

I further authorize Ryerson University to produce this thesis by photocopying or by other means, in total or in part, at the request of their institutions or individuals for the purpose of scholarly research.

.....
Ayad Hmood

Borrower's Page

Ryerson University requires the signatures of all persons using or photocopying this thesis.

Please sign below, and give address and date.

Name	Signature	Address	Date

Abstract

OPTIMAL PRECIPITATION OF Zn^{+2} AND Ni^{+2} FROM AQUEOUS SOLUTION: INFLUENCE OF RAPID MIXING PARAMETERS

Ayad Hmood

Master of Applied Science in Chemical Engineering
Department of Chemical Engineering
Ryerson University
Toronto, 2010

Wastewater containing Zn^{+2} and Ni^{+2} is normally treated by chemical precipitation, coagulation, flocculation followed by clarification. The metal precipitation is influenced by chemical (wastewater pH, coagulant type and dose) and physical (rapid mixing speed and time) parameters. The process usually consists of the rapid dispersal of a coagulant into the wastewater followed by an intense agitation commonly defined as rapid mixing. This study focused on the most important parameters of rapid mixing design: mixing intensity and duration. Simulated aqueous solutions containing 50 ppm Zn^{+2} and 50 ppm Ni^{+2} were treated with aluminum sulfate, ferrous sulfate and ferric chloride coagulants at different doses and different rapid mixing times and speeds. Experimental results obtained indicate that ferric chloride at 30mg/l dose was superior over aluminum sulfate and ferrous sulfate at the same dose in Zn^{+2} and Ni^{+2} removals. Rapid mixing time had a strong influence on the metal removal. An optimal combination of rapid mixing parameters was determined as: 60 s at 100 rpm for Zn^{+2} and 30 s at 80 rpm for Ni^{+2} removals. Scanning electron microscopy images for Zn^{+2} and Ni^{+2} flocs at optimum parameters of rapid mixing show that ferric chloride addition compacts the surface texture of the metals flocs. Flocs formed by Zn^{+2} are denser and larger than flocs formed by Ni^{+2} .

Acknowledgements

First of all, I would like to express my sincere thanks to my supervisors, Dr. Huu Doan and Dr. Jiangning Wu, for offering me an opportunity to study and work in their research group. Their continuous guidance and encouragement during the time of graduate study are highly appreciated.

I am very grateful for the invaluable assistance of faculty members and technologists in the Chemical Engineering Department of Ryerson University; especially those provided by Ali Hemmati and Danny Boothe during the equipment manufacture and system setup.

I would like to thank Mr. Qiang Li, Technical Officer in the Department of Mechanical and Industrial Engineering at Ryerson University for his help and guidance in using Scanning Electron Microscopy.

I would also like to express my gratitude to my family, special thanks to my wife and daughters for their patience and unconditional support to complete my study.

Finally, I would like to thank my friends and fellow graduate students for their moral support and understanding during my studies.

Table of Contents

Author Declaration	ii
Borrower's Page	iii
Abstract	iv
Acknowledgements	v
Table of Contents	vi
List of Figures	viii
List of Tables	xi
Nomenclature	xii
1 Introduction	1
2 Theoretical Background	7
2.1 Metals Removal by Hydroxide Precipitation	7
2.1.1 Hydroxide Precipitation Theory	9
2.1.2 Advantages and Disadvantages of Hydroxide Precipitation	12
2.1.3 Hydroxide Precipitation Using Caustic Soda	12
2.2 Coagulation and Flocculation	14
2.3 Coagulants and Flocculants	17
2.4 Mixing	21
2.4.1 Rapid Mixing	22
2.4.2 Slow Mixing	23
2.5 Sedimentation (Settling Time)	23
3 Literature Review	26
3.1 Coagulant, Flocculant Type and Dose	26
3.2 Rapid Mixing Parameters	27
3.3 Settling Time	28
3.4 Objectives	29

4 Experimental Method	30
4.1 Experimental Set-up	30
4.2 Experimental Procedures	31
4.2.1 Precipitation pH (first stage)	31
4.2.2 Coagulant Type and Dose (second stage)	32
4.2.3 Settling Time (third stage)	33
4.2.4 Rapid Mixing Speed and Time (fourth stage)	34
4.2.5 Metal Particle Imaging	36
4.3 Experimental sensitivity analysis	37
4.4 Analysis of Zinc and Nickel	38
4.4.1 Concentration in wastewater	38
4.4.2 Particle Size Distribution	38
5 Results and Discussions	39
5.1 Optimum Precipitation pH	39
5.2 Coagulant Type and Optimum Dose	41
5.3 Settling Time	49
5.4 Rapid Mixing Speed and Time	52
5.5 Metal Coagulated Particles Imaging	72
6 Conclusions and Recommendations	83
6.1 Conclusions	83
6.2 Recommendations	84
References	85
Appendixes	90
Appendix A: Velocity gradient verses agitator paddle speed for standard Jar Test ..	90
Appendix B: Experimental Errors	92
Appendix C: Particle Size Distribution	94
Appendix D: Optimum pH Calculation	102

List of Figures

Figure 2.1- Theoretical Solubility of Nickel Hydroxide.....	9
Figure 2.2- Theoretical Solubility of Zinc Hydroxide.....	10
Figure 2.3- Coagulation, Charge neutralization	15
Figure 2.4- Flocculation, illustrates the bridging of agglomerated colloidal particles to form settable flocs	16
Figure 4.1- Experimental Setup (standard Jar Test)	30
Figure 5.1- Effect of Precipitation pH on zinc ions removal	40
Figure 5.2- Effect of precipitation pH of on the nickel ions removal	41
Figure 5.3- Zinc removal percentage with ferric chloride, aluminum sulfate and ferrous sulfate, coagulants doses in mg/l	42
Figure 5.4- Nickel removal percentage with ferric chloride, aluminum sulfate and ferrous sulfate, with different coagulants doses	43
Figure 5.5- Particle size distribution for zinc using ferric chloride coagulant at different doses	44
Figure 5.6- Particle size distribution for zinc using ferrous sulfate coagulant at different doses	44
Figure 5.7- Particle size distribution for zinc using aluminum sulfate coagulant at different doses	45
Figure 5.8- Particle size distribution for zinc using ferric chloride, ferrous sulfate, and aluminum sulfate at 30 mg/l dosage and no coagulant	46
Figure 5.9- Particle size distribution for nickel using ferric chloride coagulant at different doses	47
Figure 5.10- Particle size distribution for nickel using ferrous sulfate coagulant at different doses	47
Figure 5.11- Particle size distribution for nickel using aluminum sulfate coagulant at different doses	48

Figure 5.12 - Particle size distribution for nickel using ferric chloride, ferrous sulfate, and aluminum sulfate at 30 mg/l dosage and no coagulant.....	48
Figure 5.13- Zinc removal percentage verses settling time using ferric chloride, ferrous sulfate, and aluminum sulfate at 30mg/l dose, no coagulant added as control	50
Figure 5.14- Nickel removal percentage verses settling time using ferric chloride, ferrous sulfate, and aluminum sulfate at 30 mg/l dose, no coagulant added as control	51
Figure 5.15- Zinc removal vs. settling time for 30 s rapid mixing	53
Figure 5.16- Zinc removal vs. settling time for 60 s rapid mixing	54
Figure 5.17- Zinc removal vs. settling time for 90 s rapid mixing	54
Figure 5.18- Zinc removal vs. settling time for 120 s rapid mixing	55
Figure 5.19- Zinc removal vs. settling time at 60 s rapid mixing	56
Figure 5.20 - Nickel removal vs. settling time for 30 s rapid mixing	57
Figure 5.21 - Nickel removal vs. settling time for 60 s rapid mixing	58
Figure 5.22 - Nickel removal vs. settling time for 90 s rapid mixing	58
Figure 5.23 - Nickel removal vs. settling time for 120 s rapid mixing	59
Figure 5.24- Nickel removal vs. settling time at 30 s rapid mixing time	60
Figure 5.25 Zinc particle size distributions for 30s mixing time	62
Figure 5.26 Zinc particle size distributions for 60s mixing time	62
Figure 5.27- Zinc particle size distributions for 90s mixing time	63
Figure 5.28- Zinc particle size distributions for 120 s mixing time	63
Figure 5.29- Zinc particle size distributions for 60 s mixing time	64
Figure 5.30- Nickel particle size distribution for 30 s mixing time	66
Figure 5.31- Nickel particle size distribution for 60 s mixing time	66
Figure 5.32- Nickel particle size distribution for 90 s mixing time	67
Figure 5.33- Nickel particle size distribution for 120 s mixing time	67

Figure 5.34 - Nickel particle size distribution for 30 s mixing time	68
Figure 5.35- Zinc and nickel removal in combined solution vs. settling time at pH 9 and 9.5	69
Figure 5.36- Zinc removal percentage vs. settling time for sole (pH 8.7) and combined zinc solution with nickel at pH 9-9.5	70
Figure 5.37- Nickel removal percentage vs. settling time for sole (pH 10.2) and combined nickel solution with zinc at pH 9-9.5	71
Figure 5.38 SEM images for zinc flocs, no coagulant used	73
Figure 5.39- SEM images for Zinc flocs, 30mg/l ferric chloride, 30 s rapid mixing time and different rapid mixing speeds, (a) 60 rpm, (b) 100 rpm, (c) 150 rpm	74
Figure 5.40 SEM images for zinc flocs, 30mg/l ferric chloride, 60 s rapid mixing time at different rapid mixing speeds, (a) 60 rpm, (b) 100 rpm, (c) 150 rpm	76
Figure 5.41- SEM images for zinc flocs, 30mg/l ferric chloride, 90 s rapid mixing time at different rapid mixing speed, (a) 60 rpm, (b) 100 rpm, (c) 150 rpm	77
Figure 5.42- SEM image of nickel flocs, with no coagulant addition	78
Figure 5.43- SEM images for nickel flocs, 30mg/l ferric chloride, 30 s rapid mixing time at different rapid mixing speeds, (a) 60 rpm, (b) 80 rpm, (c) 120 rpm	80
Figure 5.44- SEM images for nickel flocs, 30mg/l ferric chloride, 60 s rapid mixing time at different rapid mixing speeds, (a) 60 rpm, (b) 80 rpm, (c) 120 rpm	81
Figure 5.45- SEM images for nickel flocs, 30mg/l ferric chloride, 90 s rapid mixing time at different rapid mixing speeds, (a) 60 rpm, (b) 80 rpm, (c) 120 rpm	82
Figure A.1- Velocity gradient vs. rpm for a 2-liter square beaker (11.5x11.5x25cm), using a Phipps & Bird stirrer (2.5x7.6 cm)	90
Figure A.1- Velocity gradient vs. rpm for a 2-liter square beaker (11.5x11.5x25cm), using a Phipps & Bird stirrer (2.5x7.6 cm) at 22°C	91

List of Tables

Table 1.1- Industrial effluent discharge limits for nickel and zinc ions.....	3
Table 2.1- Solubility (S) of zinc hydroxide, S unit mol of zinc per kg of water.....	11
Table 2.2- Various sizes of particles in raw water and their settling velocity.....	14
Table 2.3- Relative Coagulating "Power" of Cations.....	16
Table 2.4- Advantages and Disadvantages of Alternative Inorganic Coagulants.....	18
Table 4.1- Levels of investigated parameters for zinc and nickel removal	35
Table C.1- Particle size distribution for zinc using ferric chloride, ferrous sulfate, and aluminum sulfate at 30mg/l dosage and no coagulant	94
Table C.2 - Particle size distribution for nickel using ferric chloride, ferrous sulfate, and aluminum sulfate at 30mg/l dosage and no coagulant	95
Table C.3- Zinc particle size distributions for 30 and 60 s mixing time	96
Table C.4- Zinc particle size distributions for 90 and 120 s mixing time	97
Table C.5- Nickel particle size distribution for 30 and 60 s mixing time	98
Table C.6- Nickel particle size distribution for 30 and 60 s mixing time	99
Table C.7- Zinc particle size distributions for 60 s mixing time	100
Table C.8- Nickel particle size distribution for 30 s mixing time.....	101

Nomenclature

Symbols

C_i	Initial metal concentration, mg/l
C_f	Final metal concentration, mg/l
G	Velocity gradient, 1/s
P	Power, W (N-m/s)
T	Temperature, °C
μ	Fluid viscosity, N-s/m ²
μm	Micro meter, 10 ⁻⁶ m
V	Mixing vessel volume, m ³
V_s	Sedimentation rate
R	The radius of the spherical particle
ρ_p	Density of the particle
ρ_f	Density of the fluid
g	Gravitational constant

Abbreviations

AA	Atomic Absorption Analysis
min	minute, time
PA	Particle Size Analysis
ppm	Part per million (mg/l)
rpm	Rotational speed (revolution per minute)
pH	Potentiometric Hydrogen Ion Concentration
s	second, time
SEM	Scanning Electron Microscopy
Vol	Volume
EPA	Environmental Protection Agency
ACE	U.S. Army Corps of Engineers

1 Introduction

One of the main causes of industrial pollution is the discharge of effluents containing heavy metals. Heavy metal refers to any metallic chemical element that has relatively high density and is toxic or poisonous at low concentration. Heavy metals can have serious effects on human and animal health. Beside the health effects, heavy metals are nonrenewable resources. Therefore, effective recovery of heavy metals is as important as their removal from waste streams. Disposal of industrial wastewater has always been a major environmental issue. Pollutants in industrial wastewater are almost invariably so toxic that wastewater has to be treated before its reuse or disposal in water bodies. Industrial processes generate wastewater containing heavy metal contaminants. Since most of heavy metals are non-degradable into non-toxic end products, their concentrations must be reduced to acceptable levels before discharging them into environment. Otherwise these could pose threats to public health and/or affect the aesthetic quality of potable water.

According to World Health Organization (WHO), the metals of most immediate concern are chromium (Cr), zinc (Zn), nickel (Ni), iron (Fe), mercury (Hg) and lead (Pb) (World Health Organization, 1984). Maximum allowed limits for contaminants in “treated” wastewater are enforced in removal techniques in many developing countries. The treatment of contaminated waters is as diverse and complicated as the operation from which it comes. A number of conventional treatment technologies have been considered for treatment of wastewater contaminated with heavy metals.

Some of the conventional techniques for removal of metals from industrial wastewater include chemical precipitation, adsorption, solvent extraction, membrane separation, ion exchange, electrolytic techniques, coagulation/flotation, sedimentation, filtration, membrane process, biological process and chemical reaction (Gardea et al., 1996; Gloaguen et al., 1997; Jeon et al., 2001; Kim et al., 1998; Lee et al., 1998; Lujan et al., 1994; Mofa, 1995; Blanco et al., 1999). Each method has its merits and limitations in application. Combination of different types of treatment should be considered, as well as

the ease of application, economy, efficiency and safety. In the industry, effluents from steelworks, rayon yarn and fiber manufacturing, wood pulp production, plating, and metal processing contain zinc. Likewise, wastewater streams from metal processing industries, steel foundries, motor vehicle and aircraft industries, printing and chemical industries contain nickel (Eckenfelder, 2000). In automotive industry, which is one of the major manufacturing sectors in southern Ontario, the electro coating process usually generates, on average 0.25 gallons of wastewater per square foot of the metal parts being processed. The wastewater flow rate exiting an automotive plant can be very large, e.g. 1.4 million gallons of wastewater is generated per day at the Toyota plant in Georgetown, Kentucky (www.afonline.com).

Unlike organic pollutants, heavy metals are non-biodegradable and hence are accumulated in living organisms through their food chains. Some metals, such as Cd, Hg, Ag, and Pb, can be extremely toxic for the cycle of living beings. Others, such as Cu, Zn, Mn, Fe, Ni, and Co, are essential for plants and animals in small quantities. However when present in concentrations above certain limits, they can be very harmful to living organisms (Malkoc, 2006). Toxic heavy metal contaminants in aqueous waste streams have caused serious water pollution problems that are being faced over the world (Dundar et al., 2008). The characteristics of heavy metals and their toxicity are:

- The toxicity of heavy metals can be very long lasting in nature;
- Some heavy metals can be transformed from species of relatively low toxicity into more toxic forms in certain environments (mercury is one example);
- The bioaccumulation of heavy metals in the food chain can damage normal physiological activity in wildlife and eventually endanger human life;
- Metals can be transformed only in valence and species, but cannot be degraded by any method, including bio-treatment;
- Toxicity from heavy metals occurs even at low concentrations of about 1.0–10 mg/L. Some strongly toxic metal ions, such as Hg and Cd ions, are very toxic even at lower concentrations of 0.001–0.1 mg/L (Volesky, 1990; Wang et al., 2006).

Zinc and nickel has been chosen in this study due to rapid increases in their quantities in industrial wastewater. The effluent discharge limits becoming ever more stringent. The concentration of metal ions has to be reduced to a permissible maximum before discharging the wastewater to a sewer. In 2003, United State Environmental Protection Agency (US EPA) imposed stringent daily effluent discharge limits for existing Metal Product and Machinery (MP&M) sector. Table 1.1 summarizes the current (2003) (US EPA, 2003) and previous (before 2003) maximum daily discharge limits for zinc and nickel in the MP&M sector. Discharge limits for zinc and nickel in the sanitary sewer were enacted by the Council of the City of Toronto in 2000 (Toronto Municipal Code Sewers, 2000); for the comparison, these limits (current 2000; previous: before 2000) also provided in Table 1.1

Table 1.1 Industrial effluent discharge limits for nickel and zinc ions.

Jurisdiction	Ionic species	Daily max: current (mg/l)	Daily max: previous (mg/l)
City of Toronto limits,	Zinc	2	4
	Nickel	2	4
US EPA limits,	Zinc	0.35	4.2
	Nickel	1.5	4.1

Chemical precipitation is the most common technique used for treatment of metal-contaminated waters (Patterson et al., 1975; US EPA, 1980; Peters et al., 1985). Chemical precipitation of heavy metals has long been used as the primary method of treating wastewaters in industrial applications, such as metal finishing and plating. Owing to this past success, chemical precipitation is often selected to remediate hazardous, toxic, and radioactive waste sites containing ground water contaminated by heavy metals or landfill leachate, or both. For the precipitation process to be effective, an efficient solid removal process must be employed. To separate the solid and liquid phases of the waste stream, coagulation, flocculation, and clarification or filtration, or both, are typically used.

All precipitation processes operate under the same fundamental chemical principles. Precipitation is a physical–chemical process, in which soluble metals and inorganic are converted to relatively insoluble metal and inorganic salts (precipitates) by the addition of a precipitating agent. Most often, an alkaline reagent is used to raise the solution pH to lower the solubility of the metallic constituent, and, thus, bring about precipitation.

In precipitation, dissolved metal ions react with added precipitants by forming insoluble compounds. These solids sediment can be removed from the supernatant liquid by different solid/liquid separation techniques. The main chemical parameters, which are of importance in the precipitation process, are pH and metal concentration. In general, heavy metals tend to be present in ionic form at low pH levels, while they tend to precipitate when pH is raised. Heavy metals can be precipitated as insoluble hydroxides, sulfides, carbonates, and others (Bradl, 2005).

Precipitation of soluble, semi-colloidal, colloidal, and small precipitate particles is necessary followed by coagulation, flocculation, settling, clarification and/or filtration. Hydroxide precipitation effectively removes heavy metals, such as: cadmium, chromium (+3), copper, manganese, nickel, lead, and zinc, while sulfide precipitation removes effectively cadmium, chromium (+6), cobalt, copper, iron, mercury, manganese, nickel, silver, tin and zinc. Finally, carbonate precipitation is often times preferred over hydroxide precipitation for the removal of cadmium, lead, and nickel. Industry prefers the precipitate cadmium carbonate to cadmium hydroxide for metals recovery processes. Also, lead and nickel precipitation using calcium carbonate gives lower final residual metal concentrations than those of hydroxide. Both carbonate and hydroxide can remove many non-metal pollutants (mainly organic load). Hydroxide can also precipitate soaps and fluorides (Bradl, 2005).

In assessing the effectiveness of the design and operation of a chemical precipitation system, US EPA examines the following parameters: pH value; precipitation temperature; residence time; amount and type of precipitating agents, coagulants, and flocculants; degree of mixing; and settling time (Noyes, 1994; US Army Corps of Engineers, 2001)

The pH value in continuous chemical precipitation systems is used as an indicator of the concentration of precipitating agents in the reaction tank and thus is used to regulate their addition to the tank. The pH value also affects the solubility of metal precipitates formed and therefore directly impacts the effectiveness of their removal.

The precipitation temperature affects the solubility of the metal precipitate. Generally, the lower the temperatures, the lower the solubility of the metal precipitate and vice versa. The operating temperature is usually between 20-25°C.

The residence time impacts the extent of the chemical reactions to form metal precipitates and, as a result, the amount of precipitates that can be settled out of solution. For batch systems, the residence time is controlled directly by adjusting the treatment time in the reaction tank. For continuous systems, the wastewater feed rate is controlled to make sure that the system is operating at the appropriate design residence time. For example, the detention time for sulfide precipitation of nickel ion could be varied; however, the detention time of 30 minutes is commonly used.

The amount and type of precipitating agent used to effectively treat the wastewater depends on the amount and type of metal and inorganic constituents in the wastewater to be treated. Other design and operating parameters, such as: the pH value, the precipitation temperature, the residence time, the amount and type of coagulants and flocculants, and the settling time, are determined depending on the amount and type of metal that need to be removed. The addition of coagulants and flocculants improves the settling rate of the precipitated metals and inorganic and allows for smaller settling systems (i.e., lower settling time) to achieve the same degree of settling as a much larger system.

Mixing provides greater uniformity of the wastewater feed and disperses precipitating agents, coagulants, and flocculants throughout the wastewater to ensure the most rapid precipitation reactions and settling of precipitate solids possible. The quantifiable degree of mixing is a complex assessment that includes, among other things, the amount of energy supplied, the length of time the material is mixed, and the related turbulence effects of the specific size and shape of the tank. This is beyond the scope of simple measurements. The goal of the rapid mixing operation is to first raise the wastewater pH to form metal hydroxide particles, as discussed above. After the addition of caustic, the next step is to add aluminum or iron salts, or organic polymers (coagulants) directly to the wastewater. These polymers attach to the metal solids particles. The small metal hydroxide particles become entangled in these polymers, causing the particle size to increase (form flocs), which promotes settling.

Adequate settling time must be provided to make sure that removal of the precipitated solids from the wastewater has been completed. Once particles become enmeshed in the polymer, they are allowed to settle so that they are removed from the wastewater. The particles settle since they are heavier than water. This settling occurs in the sedimentation tanks. Sedimentation tanks, in contrast to rapid mixing units, are designed to have no mixing, to produce a calm flow for settling.

2 Theoretical Background

2.1 Heavy Metal Removal by Hydroxide Precipitation

As metals enter the treatment process, they are in a stable dissolved aqueous form and unable to form solids. In the metal treatment by hydroxide precipitation, the pH (hydroxide ion concentration) of the water is adjusted so that the metal forms insoluble precipitate. Metal precipitation is primarily dependent upon two factors: the concentration of the metal, and the pH of the water. Heavy metals are usually present in wastewaters in dilute quantities (1 - 100 mg/l) and at neutral or acidic pH values below 7.0 (US Army Corps of Engineers, 2001). Both of these factors are disadvantageous with regard to metal precipitation. However, when one adds caustic to water which contains dissolved metals, the metals react with hydroxide ions to form metal hydroxide solid.

Two alkalis most commonly used for hydroxide precipitation are sodium hydroxide (NaOH, or, as it is commonly referred to, caustic soda or simply caustic) and lime (calcium hydroxide, $\text{Ca}(\text{OH})_2$). Of the survey respondents that have metal precipitation processes, 84% use caustic only, 5% use lime only and 9% use a combination of caustic and lime. Several other treatment reagents are used as either the sole alkali ingredient or as an adjunct to caustic or lime. The other primary alkalis are magnesium hydroxide (used by 4.3% of all respondents that perform metal precipitation, but not as the sole source of alkali) and calcium chloride (used by 11.9% of respondents that perform metals precipitation, but only 2% use it as their sole source of alkali). Other alkalis used by metal finishers are sodium carbonate and sodium bicarbonate. When magnesium hydroxide and calcium chloride are used in conjunction with either caustic or lime, this is sometimes done as a pretreatment step prior to metal precipitation (US Army Corps of Engineers, 2001).

Each alkali has advantages and disadvantages. For example, of the two most common alkalis, hydrated lime has the advantage over caustic soda of lower cost per unit of neutralizing capacity. Also, the metal hydroxide precipitants produced with the use of lime have much faster settling rates because of co-precipitation of calcium. Further, the

settled sludge from lime treatment is higher in solid content and much more amenable to dewatering. On the other hand, lime takes longer to react in the neutralizer than caustic soda, has a more complicated feed system and, most significantly, it generates a considerably higher mass of sludge (www.waterspecialists.biz).

Metal hydroxides are amphoteric, i.e., they are increasingly soluble at both low and high pH, and the point of minimum solubility (optimum pH for precipitation) occurs at a specific pH value for a metal. At an optimum pH at which the solubility of one metal hydroxide may be minimized, the solubility of another may be relatively high. Since metal hydroxides are quite soluble, many such hydroxides re-dissolve into the solution when the pH changes even slightly.

Wastewater from industrial processes usually contains several metals. For example, the typical process wastewater from printed circuit board manufacturing contains copper, tin, lead and nickel. Such mixed metals create a problem when using hydroxide precipitation since the ideal pH for one metal may put another metal back into the solution. In addition, chelators, sequestering agents, bath additives, cleaners and electroless formulations interfere with the hydroxide precipitation. From a practical point of view, it is impossible to eliminate such components from a waste stream. Good treatment practices, such as segregation and pretreatment of some process waste streams, would minimize the anti-precipitant effects of such ingredients. Otherwise, an addition of precipitant may be required in conjunction with pH adjustment. Solubility is generally much more complicated than what has been discussed earlier. Complex formation in wastewaters or natural waters must be considered to make realistic solubility calculations. Reactions of the cations or anions with water to form hydroxide complexes or protonated anion species, such as: phosphates, tartrates, EDTA (ethylene- diamine- tetra- acetic acid) and ammonia that are commonly found in cleaner and plating formulations may have an adverse effect on metal removal efficiencies. In addition, the cations or anions may form complexes with other materials in solution, thus reducing their effective concentration. Soluble molecules or ions, which can act to form complexes with metals, are called

ligands. Common ligands include OH^- , CO_3^{-2} , NH_3 , F^- , CN^- , $\text{S}_2\text{O}_3^{-2}$, as well as numerous other inorganic and organic species (US Army Corps of Engineers, 2001)

2.1.1 Hydroxide Precipitation Theory

A high pH corresponds to a high hydroxide concentration. Visual representations of the pH values that promote metal precipitation are shown in Figures 2.1 and 2.2. Each figure represents the solubility of an individual metal nickel and zinc at various pH values. Notice the wide variation in scale. The upper part of the scale shows a dissolved concentration of 100 mg/l. The lowest number on the scale is 0.001 mg/l. These solubility graphs display regions where the metals are soluble or insoluble. The region above the dark line for each metal signifies that the metals should precipitate as metal hydroxides. This is referred to as the precipitation region. The region below or outside of the dark lines illustrates where the metals are dissolved in solution, no precipitation occurs, and no metal removal takes place (US EPA, 1987).

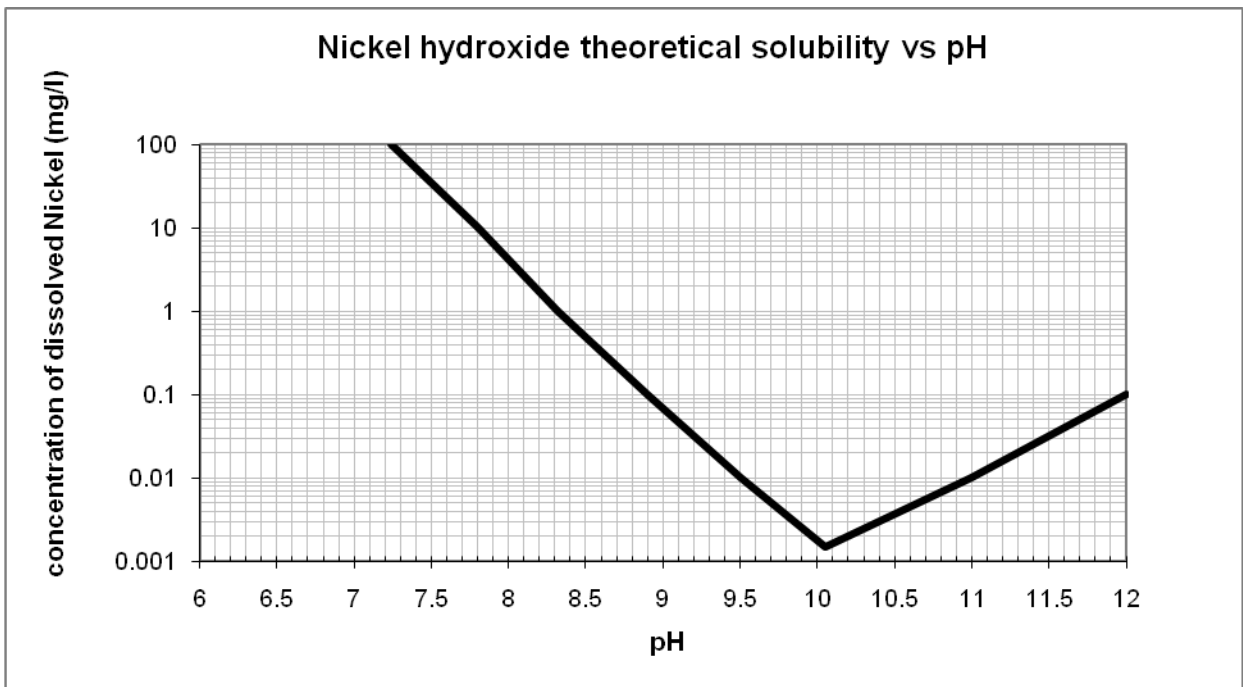


Figure 2.1- Theoretical Solubility of Nickel Hydroxide (US EPA, 1987).

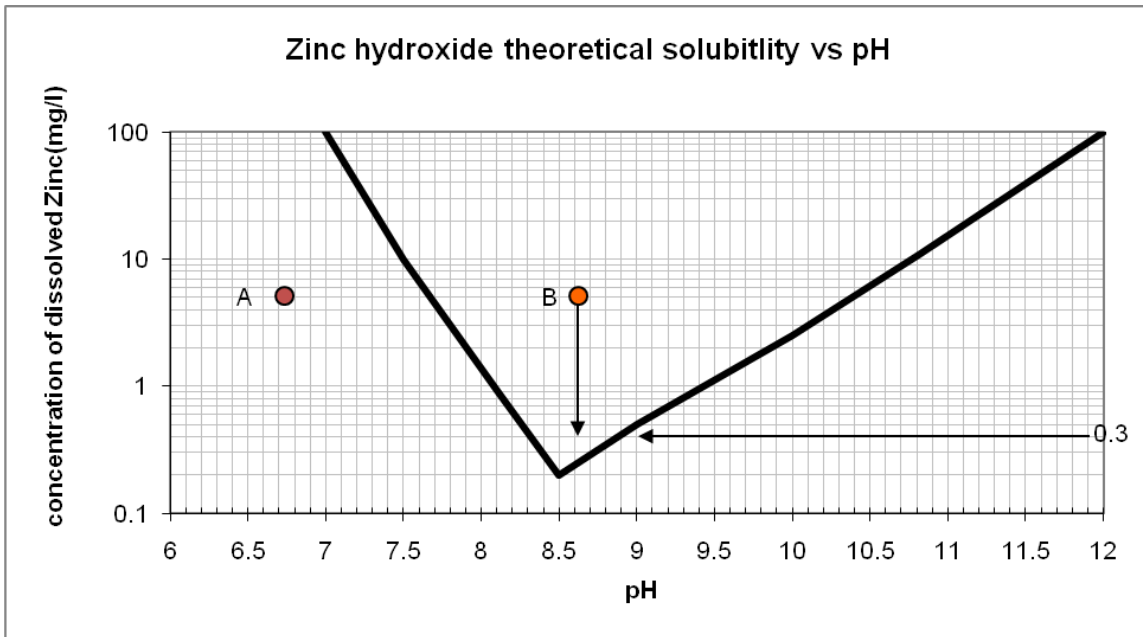


Figure 2.2- Theoretical Solubility of Zinc Hydroxide (US EPA, 1987).

In Figure 2.2, for example a wastewater contains dissolved zinc at 4 mg/l and is at pH = 6.8, this is shown at point A. Since this point is below the bold lines in the solubility graph, this indicates that zinc is only present as a dissolved metal. It is not in a solid form and under these conditions it will not precipitate. Therefore, in order to promote zinc precipitation the pH of the water needs to be adjusted to point B (pH= 8.6) by adding caustic. At this new pH value, most of zinc forms zinc hydroxide and precipitates out of solution. The dissolved zinc concentration can be obtained from the solubility line at this pH (*i.e.*, 0.3 mg/l). This is the theoretical amount of zinc that would be in the discharged wastewater after this treatment (US EPA, 1987).

Thus, simply adjusting the pH from 6.8 to 8.6 has effectively precipitated most of the dissolved metal in the water. Since all metals have some solubility dependency on pH the adjustment of pH is critical when the metal is to be removed from the wastewater. However, the metals now exist in another phase or state (*i.e.*, small solid particles). Metal removal is not complete until physically removed from the wastewater, typically by subsequent sedimentation and filtration processes. The metal solubilities presented in Figures 2.1 and 2.2 are based on solutions with single metal and no other components.

Some variations in the exact values of the metal concentrations would occur due to the presence of other substances in the wastewater. Compounds such as cyanide or ammonia can inhibit precipitation of metals, and limit their removal to the point where discharge limits can be exceeded. Also, not all metals have the same minimum solubility. Therefore in a wastewater with multiple metals, as a general rule, pH should be adjusted to an average value, approximately 9. In addition solubility depends on temperature; solubilities of inorganic and metal precipitates generally increase with increasing solution temperatures (US EPA, 1987). In the present study, all experiments were carried out at room temperature of 20-25°C. The effect of the temperature variation from 20-25°C on the percentage metal removal was insignificant (in the order of $\pm 0.2\text{mg/l}$ out of 50mg/l concentration of metal used). The temperature change has slightly effect on the zinc hydroxide solubility at optimum pH as shown in Table 2.1 (Reichel, 1975).

Table 2.1- Solubility (S) of zinc hydroxide, S unit mol of zinc per kg of water (Reichel, 1975).

12.5°C		25°C		50°C		75°C	
pH	S x10 ⁵	pH	S x10 ⁵	pH	S x10 ⁵	pH	S x10 ⁵
13.18	25.2	13.19	178	12.50	261	12.12	1029
12.85	6.12	12.97	67.3	12.24	88.7	11.95	319
12.21	1.68	12.29	5.74	11.99	33.7	11.68	104
11.51	0.50	11.05	0.54	11.25	2.92	11.14	12.6
11.10	0.24	10.84	0.46	10.99	2.14	10.85	5.27
9.83	0.23	10.14	0.31	10.02	0.84	10.01	2.06
9.49	0.23	9.43	0.38	9.55	0.76	9.71	1.84
9.27	0.31	9.18	0.54	9.08	0.87	9.54	1.76
8.99	0.46	8.91	0.61	8.77	0.99	8.93	1.68
8.55	1.33	8.41	1.30	8.52	1.15	8.38	2.06
7.96	13.2	7.90	4.74	7.82	2.43	7.89	2.06
7.70	48.3	7.63	17.2	7.54	4.97	7.65	2.37
7.32	265	7.31	49.7	7.26	10.7	7.18	7.22
7.06	844	7.00	204	7.05	19.6	6.94	13.1

2.1.2 Advantages and Disadvantages of Hydroxide Precipitation

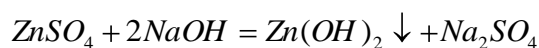
Removing metals via hydroxide precipitation has several advantages. Hydroxide precipitation is a well-established, simple technology, which is relatively inexpensive. It has proven its ability to achieve regulatory effluent limits for several metals, and it is well suited for automation. In addition to heavy metals, hydroxide precipitation can also remove many non-metal pollutants, such as soaps and fluorides (US Army Corps of Engineers, 2001).

Hydroxide precipitation of heavy metals also has several disadvantages. Some metals, including lead, manganese, and silver, may not be adequately treated by hydroxide precipitation. Some metals require reduction before they can be precipitated as a hydroxide. For example, chromium (+6) must be first reduced to chromium (+3). Similarly, selenium (+6) should be reduced to selenium (+4). Other metals may require oxidation before they can be effectively precipitated as a hydroxide. For example, arsenic (+3) must be oxidized to arsenic (+5), so as iron and manganese. In addition, strong chelating agents, organic-metallic complexes, and metal-cyanide complexes inhibit the formation of the hydroxide precipitate, making it impossible to achieve minimum theoretical solubility. Introducing a strong oxidant (e.g., ozone) before the precipitation step may decompose some of the metal complexes.

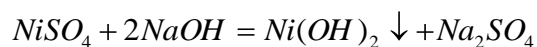
2.1.3 Hydroxide Precipitation Using Caustic Soda

Caustic soda (or caustic) is a highly alkaline sodium hydroxide solution. Caustic soda is commonly used to precipitate heavy metals and to neutralize strong acids. The following reactions occur when using sodium hydroxide as precipitant agent for zinc and nickel:

For Zinc Sulfate:



For Nickel Sulfate:



Sodium hydroxide solution (50%) is usually used in metal precipitation. It is easier to store, handle, and pump than is lime. In addition, it doesn't clog valves, form insoluble reaction products, or cause density control problems. However, in caustic storage areas where ambient temperatures are likely to fall below 12°C, heated tanks should be used to prevent reagent freezing (US Army Corps of Engineers, 2001; US EPA, 1987).

Caustic soda, after lime, is the most commonly used hydroxide-precipitating reagent. Its main advantage is that it rapidly dissociates into available hydroxyl (OH⁻) ions, resulting in minimal holdup time, and reducing feed system and tankage requirements. The main disadvantage of caustic is a higher cost in comparison with lime. Because caustic is a monohydroxide, precipitating one mole of a divalent metal requires two moles of hydroxide. In contrast, lime, a dihydroxide base, only requires one mole per one mole of metal. Increased reagent requirements, combined with a higher cost/mole (roughly five times that of hydrated lime), make precipitation using caustic soda more expensive than that with lime.

Generally, lime is the reagent of choice in applications where reagent costs constitute the bulk of the operating expenses. However, in low flow applications where a reagent is selected on the basis of limited space, rapid reaction rates, and ease of handling, caustic is more suitable. In addition, caustic would be a better choice when sludge disposal costs are high since it generates much less sludge.

Sodium hydroxide is approximately 100 times more soluble in water than lime (at 25°C). This reduces the need for complex slaking, slurring, and pumping equipment. Typically, caustic is added through an air-activated valve controlled by a pH analyzer. Caustic is added as long as the pH of the waste stream remains below the control set point required for optimum precipitation. A mechanical mixer agitates the waste stream to prevent excessive lag time between reagent addition and observable change in pH. Precipitation using caustic is usually conducted under normal temperature and pressure (US Army Corps of Engineers, 2001; US EPA, 1987).

2.2 Coagulation and Flocculation

Coagulation is used to agglomerate the insoluble and colloidal heavy metal precipitates formed during the precipitation step. Colloidal heavy metal precipitates are tiny particles that possess electrical properties, which create repelling forces and prevent agglomeration and settling. Therefore, gravity settling is almost impossible. Coagulation is the process of making the particle less stable by neutralizing its charge, thus encouraging initial aggregation of colloidal.

There are two types of colloids: hydrophilic colloids and hydrophobic colloids. Hydrophobic colloids, including clay and non-hydrated metal oxides, are unstable. The colloids are easily destabilized. Hydrophilic colloids like soap are stable. When these colloids are mixed with water, they form colloidal solutions that are not easily destabilized. Most suspended solids smaller than 0.1 mm in water carry negative charges. Since the particles have similar negative electrical charges and electrical forces to keep the individual particles separate, the colloids stay in suspension as small particles. Table 2.2 shows different size of particle in raw water and their settling velocity (Koohestanian et al., 2008).

Table 2.2- Various sizes of particles in raw water and their settling velocity

Particle diameter (mm)	Type	Settling velocity
10	Pebble	0.73 m/s (gravity settling)
1	Course sand	0.23 m/s (gravity settling)
0.1	Fine sand	0.6 m/min (gravity settling)
0.01	Silt	8.6 m/d (gravity settling)
0.0001 (10 micron)	Large colloids	0.3 m/yr
0.000001 (1 nano)	Small colloids	3 m/million yr

To remove colloids, small particles have to be destabilized first and then they would form larger and heavier flocs which can be removed by gravity settling. This process can be described by clarification mechanisms that include: coagulation, flocculation and sedimentation. Coagulation is the process of decreasing or neutralizing the negative

charge on suspended particles or zeta potential. This allows the van der Waals force of attraction to initiate aggregation of colloidal and fine suspended materials to form microflocs. Rapid, high energy mixing is necessary to ensure the coagulant is fully mixed into the process flow to maximize its effectiveness. The coagulation process occurs very quickly, in a matter of fractions of a second. Rapid mixing is very important for formation of the hydrolysis products (i.e., $\text{Fe}(\text{OH})_3$ dissociate to Fe^{+3} and OH^-) able to adsorb on the surface of colloids to initiate destabilization of colloidal particles. When suspended in water, the charge on organic and inorganic colloids is typically negative due to high pH needed for the metal precipitation. Because of electrostatic forces, the negative colloid charge attracts positive ions. Figure 2.3 illustrates how coagulants reduce the electric charges on the colloidal surfaces, allowing colloidal particles to join. The coagulation treatment is influenced by raw water characteristics, temperature, pH, coagulant type, dose and rapid mixing intensity and duration (Bratby, 2006).

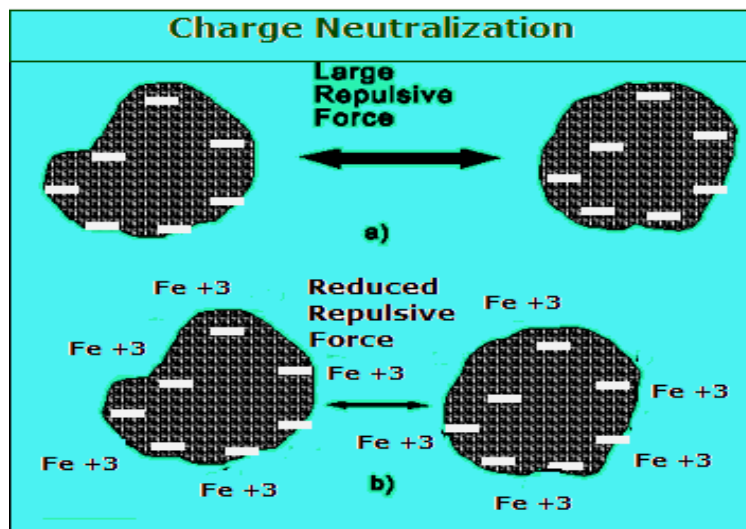


Figure 2.3- Coagulation, Charge neutralization

The effect of anionic ions coordinated with coagulants depends on the coordination strength with the cationic ions. If the anion is a strong coordinator with cation, it would not be readily replaced by hydroxyl ions, and the pH of optimum destabilization will drop sharply with increasing anion concentration. However, if the anion is only a very weak

coordinator with cation, it exerts only a slight effect on the optimum precipitation, generally in the direction of lower pH values (Bratby, 2006).

Flocculation is the process of bringing together the destabilized or “coagulated” particles to form a larger agglomeration of floc by physical mixing or addition of chemical coagulant aids, such as chain polymer, or both. Destabilization by bridging occurs when a polymer of a high molecular weight attaches to a number of adsorption sites on the surface of negatively charged particles along the polymer chain. The remainder of the polymer may remain extended into the solution and may adsorb on available surface sites of other particulates, thus creating a ‘bridge’ between the surfaces (US Army Corps of Engineers, 2001), as shown in Figure 2.4.

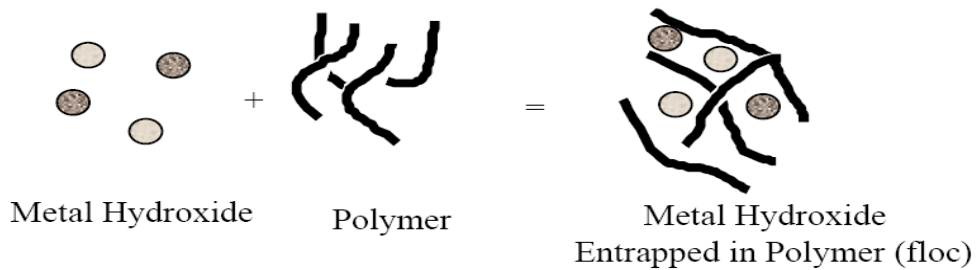


Figure 2.4- Flocculation, illustrates the bridging of agglomerated colloidal.

During dissolution of the coagulant salt, the cations generated serve to neutralize the particle charge and reduce the effective thickness of the double layer, thereby reducing the zeta potential. For inorganic coagulants, a trivalent ion can be as much as 1000 times more effective than a monovalent ion. This is the reason that alum and iron salts are very efficient coagulants. Table 2.3 illustrates the increasing coagulation “power” with cation reactivity.

Table 2.3- Relative coagulating "Power" of cations (US Army Corps of Engineers, 2001)

<i>Cation</i>	<i>Relative Coagulating Power</i>
Na ⁺	1
Mg ⁺²	63
Al ⁺³	570

Colloids can also be destabilized through the addition of polyelectrolytes, which can bring the system to the isoelectric point without a change in pH. These polyelectrolytes are 10 to 15 times more effective than alum as a coagulant; however, they are considerably more expensive. The coagulation and flocculation processes typically include the following four steps (US Army Corps of Engineers, 2001):

- If necessary, adding alkalinity (bicarbonate has the advantage of providing alkalinity without raising pH).
- Adding the coagulant and coagulant aid to the influent after precipitation.
- Rapid mixing of the coagulant throughout the liquid.
- Adding the coagulant aid, followed by slow and gentle mixing to allow for contact between small particles and subsequent agglomeration into larger flocs.

The overall success of the coagulation and flocculation processes depends on the flocculating and settling characteristics of the particles. The frequency of collisions between the particles is directly proportional to the rate at which coagulated particles coalesce. The collision frequency is proportional to the concentration of particles and the difference in settling velocities. Because the total number of particle collisions increases with time, the degree of flocculation generally increases with residence time. The agglomeration of particles cannot be predicted from collision frequency alone. The rate of flocculation depends upon several factors, which include: nature of the particle surface, presence of charges, shape of the particles and density of the particles.

2.3 Coagulants and Flocculants

Numerous chemicals are used in coagulation and flocculation processes. There are advantages and disadvantages associated with each chemical. The designer should consider the following factors in selecting these chemicals includes: cost, reliability of supply, sludge consideration, compatibility with other treatment process, environmental effect and labor and equipment requirements for storage, feeding, and handling. Coagulants and flocculants commonly used are generally classified as inorganic coagulants and polyelectrolytes which they are further classified as either synthetic-

organic polymers or natural-organic polymers. The three main classifications of inorganic coagulants are aluminum derivatives, iron derivatives and lime. Table 2.4 lists several common inorganic coagulants along with associated advantages and disadvantages (US Army Corps of Engineers, 2001).

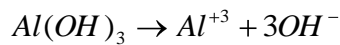
Table 2.4-Advantages and disadvantages of alternative inorganic coagulants

Coagulant Name	Advantages	Disadvantages
Aluminum Sulfate (Alum) $Al_2(SO_4)_3 \cdot 18H_2O$	Easy to handle and apply; most commonly used; produces less sludge than lime; most effective between pH 6.5 and 7.5	Adds dissolved solids (salts) to water; effective over a limited pH range.
Sodium Aluminate $Na_2Al_2O_4$	Effective in hard waters; small dosages usually needed	Often used with alum; high cost; ineffective in soft waters
Polyaluminum Chloride (PAC) $Al_{13}(OH)_{20}(SO_4)_2 \cdot Cl_{15}$	In some applications, floc formed is more dense and faster settling than alum	Not commonly used; little full scale data compared to other aluminum derivatives
Ferric Sulfate $Fe_2(SO_4)_3$	Effective between pH 4–6 and 8.8– 9.2	Adds dissolved solids (salts) to water; usually need to add alkalinity
Ferric Chloride $FeCl_3 \cdot 6H_2O$	Effective between pH 4 and 11	Adds dissolved solids to water; consumes twice as much alkalinity as alum
Ferrous Sulfate (Copperas) $FeSO_4 \cdot 7H_2O$	Not as pH sensitive as lime	Adds dissolved solids (salts) to water; usually need to add alkalinity
Lime $Ca(OH)_2$	Commonly used; very effective; may not add salts to effluent	Very pH dependent; produces large quantities of sludge; overdose can result in poor effluent quality

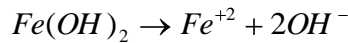
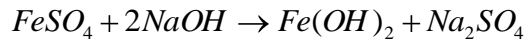
With exception of sodium aluminate, all common iron and aluminum coagulants are acid salts and, therefore, their addition lowers the pH of the treated water. Depending on the influent pH and alkalinity (presence of HCO_3^- , CO_3^{2-} , and OH^-), an alkali, such as lime or caustic, may be required to counteract the pH depression of the coagulant. This is important because pH affects both particle surface charge and floc precipitation during

coagulation. The optimum pH levels for forming aluminum and iron hydroxide flocs are those that minimize the hydroxide solubility (US EPA, 1987). However, the optimum pH for coagulating suspended solids does not always coincide with the optimum pH for the minimum hydroxide floc solubility. Aluminum sulfate, ferrous sulfate and ferric chloride have been used in this study due to their effectiveness at a high pH value. The coagulant salts used alkalinity (sodium hydroxide) to form hydroxide products. The coagulation reactions as follows (Koohestanian et al., 2008):

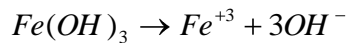
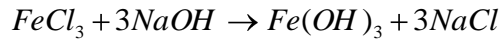
Aluminum Sulfate;



Ferrous Sulfate;



Ferric Chloride;



Aluminum, ferrous and ferric hydroxides, in solution, immediately dissociates to form hydrated reaction products. The metal ions form coordination compounds with water molecules to give $Al(H_2O)_6^{+3}$ and $Fe(H_2O)_6^{+3}$. These species, referred to as the trivalent ions of aluminum and iron, are often presented as Al^{+3} and Fe^{+3} (Bratby, 2006).

Polyelectrolytes (flocculants) are water-soluble organic polymers that can be used as either primary coagulants or coagulant aids. Polyelectrolytes are generally classified as anionic-ionization in solution to form negative sites along the polymer molecule, cationic-ionization to form positive sites and non-ionic very slight ionization. Polyelectrolyte primary coagulants are cationic, containing materials with relatively low-molecular weights (generally less than 500,000). Cationic charge density (available positive charged sites) is very high. Flocculant may be anionic, cationic, or near-neutrally

charged. Their molecular weights are relatively high (range up to 20,000,000). They function primarily through inter particle bridging. The efficiencies of polyelectrolyte primary coagulants depend greatly on the nature and amount of the particles to be coagulated, and the turbulence (mixing) available during coagulation (US Army Corps of Engineers, 2001).

The coagulation process is often enhanced through the use of coagulant aids (flocculants). Sometimes, excess primary coagulant is added to promote large floc sizes and rapid settling rates. However, in some waters, even large doses of primary coagulant will not produce a satisfactory floc. In these cases, a polymeric coagulant aid can be added after the coagulant to produce a denser floc, and thereby reducing the amount of primary coagulant required. Because of polymer “bridging,” small floc particles agglomerate rapidly into larger cohesive floc, which settles rapidly. Coagulant aids also help to create satisfactory coagulation over a broader pH range. Generally, the most effective types of coagulant aids are slightly anionic polyacrylamides with very high-molecular weights. In some clarification systems, non-ionic or cationic types have proven effective.

Synthetic organic polymers are the most commonly used coagulant aids for coagulation/flocculation of heavy metal precipitates. This is because aggregate flocs of the metal ions after treated with coagulant possess a slight electrostatic positive charge resulting from charge density separation. The negatively charged reaction sites on the anionic polyelectrolyte attract and adsorb the slightly positive charged flocs. Synthetic organic polyelectrolytes are commercially marketed in the form of dry powder, granules, beads, aqueous solutions, aqueous gels, and oil-in-water emulsions. Generally, liquid systems are preferred because they require less floor space, reduce labor requirements, and reduce the potential for side reactions because the concentrate can be diluted in the automatic dispensing systems. Usually dosage requirements for metals-containing waters are in the 0.5 to 2.0 mg/L range. Polyelectrolytes work most effectively at alkaline and intermediate pH but lose effectiveness at pH levels lower than 4.5 (US EPA, 1987).

2.4 Mixing

Mixing provides greater uniformity of the wastewater feed and disperses precipitating agents, coagulants, and coagulant aids throughout the wastewater to ensure the most rapid precipitation and subsequent settling of precipitates possible. To quantify the degree of mixing, the following factors must be considered:

- The amount of energy supplied.
- The mixing residence time.
- The mixing intensity effects on the size and shape of the particle.

The root mean square velocity gradient (typically denoted as G , units, (m/s)/m) represents a measure of shear intensity over the mixing basin. For mechanically stirred mixing basins, G as follows:

$$G = \sqrt{\frac{P}{V\mu}} \quad \rightarrow \quad P = G^2 V \mu \dots\dots\dots (1)$$

Where:

G = velocity gradient, (m/s)/m

P = power applied to stirring, W (N-m/s)

V = reactor volume, m³

μ = fluid viscosity, N-s/m²

Power applied to drive the agitator can be calculated from above equation. Velocity gradient curves (G) versus agitator paddle speed (rpm) for a standard jar test using Phipps and Bird impeller (Ebeling et al., 2003; www.phippsbird.com) are shown in Figures A.1 and A.2 in Appendix A. In present study, since the same standard jar test was used. The measured rpm can be used to obtain G values from Figures A.1 and A.2, which can be used to estimate the power required for mixing using equation (1). The calculation of Reynold's number at different rpm using standard jar test is shown in Figure A.3 in Appendix A.

2.4.1 Rapid Mixing

Chemicals such as coagulants generally require rapid mixing. Chemical mixing systems should be designed to provide a thorough and complete dispersion of the chemical throughout the influent. Rapid or flash mixing residence times depend on wastewater characteristics and the coagulant used. Some researcher suggested a range from 30 seconds to 3 minutes. The intensity and duration of the mixing of the coagulant must be controlled to prevent under-mixing or over-mixing. Over-mixing may breakup newly formed floc, whereas under-mixing can cause inadequate dispersion of the coagulant, resulting in uneven dosing. For rapid mixing applications, mixing speeds of 100-200 rpm are suggested by some researchers (US Army Corps of Engineers, 2001; US EPA, 1987; Koohestanian et al., 2008; Rossini et al., 1998).

Mixing conditions can have a very significant effect on the performance of coagulants and flocculants. The first requirement is for the additive to be distributed uniformly among the suspension and this can be achieved by some form of rapid mixing. The particles then need to collide in order to form aggregates and this process can be greatly assisted by some form of agitation, either in a stirred tank or some form of flow-through unit. In the case of charge neutralization or polymer bridging, rapid mixing is especially important since poor mixing can lead to local overdosing and re-stabilization of some particles. The formation of hydrolysis products of the coagulant occurs very rapidly. Competing processes, such as intended adsorption of the hydrolysis products on the particle surface and unwanted precipitation of the hydrolysis products, could depend on mixing conditions (Amirtharajah et al., 1990). In the case of sweep flocculation it has been suggested that initial mixing conditions are not so important, but this is not well established (Amirtharajah et al., 1982).

After coagulant dosing and mixing, flocs grow initially at a rate that is determined mainly by the applied mixing, the particle concentration and the collision efficiency and hence on the degree of particle destabilization caused by the added coagulant. As flocs become larger, further growth is restricted by the applied shear for essentially two reasons; existing flocs may be broken as a result of disruptive forces (Blaser, 2000) and the

collision efficiency of particles in a mixing field becomes lower as particle size increases (Brakalov, 1987).

A dynamic balance between floc growth and breakage can lead to a steady-state floc size distribution, where the limiting size is dependent on the applied shear rate (Muhle, 1993). When flocs are subjected to an increased shear rate, breakage can occur. This may be by rupture of flocs into roughly equal-sized fragments or erosion of small particles from the surface of flocs. In turbulent flow the mode of breakage depends on the floc size relative to the turbulence microscale. Breakage depends greatly on the intensity of shear and on floc strength, which is not a well-defined concept.

The strength of flocs depends on the nature of the interaction between particles and on the average number of bonds per particle or on the floc density. In practice, floc strength is often approached in an empirical manner, usually by observing the limiting floc size under given shear conditions (Muhle, 1993; Serra et al., 1997). After floc breakage, re-growth may occur under low shear conditions. However, in some cases floc breakage may be irreversible to some extent, in which case only limited re-growth occurs (Francois et al., 1984; Clark et al., 1991). There have been only limited studies on this aspect and the influence of mixing conditions on the re-formation of flocs has not been evaluated.

2.4.2 Slow Mixing

Slow mixing is considered to be instrumental for the formation of readily settleable suspension. Its purpose is to facilitate the formation of large, kinetically unstable flocs. For the formation of large flocs, the intensity of agitation should not exceed a certain limit beyond which floc breakage occurs. Therefore, slow mixing is often designed such that its intensity decreases as the process of flocculation progresses. The basic changes taking place during the flocculation process include the changes in the number of the destabilized particles, the number of flocs being formed from these particles, the size, shape and density of the formed flocs. The flocs formed under the flocculation conditions are large, voluminous and of geometrically loose, widely branched, spatially extended lattice structures containing large volumes of voids filled with water. They are of low density and very fragile with a tendency to fragment. Such flocs are grossly non-

homogenous in size as well as in density (Hereit et al., 1983). Slow and even mixing allows the particles to collide and contact with the flocculant so as to form flocs, the detention time typically between (10-30 minutes). The efficiency of floc formations is contingent on the frequency of particle-to-particle contact. Values of G for flocculation units typically range from 20 to 80 $1/s$ (20-50 rpm) (US Army Corps of Engineers, 2001; US EPA, 1987).

2.5 Sedimentation (Settling time)

Once particles become enmeshed in the polymer, they are allowed to settle so that they are removed from the wastewater. The particles settle since they are heavier than water. This settling occurs in a sedimentation tank. A sedimentation tank, in contrast to rapid mixing units, is designed to have no mixing, to produce a calm flow for settling

Settling rate is a result of several forces acting on a particle inside a fluid. The main forces to consider are the downward force of gravity, the upward force of buoyancy, and the force of drag which opposes the particle's motion through the fluid. Gravity and buoyancy are "static" forces in that they are always the same for a given particle regardless of how fast it is moving. The force of drag depends on the particle's speed relative to the fluid, and also on its shape and cross-sectional area. The simplified equation for spherical particle (called Stokes' Law) would give a feel for the variables that are important (Kan et al., 1998):

$$V_s = \frac{2 (\rho_p - \rho_f)}{9 \mu} gR^2 \dots\dots\dots (2)$$

Where:

V_s = Sedimentation rate

R = The radius of the spherical particle

ρ_p = Density of the particle

ρ_f = Density of the fluid

g = Gravitational constant

μ = Viscosity of the fluid

The larger the particle is, and the denser it is, the greater the gravitational force acting downward on it. The force of buoyancy on the object is how much the water pushes it upward. The strength of this buoyancy force is proportional to the volume of the object. (It is actually equal to the weight of the water displaced by the particle, which is equal to the weight of a volume of water equal to the volume of the particle). If the particle is denser than water, its gravitational force exceeds its buoyancy force and the net force on the particle is downward. If the particle is less dense than water, its buoyancy force is stronger than the gravitational force and the net force on the particle is upward. The greater the mass of the particle, the faster this speed will be at which drag stops further acceleration. The larger the particle is, the greater the force of drag at a given speed. These two effects work somewhat at cross-purposes, as a larger object would have a greater mass. But the force of gravity increases as the mass of the object, which scales with the cube of its size (i.e, its diameter for a spherical particle), while the force of drag increases as the cross-sectional area of the object, which scales with the square of its size. So if two objects have the same density but different sized, the larger one settles faster. If two objects have the same size but different densities, the denser one settles faster.

3 Literature Review

3.1 Coagulant, Flocculant Type and Dose

Coagulant dose is depending mostly on the metal concentration in wastewater (Reichle et al., 1975). Koohestanian et al. (2008) found that coagulation and flocculation of colloidal particles from raw water was optimal at a temperature range of 20-24°C. Moreover, they found that temperature effects on aluminum sulfate in removing water turbidity are more but susceptibility of ferric chloride is less. In low temperature, ferric chloride is able to decrease turbidity of the raw water easier comparing with aluminum sulfate.

Some researchers studied various coagulants for heavy metal removal but very few researchers studied coagulants with the objective of finding the optimal values of coagulant dosage and its effect on the metal precipitate particle size as well as the optimum rapid mixing operating parameters. In the reported literature, Patoczka et al. (1998) reported a high removal of nickel from an initial concentration of 30 mg/l down to 0.8 mg/l using 30mg/l ferric chloride at pH 10.5. However, they didn't investigate optimum rapid mixing parameters, resulting in longer settling time (up to 24 hours) than suppose the process should take. They reported poor zinc removal from 8.5 down to 1.0mg/l at pH of 8.7 but with elevated ferric chloride dose of 500mg/l. Ebling et al. (2003) suggested that both ferric chloride and aluminum sulfate demonstrated high removal of suspended solids in solution containing nickel and zinc from initial value of 100 down to 10mg/l at a dose of 60mg/l. However, they reported that rapid mixing speed and time played only minor role on heavy metal removal. Johnson et al. (2008) reported that ferric chloride was more effective for zinc and nickel removal than aluminum within pH range 6.5 to 7.0 at a dose of 40mg/l, but they didn't optimize the rapid mixing operating parameters or precipitation pH. As a result, poor zinc (57%) and nickel (17%) removal was achieved. They also reported 82% removal of zinc and nickel suspended solid after 45min settling time using 1min mixing at 160 rpm. Abdul Aziz et al. (2007) suggested that ferric chloride was capable of removing suspended solids of leachate from a landfill site at lower dose than that for aluminum sulfate or ferrous sulfate, and better removal was observed at pH 4 and pH 12 than at pH 6. They also obtained optimum rapid

mixing speed of 300 rpm with average particle size of 60 μ m after coagulation with ferric chloride. However they didn't investigate wide range of rapid mixing speed or time.

Some researchers focused their attention on the flocculation step. Mooyoung and Lawler (1992) claimed that the main importance of mixing in flocculation was to keep a largest number of particles suspended i.e. that mixing in flocculation was not as critical as previously thought. The slow mixing intensity rate must be at a minimal level able to suspend particles without floc breakage. Dharmappa et al. (1993) found that the most important parameters for the whole optimization process are the rapid mixing parameters. Many researcher studied the slow mixing optimum parameters and suggested that mixing speed is between 20-50 rpm and detention time is 10-25 minutes and flocculant dose is 0.5- 1.0 mg/l (US EPA, 1987; Kawamura, 1976; Johnson et al., 2008; Stnadova and Schejbal, 1997; Patoczka et al., 1998). In this study, operating parameters for flocculation are set as 0.5 mg/l dose for the flocculant (polymer) and slow mixing for 15 minutes at 50 rpm.

3.2 Rapid Mixing Parameters

Some researchers studied various rapid mixing devices but very few researchers (Mhaisalkar et al., 1991; Suleyman and Evison, 1995) studied rapid mixing with the objective of finding the optimal values of velocity gradient (speed) and mixing time. Different sources suggested conflict recommendations on the rapid mixing speed and time. Hudson et al. (1967), Kawamura (1976) and Vrale et al. (1971) suggested instantaneous mixing based on chemical theories of adsorption-destabilization was appropriate for metal precipitation, while Camp (1968) and Lettermann et al. (1973) recommended detention times of minutes in the rapid mixing unit. Mhaisalkar et al. (1991) suggested some values for the optimal time and intensity for rapid mixing. The reasons for the conflicting results in the literature were not provided. Many researchers studied coagulation of suspended solids of heavy metals and they suggested optimal values for rapid mixing parameters. Park et al. (2006) reported that rapid mixing optimum conditions, corresponding to a minimum number of small microflocs as well as a maximum number of large microflocs in a 14-25 μ m range, were at mixing speed of 180

rpm and a mixing time of 150 s for turbidity removal. Kan et al. (1998) found that a rapid mixing speed range from 200-225 rpm at 10 s was the optimal condition in turbidity removal. They also suggested that the determination of the optimum dosage of the coagulant would not be affected by the mixing intensity. Rossini et al. (1998) reported that increasing the rapid mixing speed raises the contribution of the adsorption – destabilization to turbidity removal and they suggested optimal values of mixing time and speed of 250 rpm at 120 s, respectively. Kan et al. (2002) reported a good mixing speed range of 180- 250 rpm at 150 s for coagulation of high turbidity water.

3.3 Settling Time

Settling process is a gravitational process that requires no chemical addition. Although some workers realized the importance of the settling process, there is little information available in the literature on the effect of the settling time on the heavy metal removal capacity. Most studies on the treatment of wastewater were focused on reducing settling time of these heavy metal particles so to reduce the clarifier tank size and thus the capital cost. Some researchers studied the settling time but very few researchers (Hereit et al., 1983; Strnadova and Schejbal, 1997) studied settling time with the objective of finding the optimal values of settling time using different coagulants. Different sources suggested different settling times. Johnson et al. (2008) suggested 25 minute settling time using ferric chloride in removing total suspended solid in solution containing heavy metals. On the other hand, Patoczka et al. (1998) suggested 30 minute settling time for heavy metals precipitates removal by ferric chloride. Abdul Aziz et al. (2007) suggested that almost complete removal of suspended solids was achieved after 60min settling.

3.4 Objectives

The aim of the present study is to obtain the optimal operating parameters for the removal of zinc and nickel by chemical precipitation/coagulation. In addition, explanation for the apparent contradiction of the literature data on optimum parameters for the chemical precipitation, coagulation and mixing intensity was also attempted.

In order to achieve the project objectives, experimental work was carried out to find:

- Solution pH value for the optimum removal of nickel and zinc in the wastewater.
- Coagulant type and dosage that would give a highest removal of the metals.
- Optimal mixing time and impeller speed in coagulation stage (rapid mixing)
- Optimal settling time required for metal particles to settle.
- The mechanism of the particle formation during rapid mixing coagulation as well as the coagulation mechanism.

4 Experimental Method

4.1 Experimental setup

Many researchers used standard jar test by Phipps & Bird (Sheng et al., 2006; Park et al., 2006; Lee et al., 1994; Kan et al., 2002; Young et al. 2000) to conduct the experiments. In this study, the same standard jar test as shown in Figure 4.1 had been built as follow:

- Glass mixing vessel (L x W x H, 11.5 cm x 11.5 cm x 25 cm) ,2000 ml
- Mixing provided by 7.6 cm x 2.5 cm flat rectangular blade centrally located in the vessel and placed at 5 cm from the vessel bottom
- Overhead stirrer with 1/25 hp constant speed range 50-1000 rpm (Model- VOS14, VWR, Canada)
- Tachometer with speed range 50-2000 rpm (Model- DMMI- DUT371, Digital Measurement Metrology Inc., Canada)
- pH meter and temperature (Model- PH 2100e, Mettler Toledo , Germany)

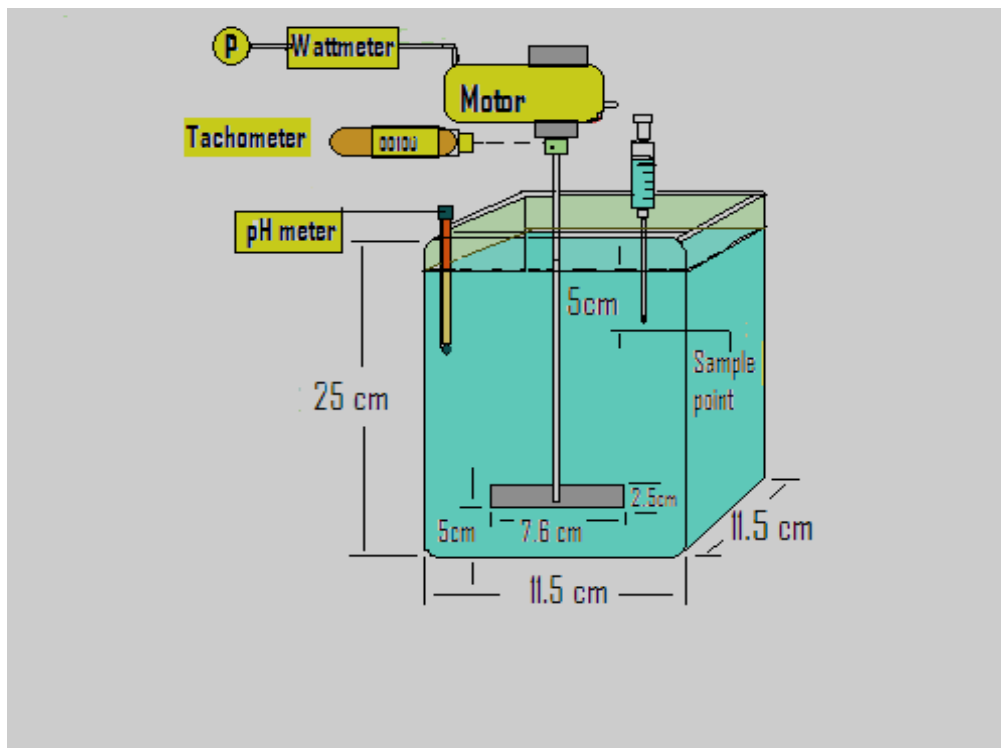


Figure 4.1 Experimental Setup (standard Jar Test)

4.2 Experimental Procedures

The stock solutions of metal salt were prepared by dissolving 50g of analytical grade nickel sulfate (NiSO_4 , AlfaAesar, USA)/ zinc sulfate (ZnSO_4 , J.T.Baker, USA) in 1 liter deionized water. The stock solutions of the coagulants were prepared by dissolving 2g analytical grade of aluminum sulfate ($\text{Al}_2(\text{SO}_4)_3 \cdot 16\text{H}_2\text{O}$, Mallinckrodt Inc., USA) / ferrous sulfate ($\text{FeSO}_4 \cdot 7\text{H}_2\text{O}$, EMD, USA) / ferric chloride ($\text{FeCl}_3 \cdot 7\text{H}_2\text{O}$, J.T.Baker, USA) in 200ml deionized water. Flocculant, polyacrylamide (anionic) (A-PAM, Water Energy Technologies, Canada), was prepared and ready to use by manufacturer. The simulated wastewater initial concentration was 50 ppm (mg/l) zinc or nickel ions were prepared for each experimental run. To adjust the solution pH, 1 N sodium hydroxide (NaOH , MultiPharm, Germany) and 1 N sulfuric acid (H_2SO_4 , EMD, USA) solutions were used.

4.2.1 Precipitation pH (first stage)

The experimental procedure to obtain the optimum pH to precipitate zinc ions or nickel ions was as follow:

- Measuring the temperature of the solution in the jar test.
- Mixing zinc or nickel solution with an initial concentration $C_i=50$ mg/l with 2L de-ionized water in the jar test and withdraw 10ml sample for the metal concentration analysis using Atomic Adsorption Spectrophotometer (A.A.).
- Adding caustic soda / sulfuric acid to adjust the pH in the range of 6 -12 with 0.5 increments and 0.25 increments around the optimum point, throughout the precipitation process.
- Mixing the simulate solution for 10 min @ 100 rpm.
- To stop mixing and let the wastewater settled for 1hr. Withdraw 10 ml sample at 5 cm depth below the water level.
- To filter the sample with micro filter paper (Whatman, 934-AH) and use the filtered water sample for A.A. analysis. Obtain final metal concentration (C_f).

4.2.2 Coagulant Type and Dose (second stage)

The optimum pH for the precipitation of zinc and nickel ions was obtained in the first stage. This pH was used to obtain the best coagulant and the optimum dose of the coagulant that gives the highest metal removal. A test with the simulated solution and no coagulant or flocculant was used as a control run. The coagulant testing experimental steps are as follows:

- Measuring the temperature of the wastewater in the jar test.
- Mixing zinc or nickel solution with an initial concentration $C_i = 50$ mg/l with 2L de-ionized water in the jar test and withdraw 10ml sample for the metal concentration analysis using A.A.
- Adding caustic soda / sulfuric acid to adjust the pH to the optimum value that obtained from the first stage. The optimum pH was maintained throughout experiments.
- Adding coagulant (aluminum sulfate, ferrous sulfate and ferric chloride) at doses ranging from 0-50 mg/l with 10mg/l increments. The pH was adjusted back to the optimum after adding the coagulant (due to coagulant depression in pH)
- Performing rapid mixing for 120 s @ 150 rpm. To Stop mixing and withdraw 100 ml sample for Particle Analysis (P.A.)
- Adding 0.5 ml/l flocculant (polyacrylamides) followed by slow mixing for 15 min @ 50 rpm.
- To stop mixing and letting the solution settled for 30 min (Johnson et al., 2008; Patoczka et al., 1998). Withdraw 10 ml sample from 5 cm depth below water level (measuring total suspended solids).
- Adjusting the sample pH below 6 by adding sulfuric acid in order to dissolve any suspended particle that the sample might have. Using A.A. analysis to obtain final metal concentration (C_f).

4.2.3 Settling Time (third stage)

After the optimum coagulant dose had been obtained from second stage, the optimum dose was used to find the final settling time that is the time at which the metal concentration in the solution is doesn't further decrease significantly with time. The objective of this experiment was to determine the time beyond which the removal percentage showed no significant increase compared with time required for settling. The experimental steps are as follows:

- Measuring the temperature of the solution in the jar test.
- Mixing zinc or nickel solution with an initial concentration $C_i=50$ mg/l with 2L deionized water in the jar test and withdraw 10 ml sample for the metal concentration analysis using A.A.
- Adding caustic soda / sulfuric acid to adjust the pH to the optimum value that obtained from the first stage. The optimum pH was maintained throughout experiments.
- Adding coagulants (aluminum sulfate, ferrous sulfate and ferric Chloride) at the optimum dose previously obtained.
- Performing rapid mixing for 120 s @ 150 rpm, used in standard jar test method. To Stop mixing and withdraw 100ml sample for Particle Analysis (P.A.).
- Adding 0.5 ml/l flocculant (polyacrylamides) followed by slow mixing for 15 min @ 50 rpm.
- To Stop mixing and let the wastewater settled for 60 min. Withdraw 10 ml sample from 5 cm depth below water level every 1 min.
- Adjusting the sample pH below 6 by adding sulfuric acid in order to dissolve any suspended particle that the sample might have. Using A.A. analysis to obtain final metal concentration (C_f).

4.2.4 Rapid Mixing Speed and Time (fourth stage)

After the settling time was obtained from third stage, use this time to find the optimum rapid mixing speed and time. The experimental steps are as follows:

- Measuring the temperature of the wastewater in the jar test.
- Mixing zinc or nickel solution with an initial concentration $C_i=50$ mg/l with 2L deionized water in the jar test and withdraw 10ml sample for the metal concentration analysis using A.A.
- Adding caustic soda / sulfuric acid to adjust the pH to the optimum value that obtained from the first stage. The optimum pH was maintained throughout experiments.
- Adding coagulants (aluminum sulfate, ferrous sulfate and ferric chloride) at the optimum dose previously obtained.
- Performing rapid mixing for 30, 60, 90 and 120 s @ 100, 200, 300 and 400 rpm for simulate solution with zinc ions and for 30, 60, 90, 120 s @ 100, 150, 200, 250 rpm for simulate solution with nickel ions. Levels of investigated parameters are shown in Table 4.1. To Stop mixing and withdraw 100ml sample for particle analysis P.A.
- Repeating the same step above for narrow range of mixing speed and time around the optimum point.
- Adding 0.5 ml/l flocculant (polyacrylamides) followed by slow mixing for 15 min @ 50 rpm.
- To stop mixing and let the wastewater settled for 30 min. Withdraw 10 ml sample at 5 cm depth below water level every 5 min.
- Adjusting the sample pH below 6 by adding sulfuric acid in order to dissolve any suspended particle that the sample might have. Using A.A. analysis to obtain final metal concentration (C_f).

Table 4.1- Levels of investigated parameters for zinc and nickel removal.

Coagulant	Coagulant dose (mg/l)	Flocculant dose ml/l (Polyacrylamides)	Rapid mixing		Slow mixing	
			Time(s)	Speed(rpm)	Time(min)	Speed(rpm)
Ferric chloride	0	0.5	30	60	15	50
	20		60	80		
	30		90	100		
	40		120	120		
	50			140		
				150		
				160		
				200		
				250		
				300		
		400				
Ferrous sulfate	0		120	150		
	20					
	30					
	40					
	50					
Aluminum Sulfate	0		120	150		
	20					
	30					
	40					
	50					

4.2.5 Metal Particle Imaging

To analyze the structural surface of the zinc and nickel precipitate particles, scanning electron microscopy (SEM, Model- JEOL, JSM-6380 LV, Oxford Instrument, U.K) was performed in the Laboratory of Electron Microscopy and Sample Preparation of the Mechanical and Industrial Engineering Department, Ryerson University. The scanning electron microscope (SEM) provides the sample surface analysis by scanning it with a highly energetic electron beam. The electrons interact with the atoms that make up the sample producing signals that contain information about the sample's surface topography, composition, and other properties such as electrical conductivity. The SEM allows a greater depth of focus than an optical microscope does. For this reason the SEM can produce an image that is a good three-dimensional representation of the sample.

Samples for SEM analysis were prepared as follows:

- 100ml solution samples with suspended particles were collected.
- The samples were withdrawn from wastewater after rapid mixing stage.
- Samples were filtered using micro filter paper (Whatman 934-AH) and then left to dry for 48 hours in room temperature.
- Samples were coated to be more conductive.
- Blank filter paper imaged as background reference.

4.3 Experimental Uncertainty Analysis

The experimental uncertainty was conducted by considering the important instruments used for experimental data readings. In this regard the uncertainty analysis was performed as:

- **Error from instruments**

The instruments involved in the experimental study are balances, pH meter, tachometer, and atomic absorption spectrophotometer. Typical errors are given in Appendix B.

- **Error from manual readings**

The errors can come from different sources that include weighing of the chemicals, sampling the treated water, dilution of the samples and preparation of the solutions. In order to compare the discrepancy of the experimental results generated from the above mentioned possible errors, the experiments were performed three times. The average deviation from the means of all experiments was within \pm (1.0-2.5%). The average deviation from the means was calculated using the following

$$\text{Average Deviation} = \frac{1}{N} \sqrt{\sum_1^N (\bar{X} - X_i)^2} \dots\dots\dots (3)$$

Where

N = number of experimental data points

X_i = value of the individual data point

\bar{X} = average of the data points

The reproducibility of the optimum zinc and nickel removal runs are shown in Figures B.1 and B.2 in Appendix B.

4.4 Analysis of Zinc and Nickel

4.4.1 Concentration in wastewater

The concentration of zinc or nickel in simulated wastewater was measured using Atomic Adsorption Spectrophotometer (AAAnalyest 800, Perkin Elmer, Massachusetts, USA) flame technique. The samples were prepared by dilute 5 ml of the wastewater in 45ml of deionized water. The spectrometer has a detection limit of 7 mg/l for zinc and 5 mg/l for nickel. The calibration of the spectrometer was performed using four standard solutions of zinc and nickel. The calibration repeated after each 20 samples measurement. The percentage metal removal from wastewater was calculated using the following equation.

$$\text{Removal \%} = \left[\frac{C_i - C_f}{C_i} \right] \times 100 \quad \dots\dots\dots (4)$$

Where C_i and C_f are the initial and final concentration of metal in wastewater, respectively.

4.4.2 Particle Size Distribution

The particle size distribution of the zinc and nickel precipitate in wastewater was measured by Particle Analyzer (Microtrac-S3500, Microtrac Inc., USA). The detection range for particle is between 0.102 – 1408 μm . Samples of 100ml wastewater with zinc or nickel suspended particles were shaken gently to prevent particle breakage and then dropped in the sampler hopper of the particle analyzer. The calibration of the Particle Analyzer was performed using a standard solution after every 50 sample measurement. The total particle size distribution percentage (volume %) in 100ml wastewater sample was used to compare between samples. Particle size distribution measurements and calculations are given in Appendix C.

5 Results and Discussions

This chapter presents the experimental results using simulate aqueous solution with 50 ppm zinc ions and 50 ppm nickel ions individually and combined. The effect of pH on the metal removal by precipitation was investigated. Using three types of coagulants, the coagulant show highest metal removal with lower dose as well as settling time was determined. To determine optimum precipitation operating parameters, different mixing impeller speeds and times for the coagulation were also investigated. Finally, the precipitate particles surface structure and density were also evaluated using SEM imaging.

5.1 Optimum Precipitation pH

Zinc precipitation process begins with a pH adjustment. The pH is adjusted between 6.0-12.0 (beyond this range zinc ions are highly soluble as shown in Figure 2.2) with 0.5 increments and 0.25 increments around the optimum point. The results obtained, as plotted Figure 5.1, shows that zinc ions precipitate at the solution pH in the range of 8.0-9.0 with 8.7 being the optimum point at which the highest zinc removal (about 94%). Therefore, the optimum precipitation pH for zinc is considered to be 8.7, which was used for others experiments thereafter. The optimal estimation is shown in Appendix D.

Theoretical solubility of zinc hydroxide in Figure 2.2 shows that solubility for the zinc hydroxide reaches its minimum value at pH of 8.5, which is close to the observed value in the present study of 8.7. During experiment, it was noticed that zinc started to precipitate once the solution pH was increased from 7.0 to 8.0 at which few white small particles were formed. The amount and size of zinc particles increased rapidly for pH 8.0 to 9.0 and hence, the wastewater turbidity increased as well. The amount of the zinc particles and turbidity decreased gradually after the solution pH reached 9.5 and continuously dissolved back into the water as the pH was increased up to 12.

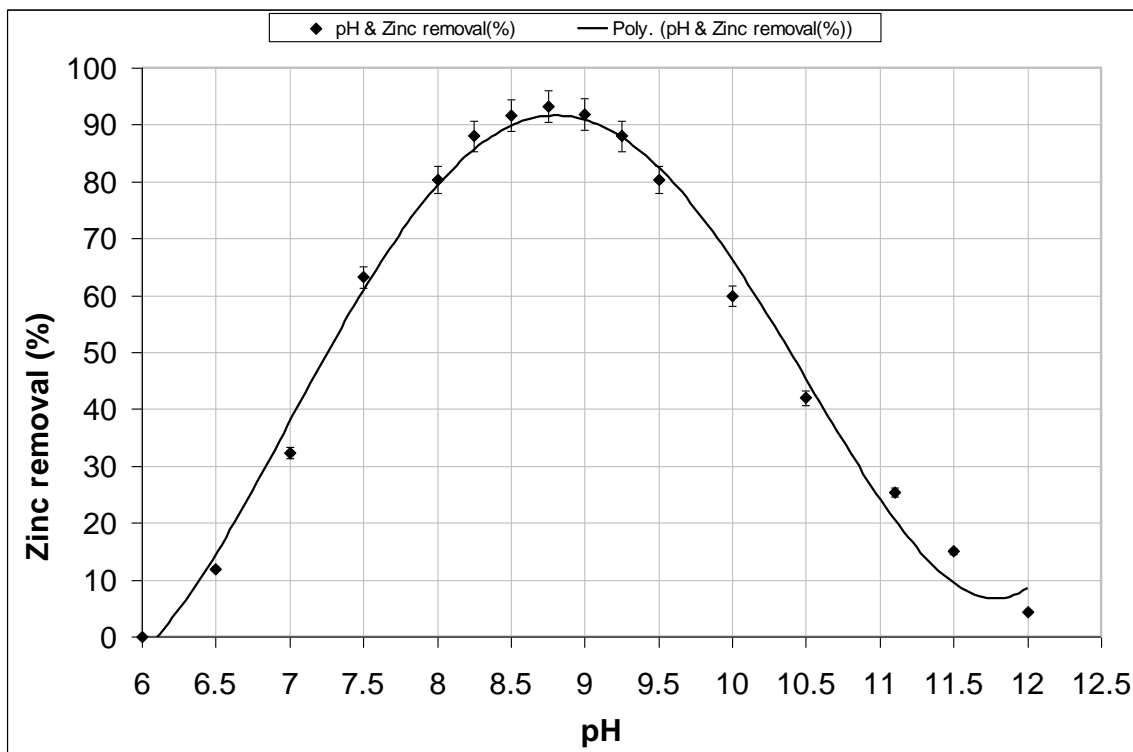


Figure 5.1- Effect of Precipitation pH on zinc ions removal. (Initial [Zn]=50 ppm, filtered samples)

Similarly, for the nickel solution pH was also adjusted between 7.0-12.0 with 0.5 increments and 0.25 increments around the optimum point. The results obtained are plotted in Figure 5.2. As can be seen in Figure 5.2, nickel ions precipitated at the pH range of 9.0-11.0 with 10.2 being the optimum point at which 93% of nickel removed. The optimum precipitation pH for nickel of 10.2 was then used for other experiments thereafter. The experimental optimum pH of 10.2 is slightly higher than the theoretical value of 9.8 based on the solubility of nickel at varied pH values as shown in Figure 2.1. It can be seen that optimum precipitation pH for nickel is higher than optimum pH for zinc. The optimum pH calculation is shown in Appendix D.

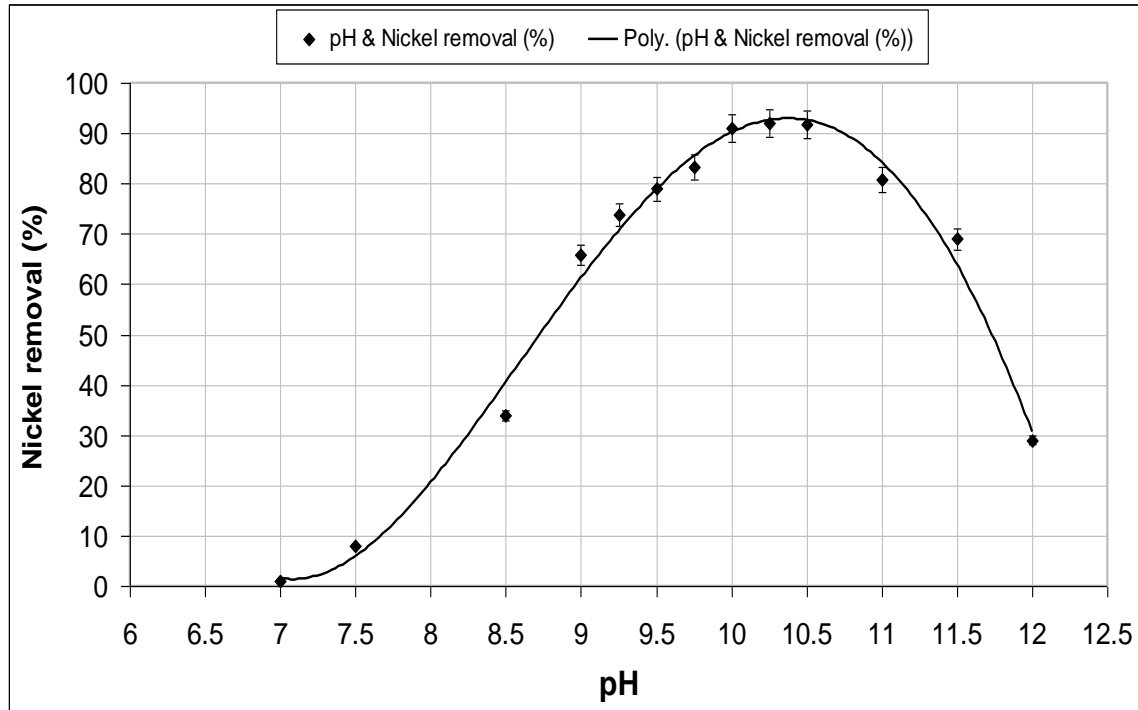


Figure 5.2- Effect of precipitation pH of on the nickel ions removal. (initial [Ni]=50 ppm, filtered samples)

5.2 Coagulant Type and Optimum Dose

Aluminum sulfate, ferrous sulfate and ferric chloride were used as coagulants in the present study. The coagulants dose was varied from 0.0 to 50.0 mg/l. The results of the percentage zinc removal with different coagulants are presented in Figure 5.3. Ferric chloride was found to be advanced to the other coagulants, since it increased the zinc ions removal from 80% to 95% at dose of 30 mg/l while aluminum sulfate and ferrous sulfate increased the zinc removal up to 92% and 88%, respectively, at the same dose.

Zinc ions removal did not increased significantly with ferric chloride dose over 30mg/l. The addition of more coagulant would not improve the settling of suspended zinc particles. In fact, it might lead to re-stabilization by charge reversal of metal particles (Strnadova and Schejbal, 1997; Patoczka, 1998). From these results, the optimum dose of ferric chloride was determined to be 30mg/l, when the corresponding pH was 8.7. Sulfate and chloride ions associate weakly with aluminum and ferric, since they are readily replaced by hydroxyl ions (Bratby, 2006). This explains the slight depression in the solution pH. Coagulation with ferric chloride dose of 30mg/l caused only a slight

decrease in the pH of the solution (0.5 pH unit maximum), which would not be detrimental to downstream processes. Both ferric chloride and aluminum sulfate increased the zinc removal significantly at 30mg/l dose. However, ferric chloride was more effective than aluminum sulfate since ferric flocs are heavier than aluminum flocs, hence, they would settle faster. Ferrous sulfate showed no significant increase in the zinc removal even at higher dose because ferrous salts are divalent ions that have less relative coagulating "power" as cations than trivalent ions such as ferric and aluminum salts (US Army Corps of Engineers, 2001).

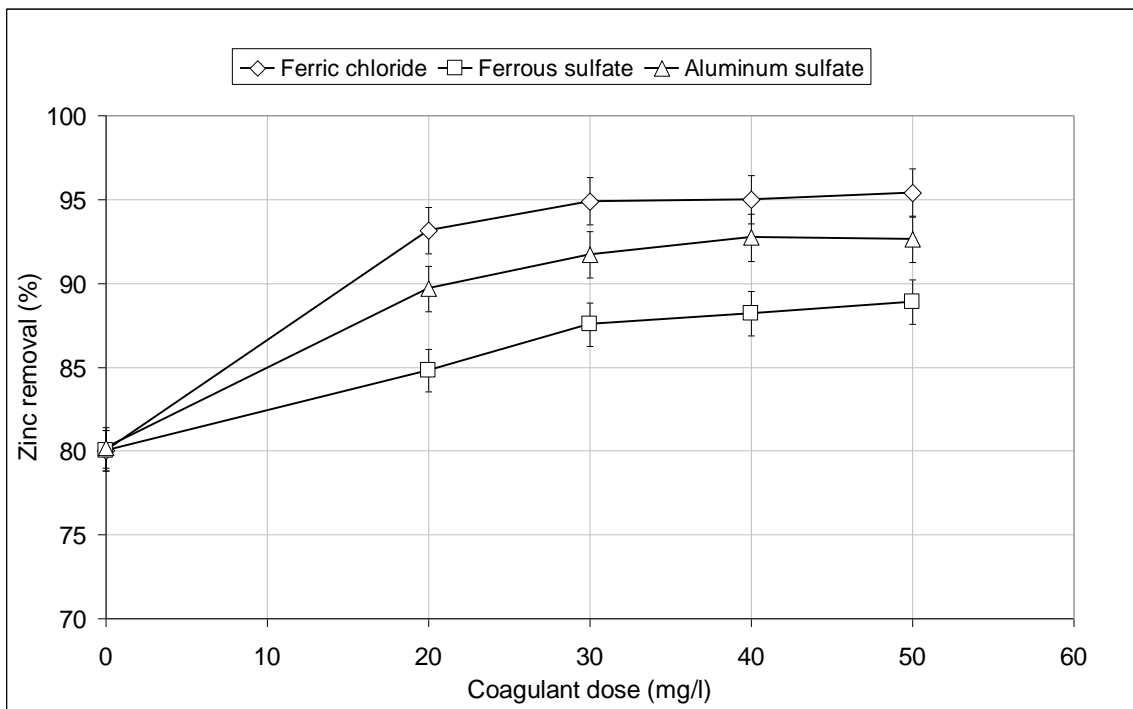


Figure 5.3- Zinc removal percentage with ferric chloride, aluminum sulfate and ferrous sulfate, coagulants doses in mg/l. (initial [Zn]= 50 ppm, pH 8.7, rapid mixing for 120 s @ 150 rpm, 0.5 ml/l flocculant, slow mixing 15 min @ 50 rpm, settling time 30min)

Similarly, the effect of the coagulant dose on the nickel removal was also investigated. The results presented in Figure 5.4 show that ferric chloride and aluminum sulfate enhanced the nickel removal at similar level, since they increased the removal of nickel ions from 76% to 89.8% and 88% respectively, at dose of 30 mg/l. For ferrous sulfate at the same dose the nickel removal only increased to 83%. Nickel ions removal did not

increased significantly for ferric chloride and aluminum sulfate dose over 30mg/l. The optimum dose of ferric chloride was thus considered to be 30mg/l. Both ferric chloride and aluminum sulfate increased the nickel removal significantly at 30mg/l dose. However, ferric chloride is slightly more effective than aluminum sulfate because ferric agglomerate is heavier than that with aluminum (US Army Corps of Engineers, 2001). Ferrous sulfate results show no significant increased in nickel removal even at doses higher than 30mg/l.

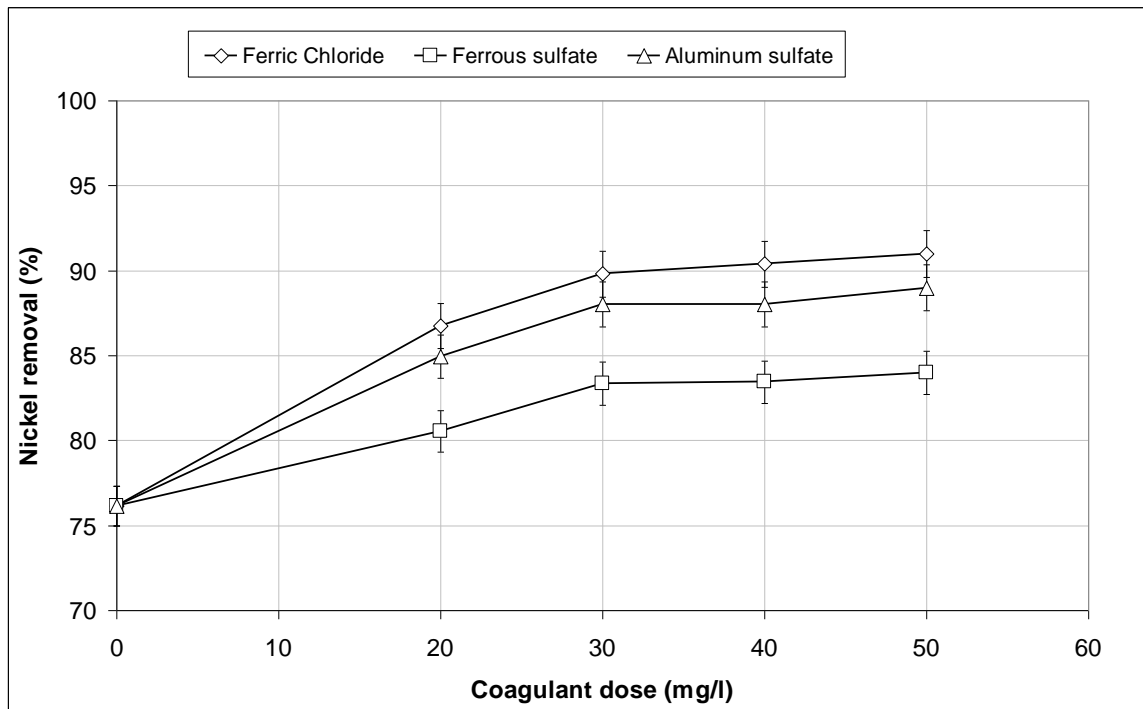


Figure 5.4- Nickel removal percentage with ferric chloride, aluminum sulfate and ferrous sulfate, with different coagulants doses.(initial [Ni]= 50 ppm, pH 10.2, rapid mixing for 120 s @ 150 rpm, 0.5 ml/l flocculant slow mixing 15 min @ 50 rpm, settling time 30 min)

The particle analysis for zinc precipitate using the three types of coagulants was also carried out. Particle size distributions obtained are presented in Figures 5.5, 5.6, and 5.7. With ferric chloride at a dose of 30 mg/l the particle size was larger than that with aluminum sulfate. Larger particle size improves the settling of the particles and thus reducing the settling time and increase metal removal. Particle size analysis results match with zinc concentration analysis in that ferric chloride is a proper choice as a coagulant for zinc removal from wastewater. Ferric chloride neutralizes the negative charge that

zinc precipitate particle hold due its strong relative coagulating power as trivalent ions (US Army Corps of Engineers, 2001). Ferric chloride particle size analysis results, in comparison with ferrous sulfate, show larger particle size for all coagulants doses that were used. Aluminum sulfate particle size analysis results show smaller particle size distribution than other coagulants. Therefore, the settling time of the particles would be longer.

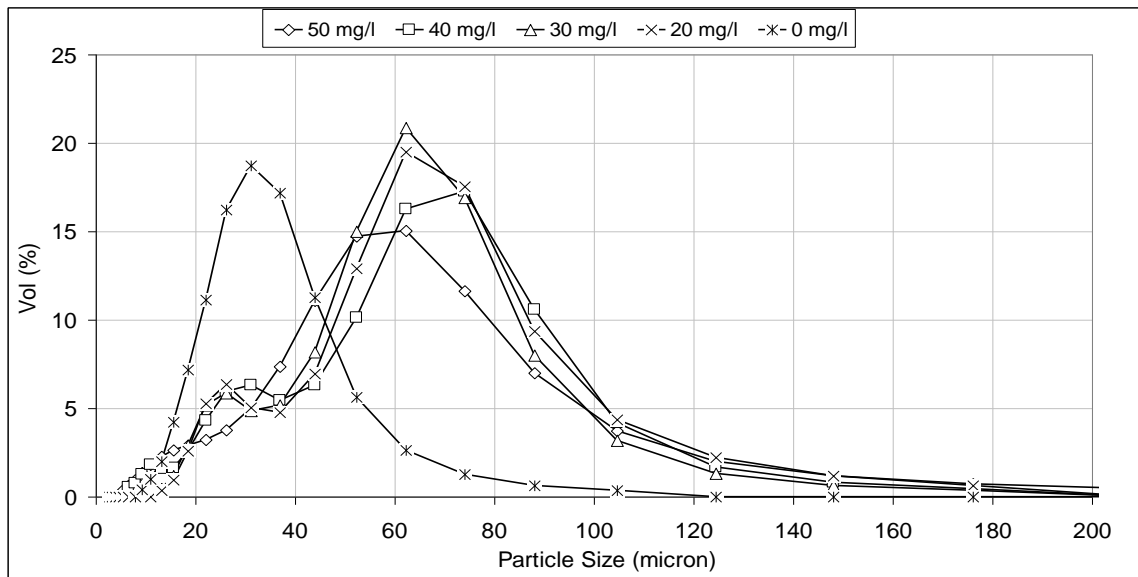


Figure 5.5- Particle size distribution for zinc using ferric chloride coagulant at different doses. (initial [Zn]=50 ppm, pH 8.7, rapid mixing for 120 s @ 150 rpm, 0.5 ml/l flocculant slow mixing 15 min @ 50 rpm)

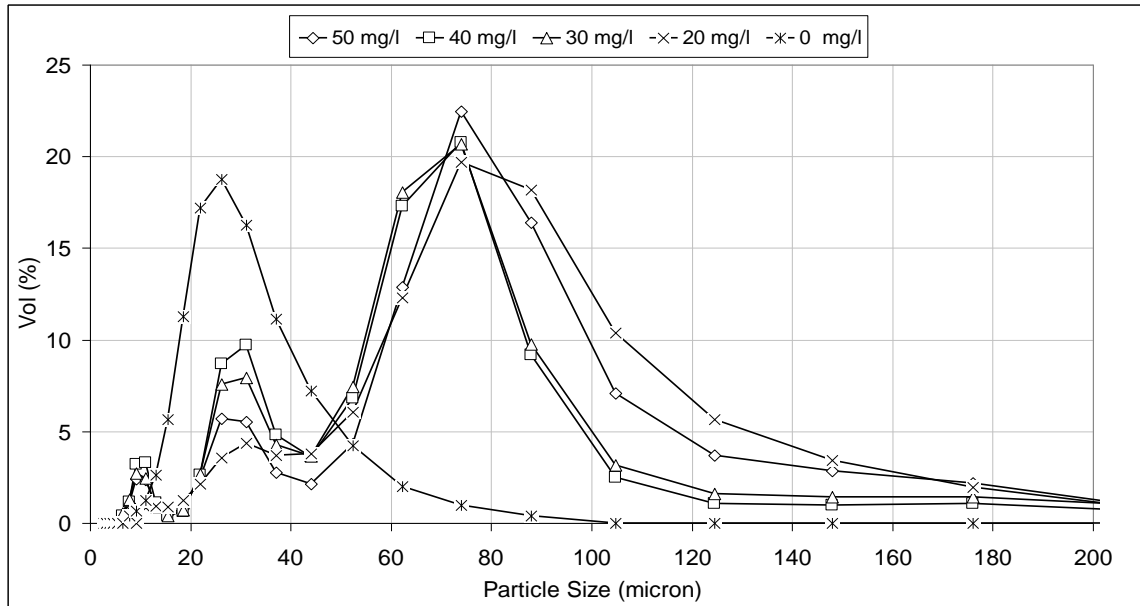


Figure 5.6- Particle size distribution for zinc using ferrous sulfate coagulant at different doses. (initial [Zn]=50 ppm pH 8.7, rapid mixing for 120 s @ 150 rpm, 0.5 ml/l flocculant, slow mixing 15 min@ 50 rpm)

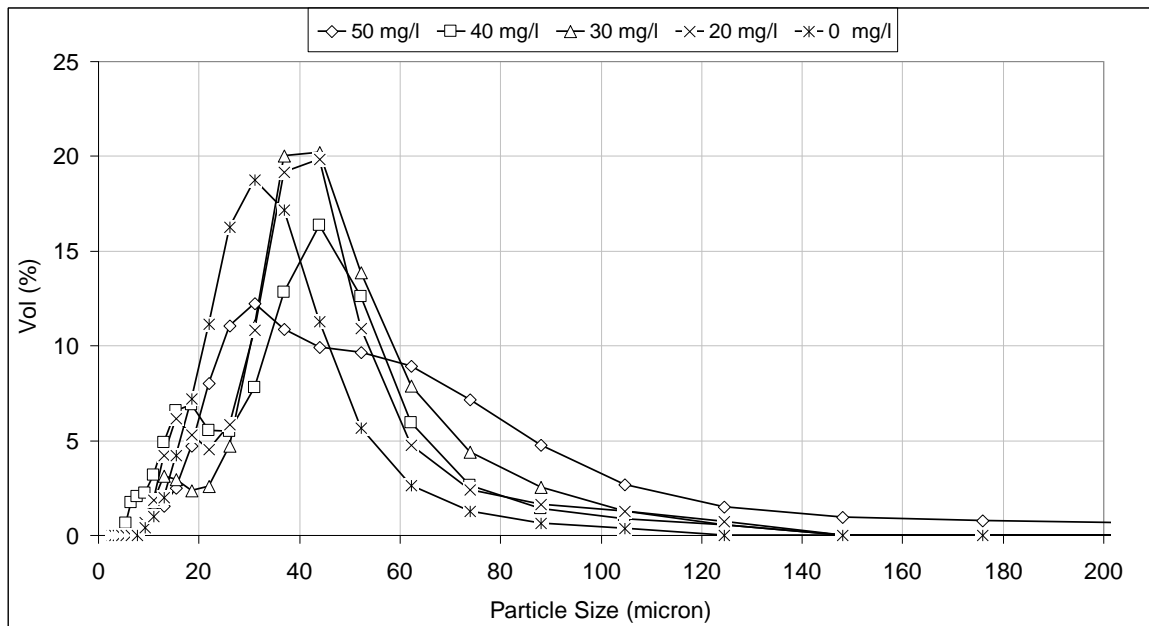


Figure 5.7- Particle size distribution for zinc using aluminum sulfate coagulant at different doses. (initial [Zn]=50 ppm, pH 8.7, rapid mixing for 120 s @ 150 rpm, 0.5 ml/l flocculant slow mixing 15 min@ 50 rpm)

For a comparison, particle size distribution for the three coagulants used at 30mg/l was plotted in Figure 5.8. It was noticed that the total particle size distribution, in terms of

volume percentage, for ferric chloride, compared with ferrous sulfate and aluminum sulfate, was highest at about 60.7% in the particle size range from 52-88 μm while ferrous sulfate, aluminum sulfate, and no coagulant yielded total particle size distribution of about 55.9%, 28.6%, and 10.2%, respectively. On the other hand, small particle size in the range of 6-11 μm for ferrous sulfate was at about 7% while it was 0% for ferric chloride. This can explain why ferrous sulfate yielded lower zinc removal percentage than ferric chloride at the same dose because small particle (less than 10 μm) still suspended in the solution even after 30 min settling. Total particle size calculation is shown in Table C.1, Appendix C.

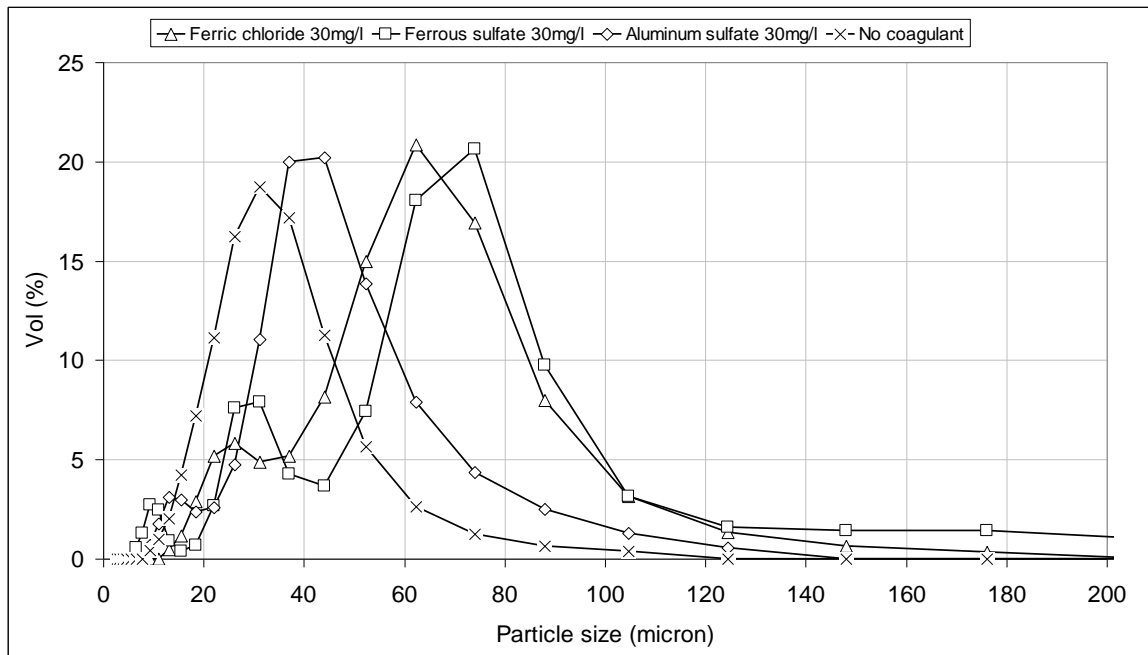


Figure 5.8- Particle size distribution for zinc using ferric chloride, ferrous sulfate, and aluminum sulfate at 30 mg/l dosage and no coagulant. (initial [Zn]= 50 ppm, pH 8.7, rapid mixing for 120 s @ 150 rpm, 0.5ml/l flocculant, slow mixing 15 min @ 50 rpm)

Particle size analysis for nickel ions removal using the three types of coagulants was also performed. The results presented in Figures 5.9, 5.10, and 5.11 show that ferric chloride formed nickel flocs at a dose of 30 mg/l were larger than those for other coagulants. Particle size analysis results agree with the metal concentration analysis in that ferric chloride is best choice as a coagulant for the nickel removal from wastewater. Ferric

chloride particle analysis results in comparison with ferrous sulfate show larger particle size for all coagulants doses that have been used. Aluminum sulfate particle size analysis results show smaller particle size distribution than ferric chloride. For a comparison, particle size distribution for the three coagulants used at 30mg/l was plotted in Figure 5.12. It was noticed that the total particle size distribution for ferric chloride, compared with ferrous sulfate and aluminum sulfate, was highest at about 62.6% in the particle size range from 13-37 μm , while ferrous sulfate, aluminum sulfate, and no coagulant gave the total particle size of about 32.2%, 58.3%, and 11.3%, respectively. On the other hand, total particle size distribution for particle less than 10 μm was 17% for ferric chloride compare to 45%, 19% and 79% for ferrous sulfate, aluminum sulfate and no coagulant, respectively. Total particle size calculation is shown in Table C.2, Appendix C.

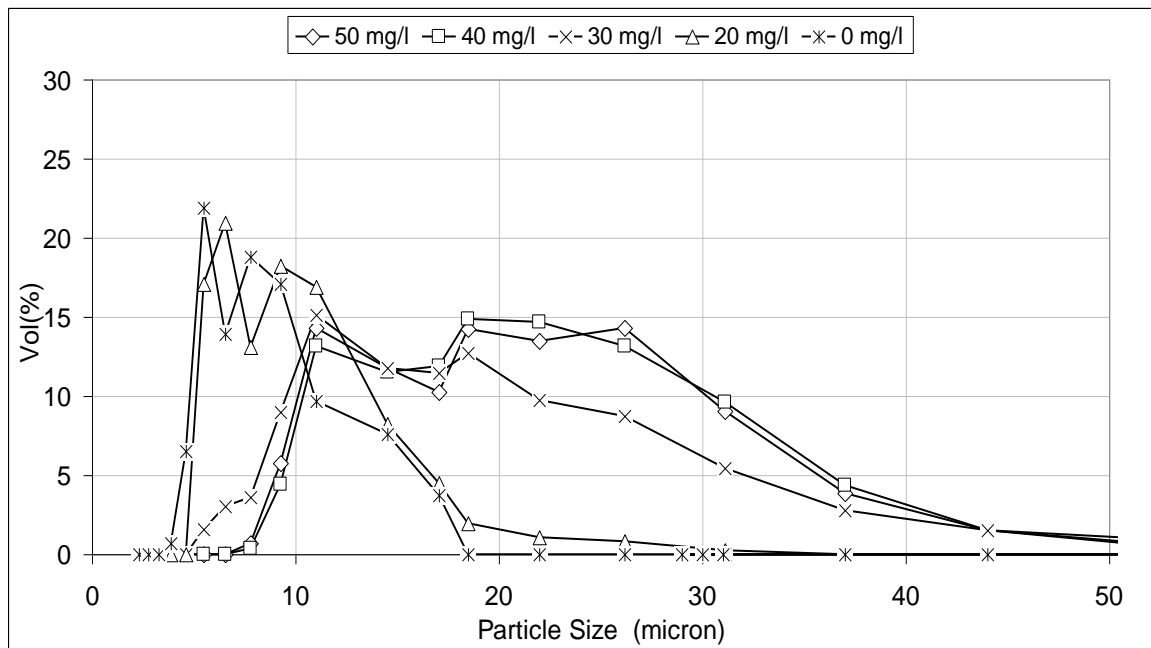


Figure 5.9- Particle size distribution for nickel using ferric chloride coagulant at different doses. (initial [Ni]=50 ppm, pH 10.2, rapid mixing for 120 s @ 150 rpm, 0.5 ml/l flocculant, slow mixing 15 min @ 50 rpm)

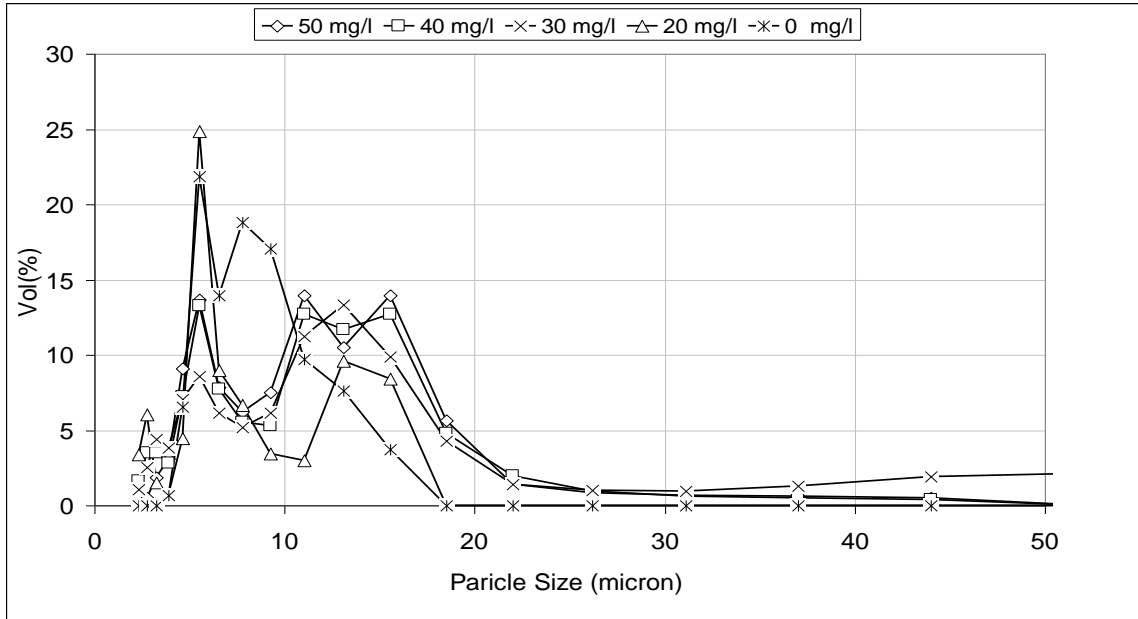


Figure 5.10- Particle size distribution for nickel using ferrous sulfate coagulant at different doses. (initial [Ni]=50 ppm, pH 10.2, rapid mixing for 120 s@ 150 rpm, 0.5 ml/l flocculant, slow mixing 15 min @ 50 rpm)

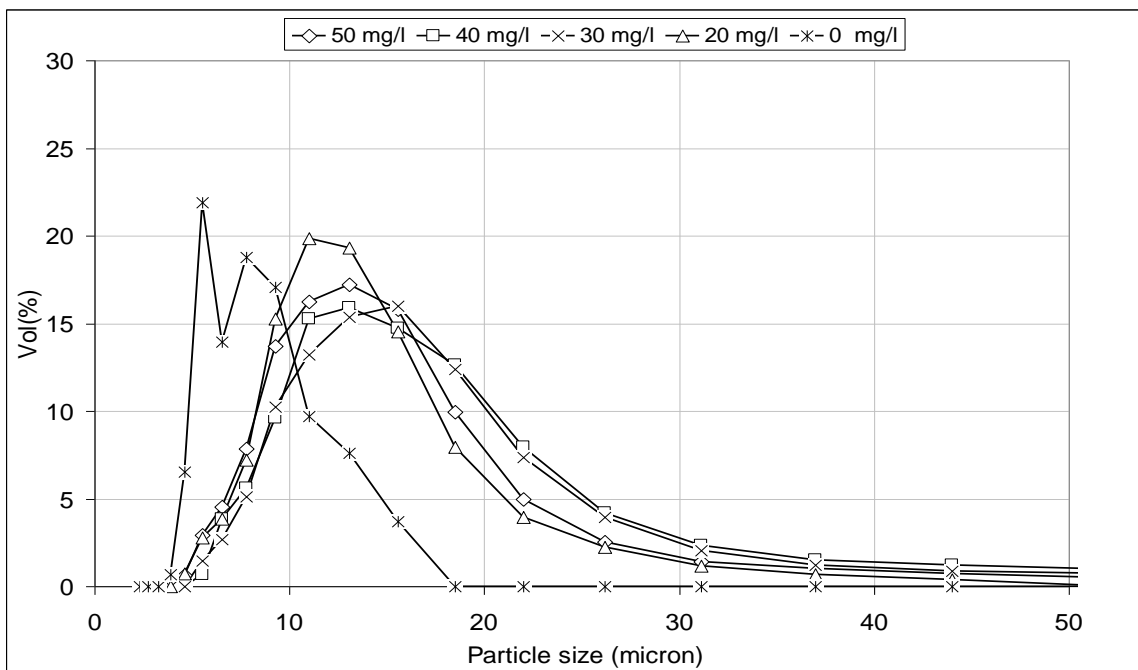


Figure 5.11- Particle size distribution for nickel using aluminum sulfate coagulant at different doses. (initial [Ni]=50 ppm, pH 10.2, rapid mixing for 120 s @ 150 rpm, 0.5ml/l flocculant, slow mixing 15 min @ 50 rpm)

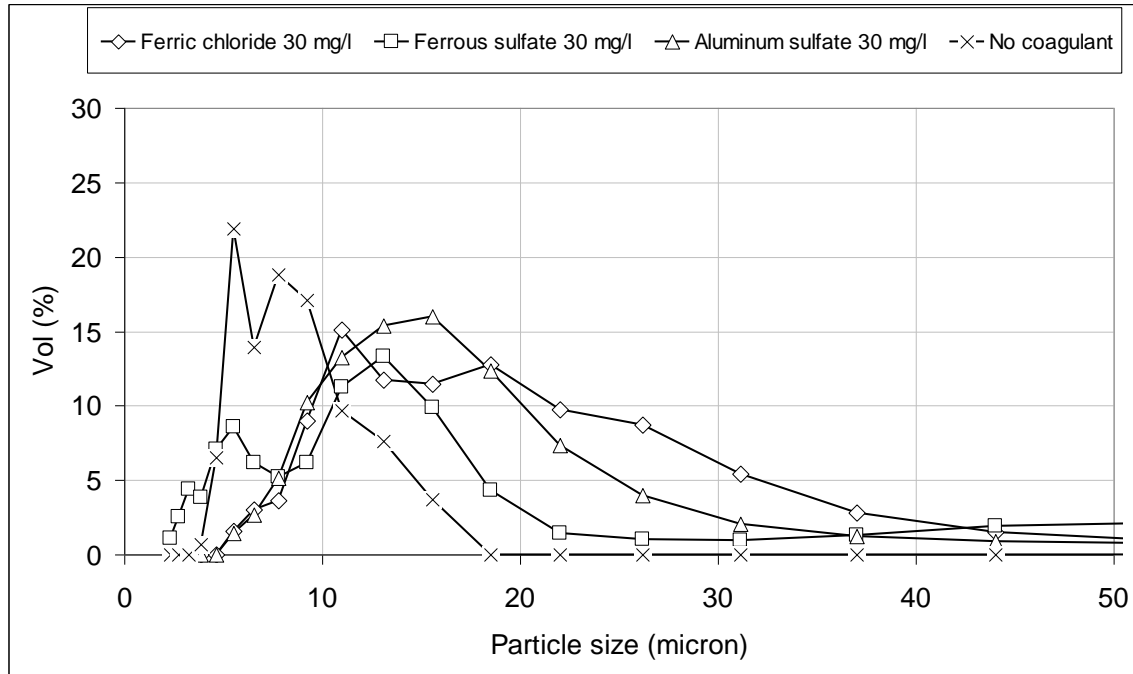


Figure 5.12 - Particle size distribution for nickel using ferric chloride, ferrous sulfate, and aluminum sulfate at 30 mg/l dosage and no coagulant. (initial [Ni]= 50 ppm, pH 10.2, rapid mixing for 120 s @ 150 rpm, 0.5 ml/l flocculant, slow mixing 15 min @ 50 rpm). Table C.2, Appendix C.

In the present study, two different measurements were used to confirm the optimal value of 30 mg/l dose of ferric chloride for both zinc and nickel at optimum pH. Ferric chloride was chosen as coagulant in zinc and nickel removal based on the particle size analysis results since it formed larger flocs than those formed by aluminum sulfate and ferrous sulfate. This is helping in reducing settling time and thus increasing metal removal. In comparison, the present study agreed with the reported literature in that ferric chloride was a proper choice as a coagulant in zinc and nickel removal from wastewater but the optimal dose was close to those used by other researchers (Johnson et al., 2008; American Water Works Association, 1997; Abdul Aziz et al., 2007; Park et al., 2006).

5.3 Settling Time

At the optimum dose of 30 mg/l of the three coagulant used in zinc removals at the pH of 8.7, the final settling time for zinc particles was investigated. The settling time is the time at which metal removal reaches its highest percentage. The results obtained are presented in Figure 5.13. As can be seen in Figure 5.13, settling time with ferric chloride was shorter than with ferrous sulfate and comparable to that with aluminum sulfate.

Ferric chloride reduced the metal removal significantly in the first 2 min of settling of about 61% compared to 10%, 43% and 48% for no coagulant, ferrous sulfate and aluminum sulfate, respectively. When using ferric chloride, it was noticed that more than 80% of zinc particles removed (settled) after 10 min and more 90% after 25 min. Ferric chloride reduced the settling time compared with the control run (no coagulant added) from 24 to 10 min at a similar metal removal of 82.6%. Zinc removal percentage after 30 min settling shows insignificant increase in maximum of 2% which is within the errors value. The final settling time for zinc particles was then set as 30 min for the next set of the experiments.

Similarly, settling time for nickel particles results are presented in Figure 5.14. It can be noticed that more than 80% of nickel particles settled after 20min and more than 90% after 30 min. Ferric chloride shows shorter settling time than other coagulants. Comparing with control run (no coagulant added), ferric chloride reduced the settling time from 30min to 12min for the same removal of 85%. In the present study, it was found that ferric chloride enhanced precipitate settling more than aluminum sulfate and ferrous sulfate for zinc removal. Settling time of 30 min is close to those used by other researchers (Johnson et al., 2008; Patoczka et al., 1998; Abdul Aziz et al., 2007). Both ferric chloride and aluminum sulfate coagulants, when used with nickel, showed shorter settling time of 30min than ferrous sulfate.

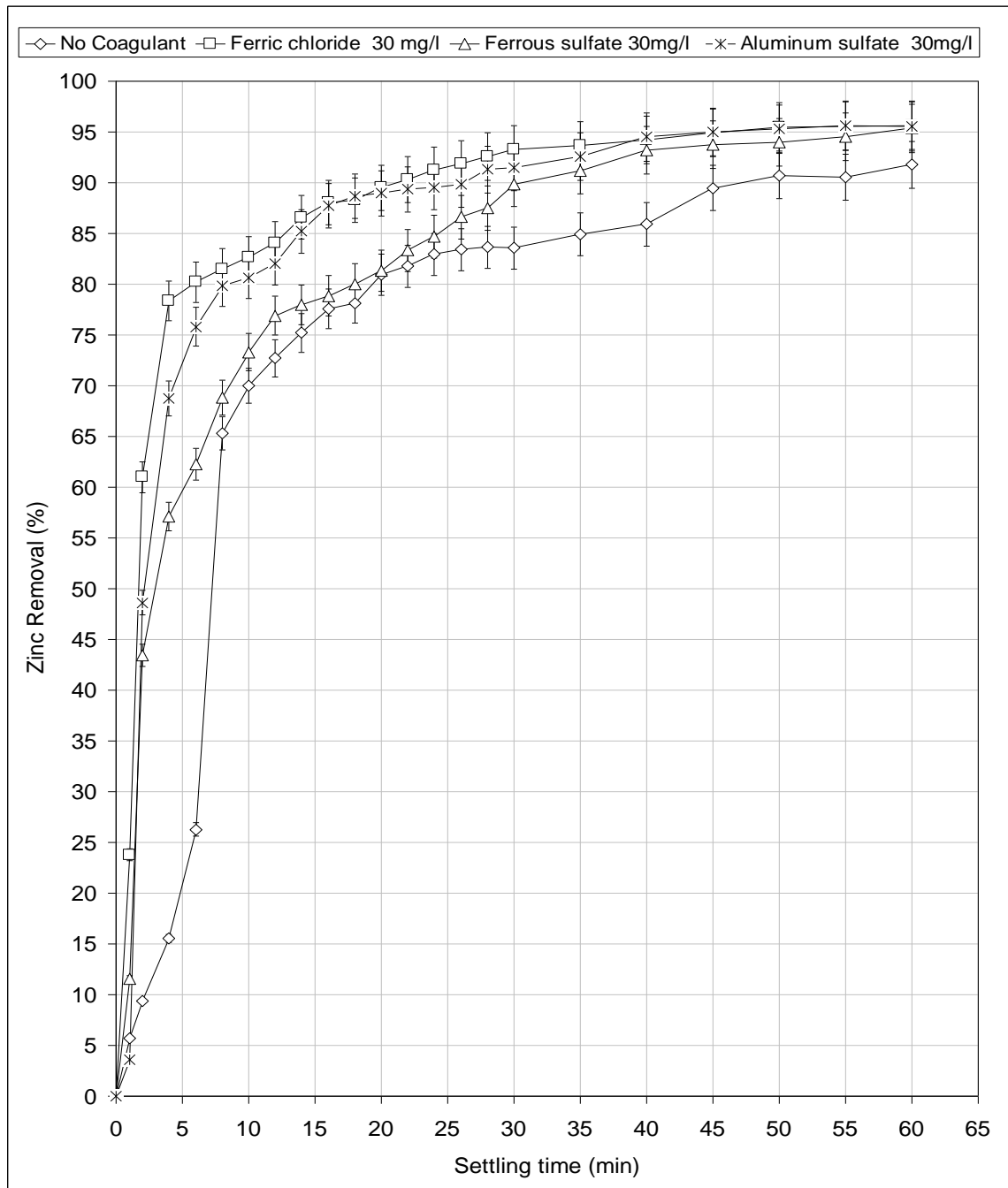


Figure 5.13- Zinc removal percentage verses settling time using ferric chloride, ferrous sulfate, and aluminum sulfate at 30mg/l dose, no coagulant added as control. (initial [Zn]= 50 ppm, pH 8.7, rapid mixing for 120 s @ 150 rpm, 0.5 ml/l flocculant slow mixing 15 min @ 50 rpm).

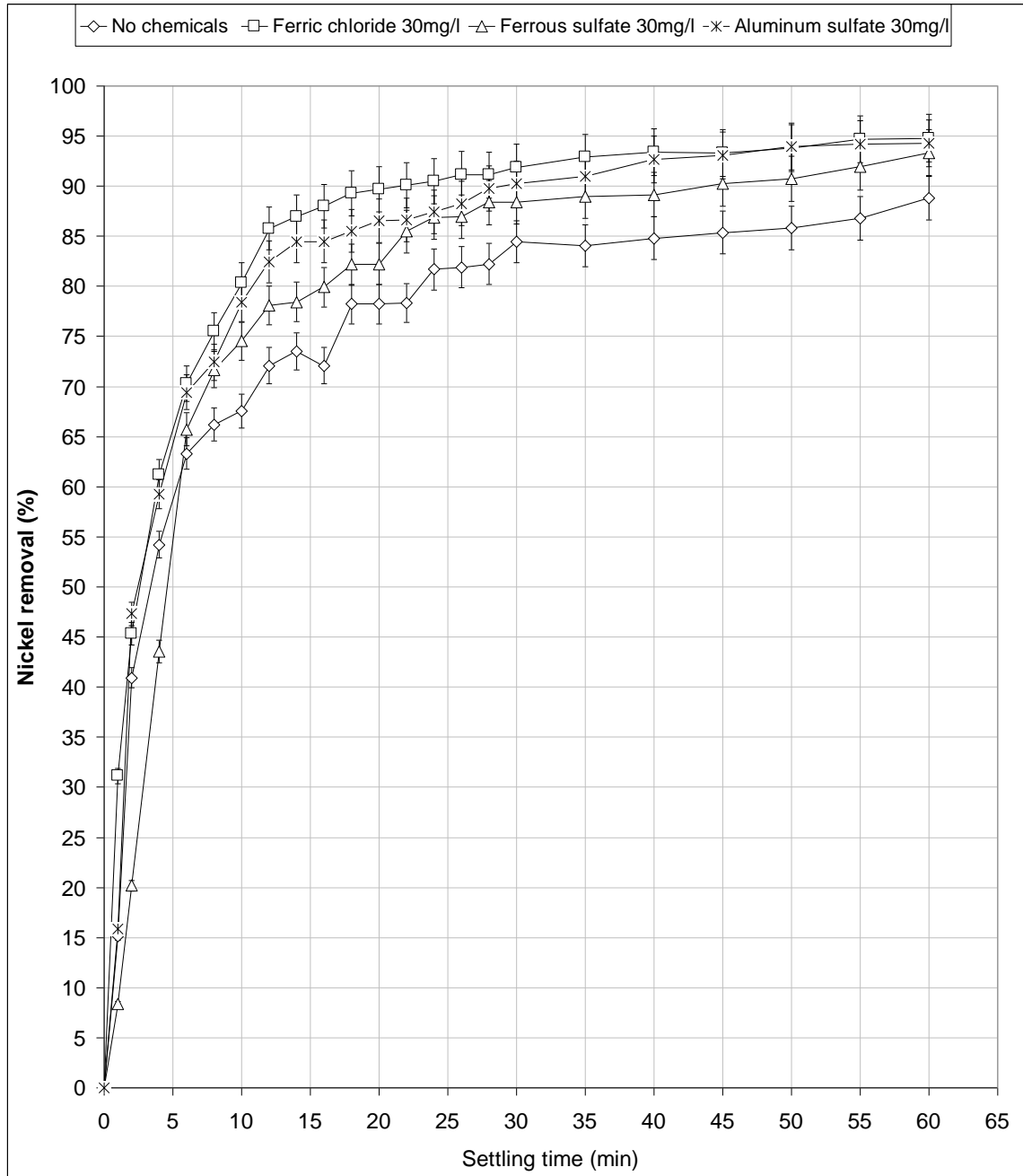


Figure 5.14 Nickel particles removal percentage versus settling time using ferric chloride, ferrous sulfate, and aluminum sulfate at 30 mg/l dose, no coagulant added as control. (initial [Ni]= 50 ppm, pH 10.2, rapid mixing for 120 s @ 150 rpm, 0.5 ml/l flocculant slow mixing 15 min @ 50 rpm).

5.4 Rapid Mixing Speed and Time

Rapid mixing with the paddle speeds of 100, 200, 300 and 400 rpm was tested using mixing times of 30, 60, 90, and 120 s. Ferric chloride was used as coagulant at 30 mg/l and the settling time was set at 30 min. The results obtained are presented in Figures 5.15, 5.16, 5.17 and 5.18. Rapid mixing with the impeller speed of 100 rpm for 60s gave the highest zinc removal of about 98.9%. The higher the mixing speeds, the more coagulant dispersed in the whole fluid bulk. Dispersion must be rapid because ferric hydrolysis products able to adsorb on the surface of the colloidal particles are produced within a second. Increasing the mixing velocity raises the adsorption-destabilization of the particles and thus the floc formation and sedimentation are enhanced, resulting in higher metal removal.

Figure 5.15 presents the results for 30 s rapid mixing time. It was noticed that the highest metal removal are achieved at 100 rpm. Also, floc size was higher at this mixing speed as it is shown later in particle size analysis. When the speed was increased to 200 rpm or higher the floc breakage exceeded the floc formation. Zinc removal for 100, 200, 300 and 400 rpm at settling time of 30 min and 30 s rapid mixing were 93.2%, 91.5%, 87.7% and 80.2%, respectively. This indicates that the more mixing intensity the less metal removal due to floc breakage. Therefore, 100 rpm mixing speed is considered to be the optimum impeller speed at this stage.

Figure 5.16 shows that 100 rpm speed achieved the highest metal removal as well. Comparing the results in Figures 5.15 and 5.16 for 100 rpm speed, mixing for 30 s was insufficient and the coagulant might not be evenly dispersed into the fluid. As can be seen in Figure 5.16 the zinc removal increased from 93.2% to 98.9% by increasing the mixing time from 30 to 60 s at the same speed of 100 rpm and settling time of 30 min. It can also be noticed that after 5 min settling, zinc removal percentage increased from 75% to 80% at 100 rpm. The coagulant had enough time to disperse into fluid bulk and aggregates the microflocs into larger ones for the case with 60 s mixing.

Figure 5.17 and 5.18 presents the results for the cases with 90 and 120 s rapid mixing times. It was noticed that increasing the mixing time to 90 and 120 s lowers the zinc removal to 95.1% and 91.8%, respectively, at the same mixing impeller speed of 100 rpm and 30 min settling. It was also noticed that after 5 min settling the zinc removal decreased from 80% to 65% for 100 rpm mixing. This might be due to the breakage of the large flocs into microflocs under prolonged mixing periods. The mixing duration of 60 s can be set as the optimum mixing time at 100 rpm speed.

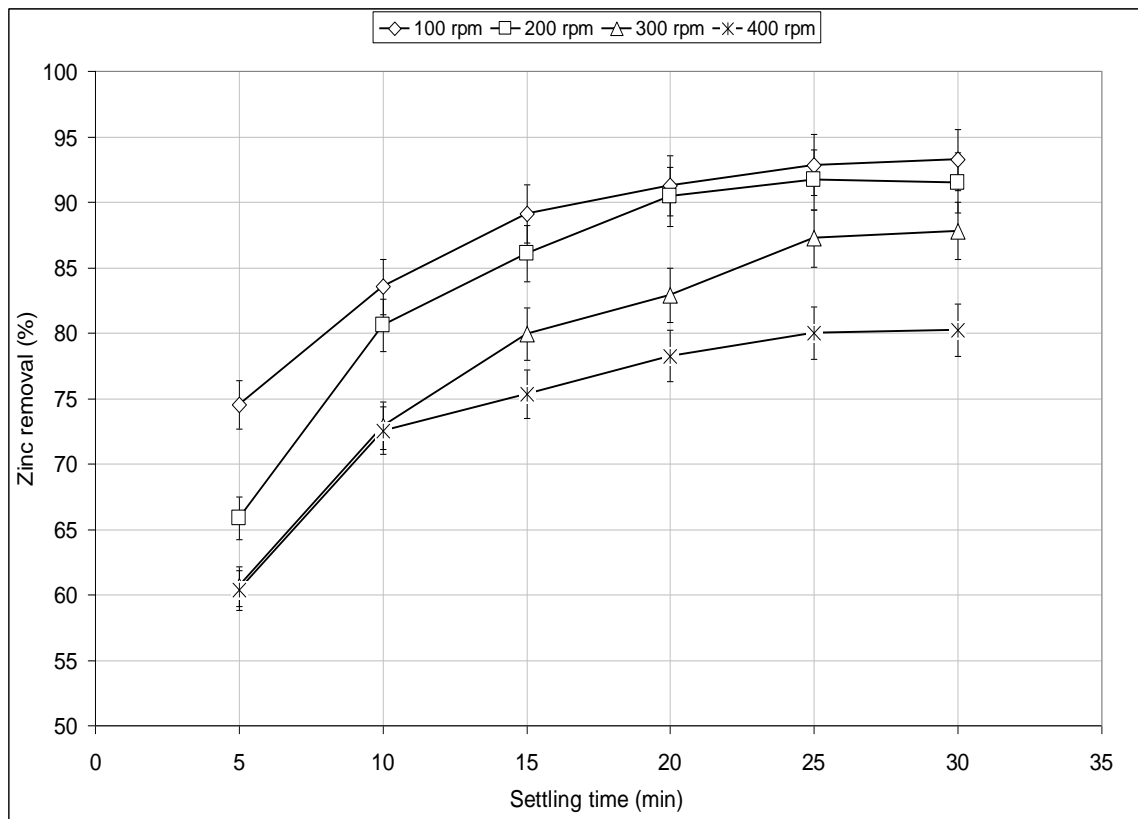


Figure 5.15- Zinc removal vs. settling time for 30 s rapid mixing. (initial [Zn]= 50ppm, pH 8.7, 30 mg/l ferric chloride coagulant, rapid mixing for 30 s @ 100, 200, 300, 400 rpm, 0.5 ml/l flocculant, slow mixing 15 min @ 50 rpm, settling time 30 min)

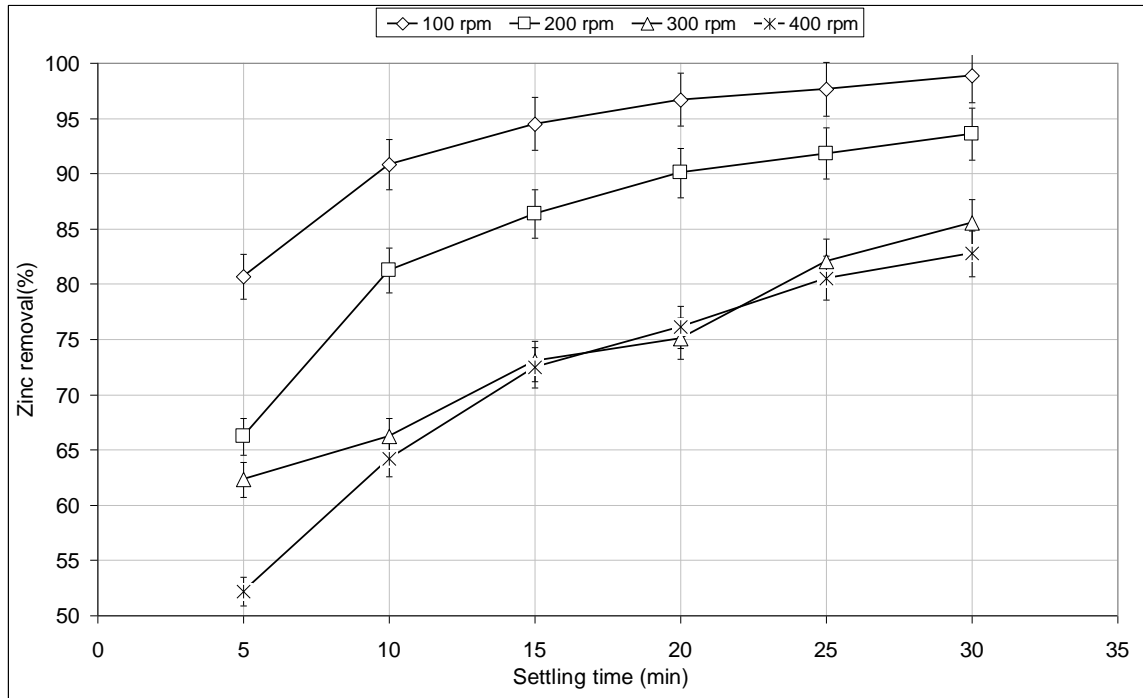


Figure 5.16- Zinc removal vs. settling time for 60 s rapid mixing. (initial [Zn]= 50ppm, pH 8.7, 30 mg/l ferric chloride coagulant, rapid mixing for 60 s @ 100, 200, 300, 400 rpm, 0.5 ml/l flocculant, slow mixing 15 min @ 50 rpm, settling time 30 min)

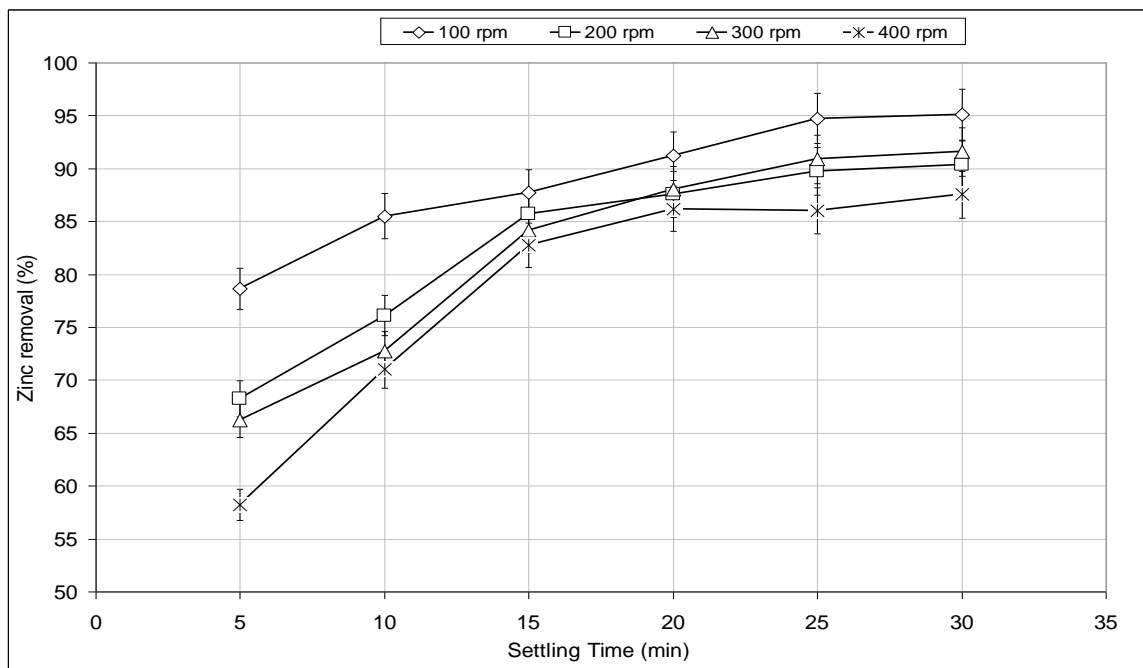


Figure 5.17- Zinc removal vs. settling time for 90 s rapid mixing. (initial [Zn]= 50 ppm, pH 8.7, 30 mg/l ferric chloride coagulant, rapid mixing for 90 s @ 100, 200, 300, 400 rpm, 0.5 ml/l flocculant, slow mixing 15 min @ 50 rpm, settling time 30 min)

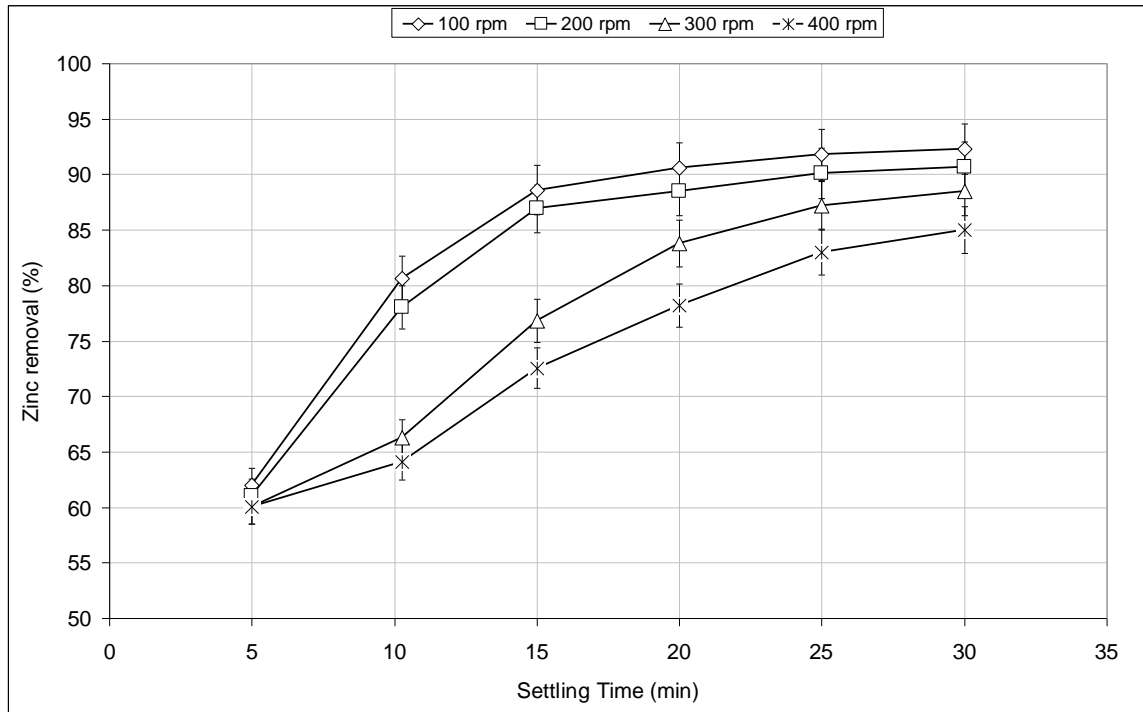


Figure 5.18- Zinc removal vs. settling time for 120 s rapid mixing. (initial [Zn]= 50 ppm, pH 8.7, 30 mg/l ferric chloride coagulant, rapid mixing for 120 s @ 100, 200, 300, 400 rpm, 0.5 ml/l flocculant, slow mixing 15 min @ 50 rpm, settling time 30 min)

From the previous experiments, the mixing time of 60 s was selected to be the optimum mixing time for zinc coagulation. It was also found that the optimum mixing speed appeared to be at 100 rpm. In order to ensure that the optimum speed was actually at 100 rpm, rapid mixing impeller speeds of 60, 80, 100, 120, 140 and 160 rpm were investigated using the optimum mixing time of 60 s. The results presented in Figure 5.19 show that rapid mixing at an impeller speed of 100 rpm and 60 s gave highest zinc removal of about 98.9%.

For the mixing speed of 60 rpm, the coagulant might be dispersed insufficiently into the fluid bulk, resulting in a low metal removal. When the mixing speed was increased to 80 rpm, the metal removal increased significantly. At mixing speed of 100 rpm, the metal removal further increased. However, further increase of the mixing speed beyond 100 rpm, the metal removal decreased due to the breakage of large flocs. It can be seen that settling time was shortened significantly when using optimum mixing speed and time.

More than 90% of zinc particles settled after 10min, comparing with figure 5.13 which shows that it took more than 20 min to settle for the same amount of metal removal.

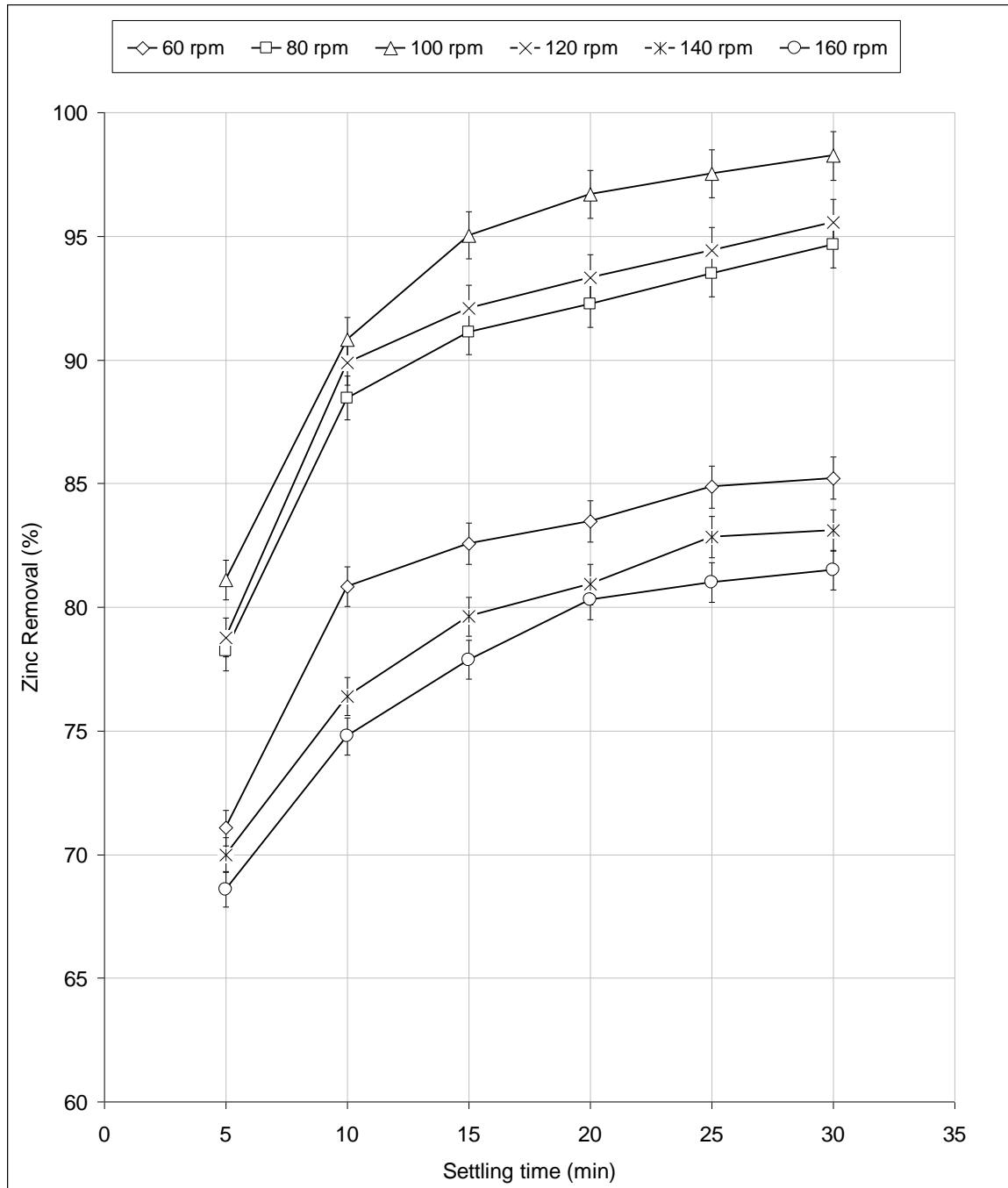


Figure 5.19- Zinc removal % vs. settling time at 60 s rapid mixing. (initial [Zn]= 50 ppm, pH 8.7, 30 mg/l ferric chloride, rapid mixing for 60 s, 0.5 ml/l flocculant, slow mixing 15 min @ 50 rpm, settling time 30 min).

Similarly, for nickel removal, rapid mixing with the paddle speeds of 100, 150, 200 and 250 rpm was tested using mixing times of 30, 60, 90, and 120 s. The rapid mixing speed range was lowered since nickel floc size was smaller than zinc floc as observed in second stage of the experiments. Ferric chloride was used as coagulant at 30mg/l and the settling time was set at 30min. The results obtained are presented in Figures 5.20, 5.21, 5.22, and 5.23. Rapid mixing speed of 100 rpm at 30 s gave the highest nickel removal at about 97.3% at the settling time of 30 min. When the mixing speed increased to 150 rpm or more, the floc might start to break gradually. This explains why the nickel removal decreased to 94.9%, 88% and 82.2% at mixing speed of 150, 200 and 250 rpm, respectively. Settling time was shortened significantly since more than 90% of nickel flocs had been removed after 10 min as shown in Figure 5.20. Comparing the results in Figures 5.21, 5.22 and 5.23, increasing mixing time to 60 s or more might lead to floc breakage and thus reducing the metal removal. As can be seen, nickel removal decreased to 88.5%, 82% and 74% for 60, 90 and 120 s, respectively, at 100 rpm mixing speed.

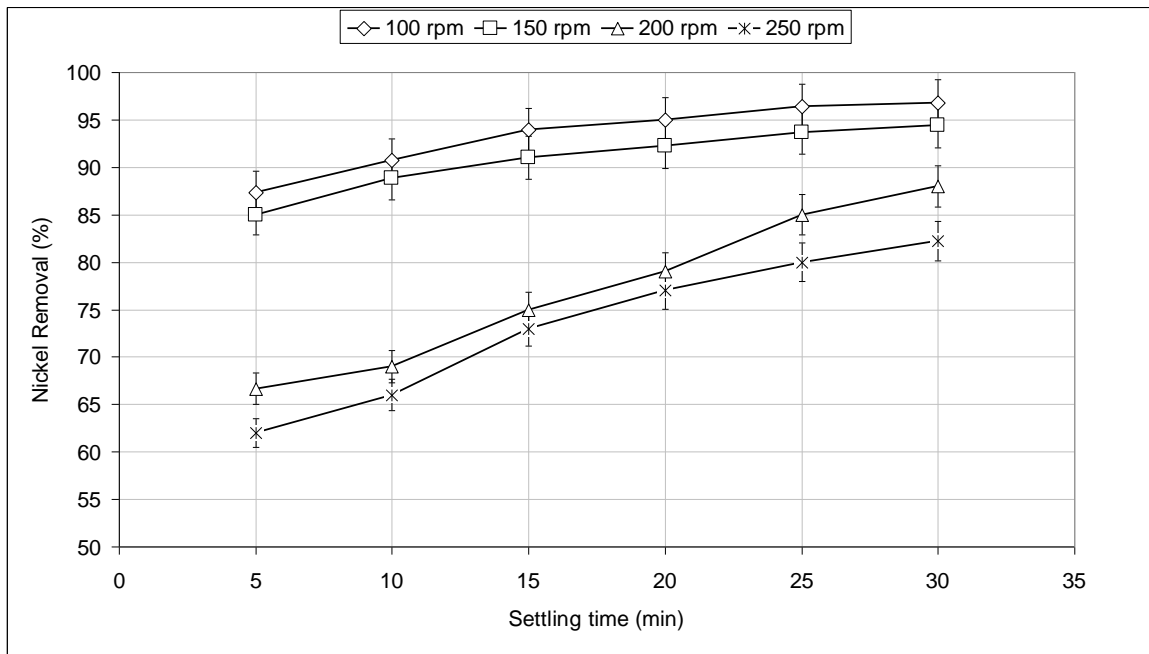


Figure 5.20 - Nickel removal vs. settling time for 30 s rapid mixing. (initial [Ni]= 50 ppm, pH 10.2, 30 mg/l ferric chloride, rapid mixing for 30 s @ 100, 150, 200, 250 rpm, 0.5 ml/l flocculant, slow mixing 15 min @ 50 rpm, settling time 30 min)

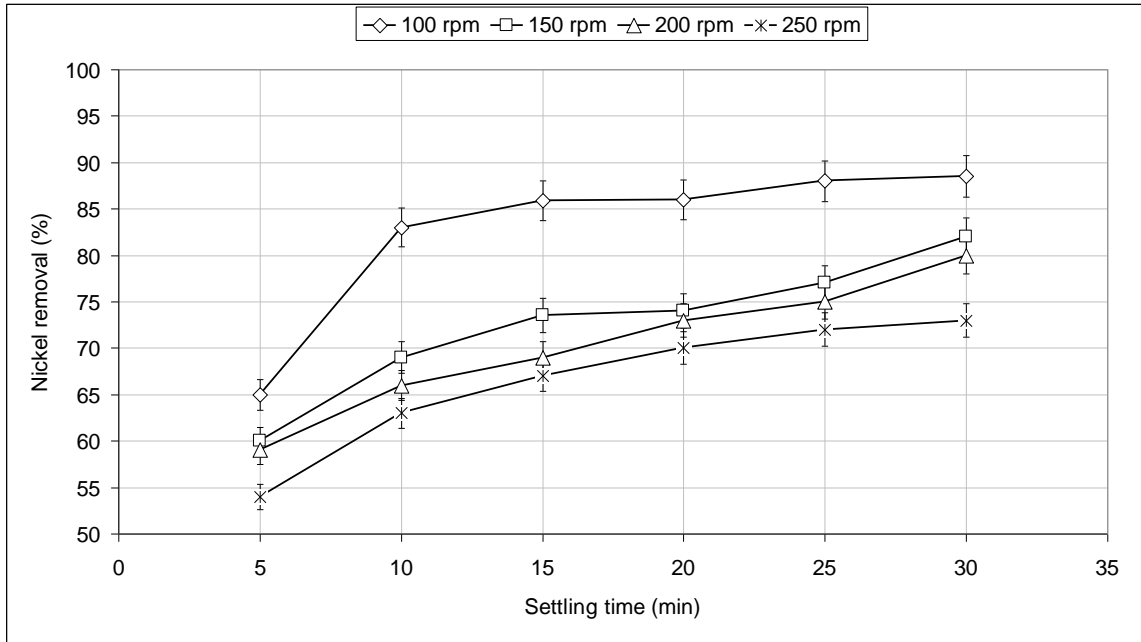


Figure 5.21 - Nickel removal vs. settling time for 60 s rapid mixing. (initial [Ni]= 50ppm, pH 10.2, 30 mg/l ferric chloride, rapid mixing for 60 s @ 100,150,200,250 rpm, 0.5ml/l flocculant, slow mixing 15 min @ 50 rpm, settling time 30 min)

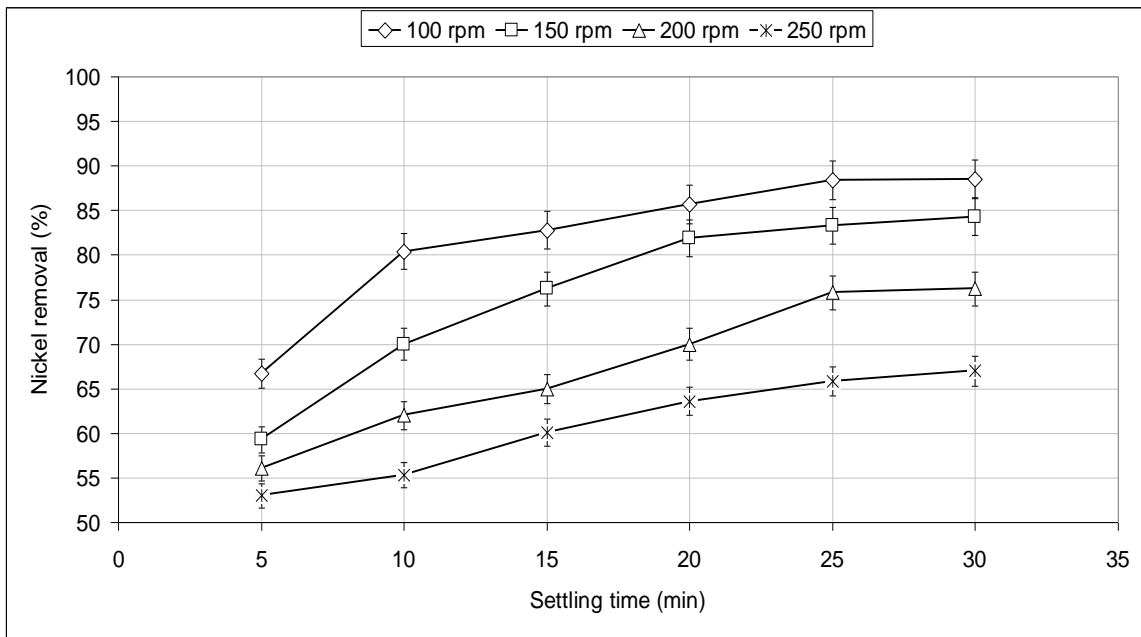


Figure 5.22 - Nickel removal vs. settling time for 90 s rapid mixing. (initial [Ni]= 50ppm, pH 10.2, 30 mg/l ferric chloride, rapid mixing for 90 s @ 100,150,200,250 rpm, 0.5ml/l flocculant, slow mixing 15 min @ 50 rpm, settling time 30 min)

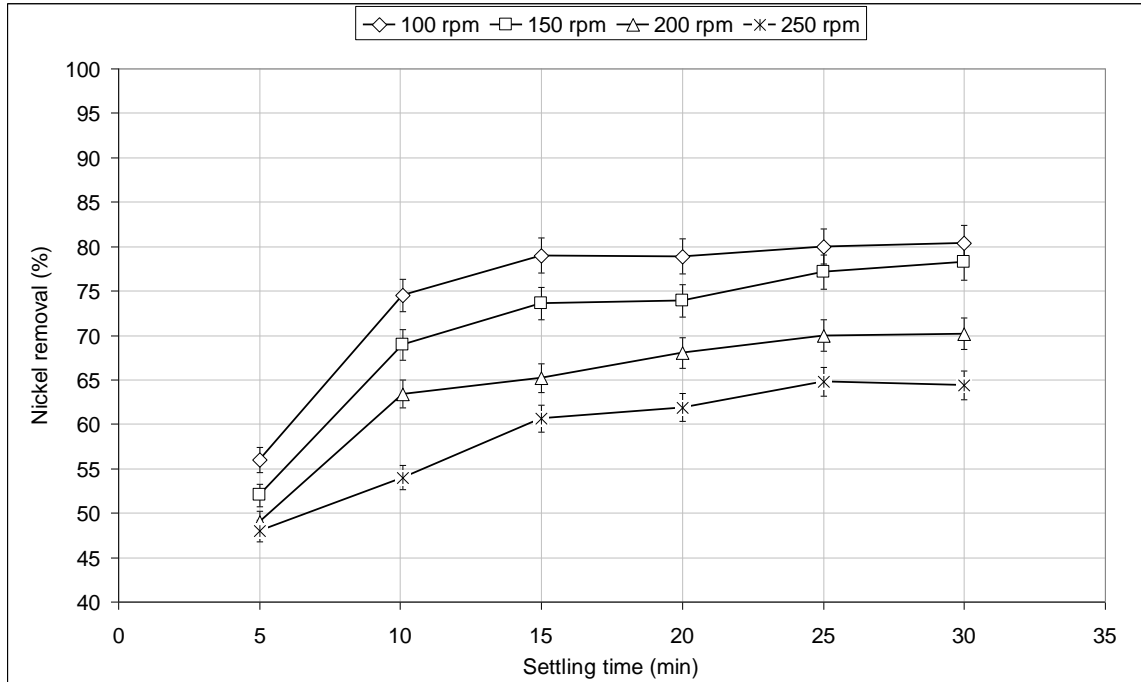


Figure 5.23 - Nickel removal vs. settling time for 120 s rapid mixing. (initial [Ni]= 50ppm, pH 10.2, 30 mg/l ferric chloride, rapid mixing for 120 s @ 100,150,200,250 rpm, 0.5ml/l flocculant, slow mixing 15 min @ 50 rpm, settling time 30 min)

Similarly, for nickel removal, the mixing time of 30 s was selected to be the optimum time. Rapid mixing speeds of 60, 80, 100, 120, 140 and 150 rpm were investigated to find the optimum rapid mixing speed in the region around 100 rpm using the optimum mixing time of 30s. The results presented in Figure 5.24 show that rapid mixing at an impeller speed of 80 rpm and 30 s gave highest nickel removal of about 97.6% after settling for 30min. At 60rpm the nickel removal was 95% then increased to 96.8% at 80 rpm and started to decrease slightly at 100 rpm and gradually for higher speeds than 100 rpm. Mixing speed of 80 and 100 rpm yielded very close nickel removal percentage. Speed of 80 rpm can be considered the optimum mixing speed for nickel removal since it is less power consumption than 100 rpm speed.

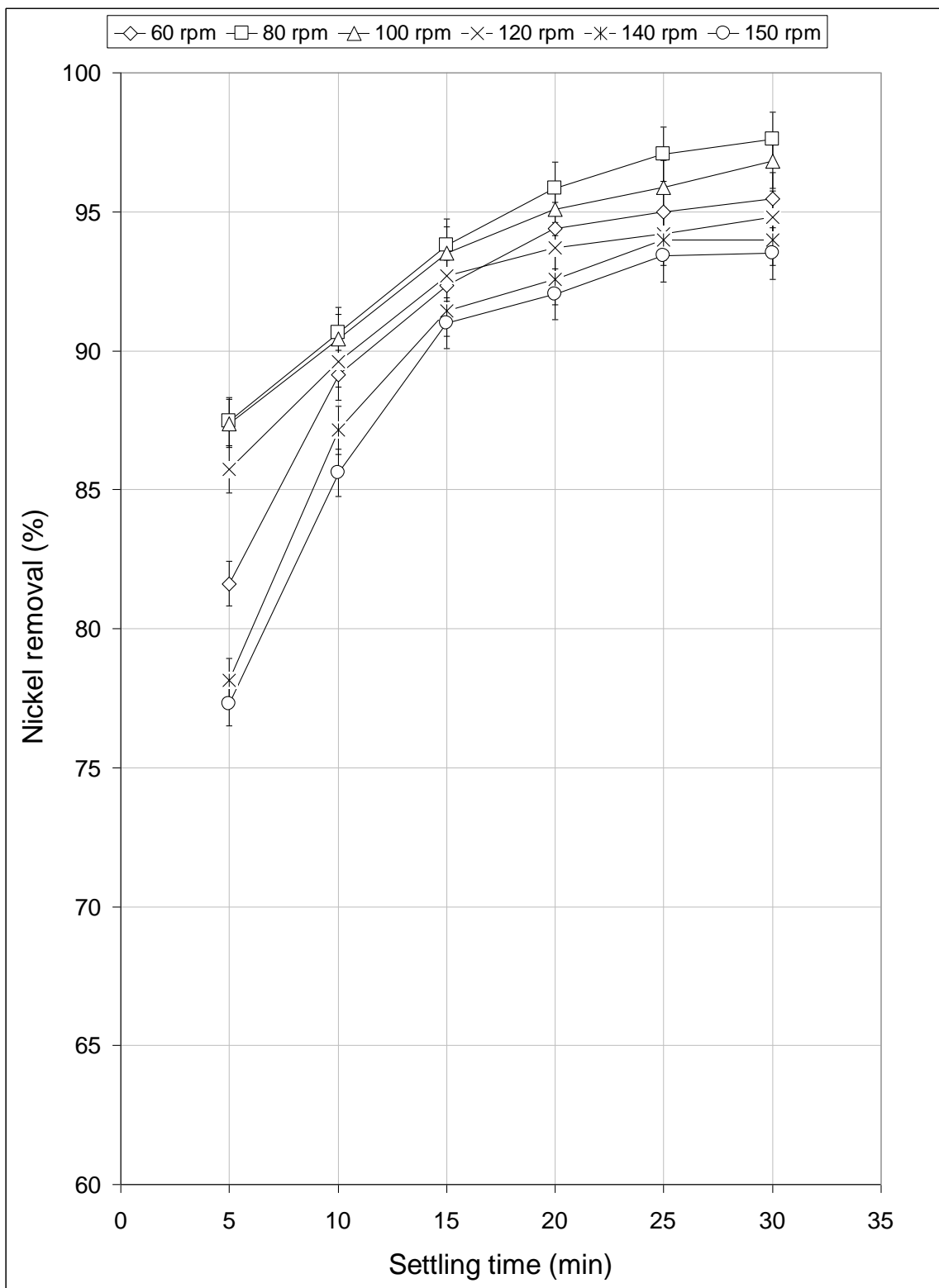


Figure 5.24- Nickel removal % vs. settling time at 30 s rapid mixing time. (initial [Ni]= 50 ppm, pH 10.2, 30 mg/l ferric chloride, rapid mixing for 30 s, 0.5 ml/l flocculant, slow mixing 15 min @ 50 rpm, settling time 30 min).

Particle size analysis for zinc was also carried out. The results presented in Figure 5.25 for the mixing time of 30 s at different mixing speeds show that for particle sizes in the range of 88-176 μm the total particle size distribution was about 22.4% at 100 rpm mixing speed while it was 12%, 6.7% and 1.2% for 200, 300, and 400 rpm, respectively. Details of the total particle size calculation are given in Appendix C. The results indicate that the formation of flocs during rapid mixing phase is greatly influenced by the duration and intensity of mixing. On increasing the mixing speed to 200 rpm, there is an immediate and rapid increase in flocs breakage more than 50%. More flocs breakage occurs with further increases in the mixing speed to 300 and 400 rpm.

The results for mixing time of 60 s are presented in Figure 5.26. For higher mixing time of 60 s, coagulant had enough time to disperse into fluid bulk and adsorb onto metal particles, enhancing agglomeration of flocs. This is reflecting through the increase of particle size distribution to 63.9% in the same range of 88-176 μm at 100 rpm mixing speed. For an additional 30 seconds mixing, the flocs rapidly grew during this time and the surface charge was reversed and then approached neutral, and the floc interior structure was compacted. For other mixing speeds of 200, 300 and 400 rpm the total particle size distribution for the range of 88-176 μm were 21.7%, 4% and 3.6% respectively. This indicates that higher mixing intensity increase the flocs breakage even with an optimum mixing duration.

The results for 90 s rapid mixing are shown in figure 5.27. At 100 rpm the particle size distribution was about 63.3% in the range of 88-176 μm which indicates that rapid mixing up to 90 s could maintain the flocs size similar to those with 60 s mixing time. On the other hand, the results presented in figure 5.28 for mixing time of 120 s shows that the particle size distribution reduced significantly to 6.7% in the same particle size range, indicating that the breakage of large flocs occurred under a longer duration of mixing even though the mixing speed of 100 rpm was at optimum.

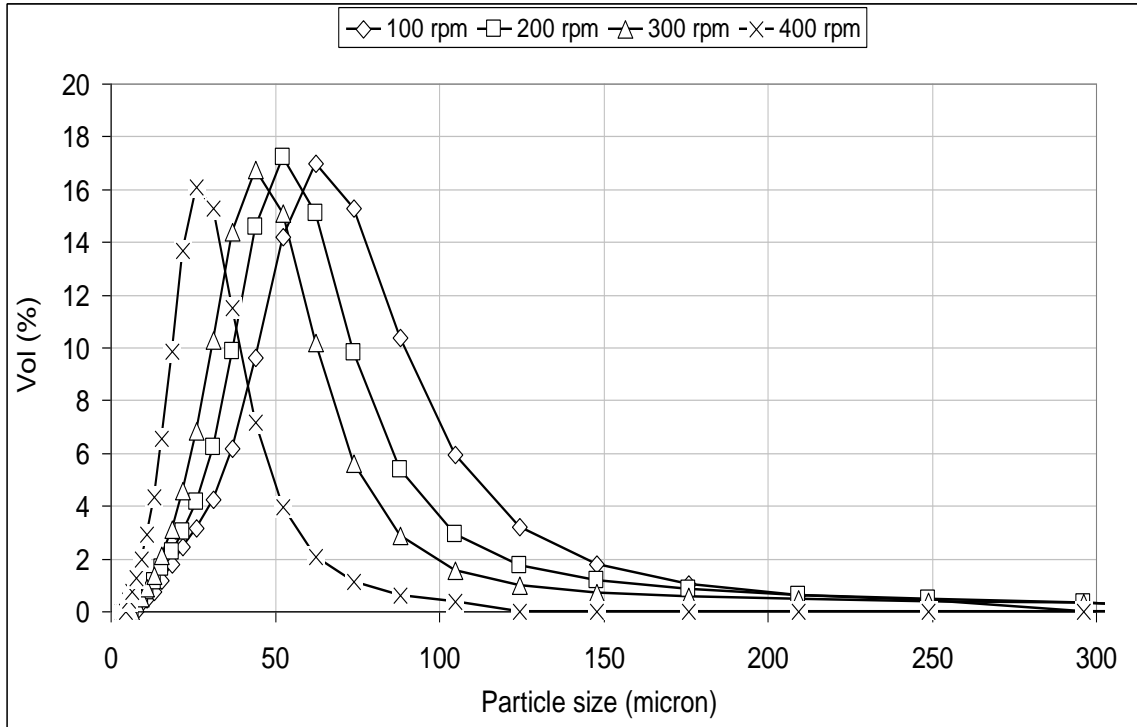


Figure 5.25 Zinc particle size distributions for 30s mixing time. (Initial [Zn]= 50 ppm, pH 8.7, 30 mg/l ferric chloride coagulant, rapid mixing for 30 s @ 100, 200, 300, 400 rpm)

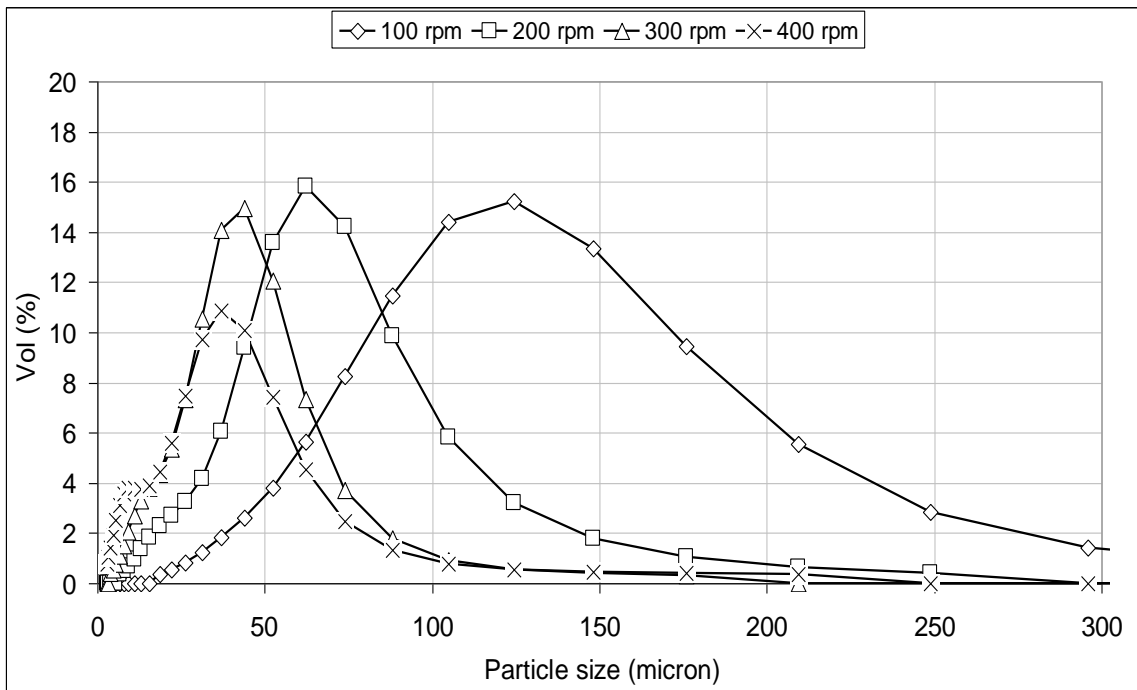


Figure 5.26 Zinc particle size distributions for 60s mixing time. (Initial [Zn] = 50 ppm, pH 8.7, 30 mg/l ferric chloride coagulant, rapid mixing for 60s @ 100, 200, 300, 400 rpm)

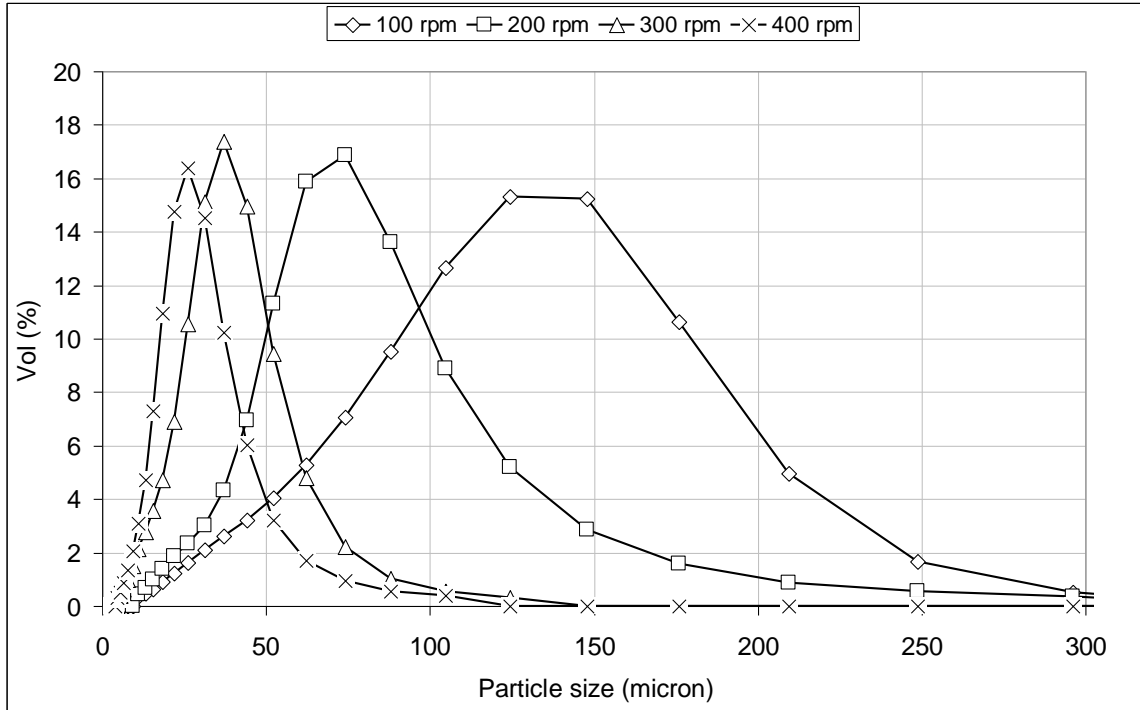


Figure 5.27- Zinc particle size distributions for 90 s mixing time. (Initial [Zn]= 50 ppm, pH 8.7, 30 mg/l ferric chloride coagulant, rapid mixing for 90s @ 100,200,300,400 rpm)

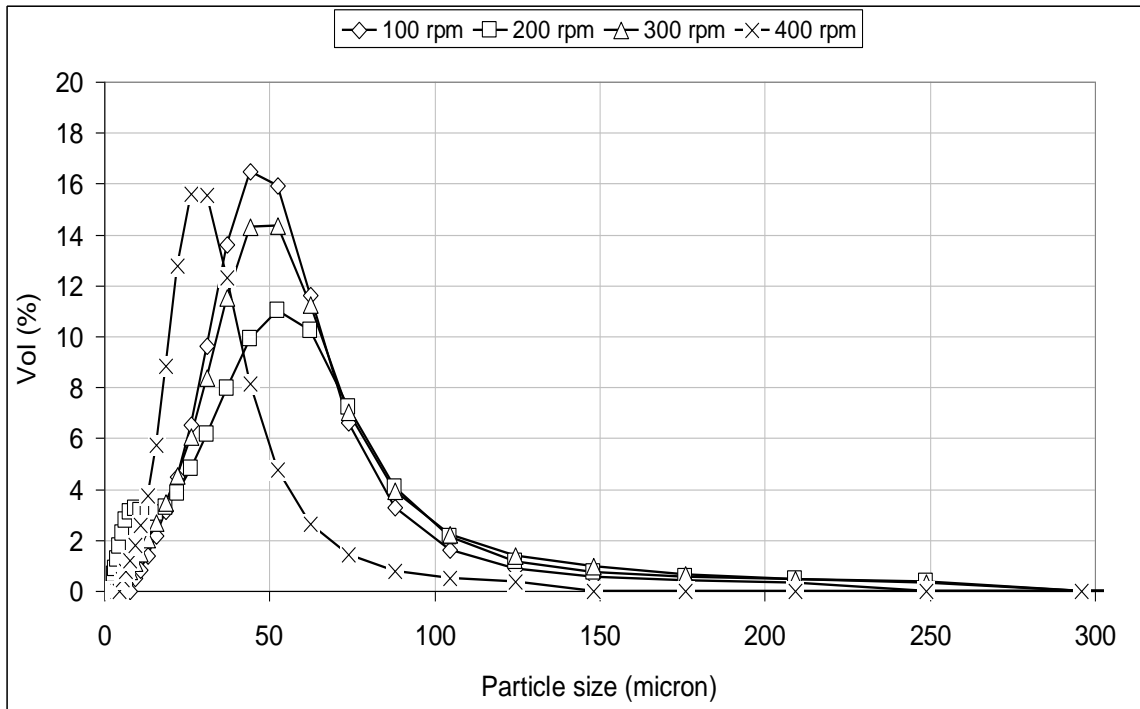


Figure 5.28- Zinc particle size distributions for 120 s mixing time. (Initial [Zn]= 50 ppm, pH 8.7, 30 mg/l ferric chloride coagulant, rapid mixing for 120 s @ 100, 200, 300 and 400 rpm)

Particle size analysis for zinc results are presented in Figure 5.29 for mixing time of 60 s at a narrow range of mixing speeds. At 100 rpm the particle size distribution was 63.9% for the particle size range from 88-176 μm . While it was 21.7%, 43.4%, 52.8%, 51.1% and 42.4% for rapid mixing impeller speeds of 60, 80, 120, 140 and 160 rpm, respectively. Calculations of the particle size range of interest for both zinc and nickel are shown in Appendix C.

The results indicate that the flocs formation was greater than the flocs breakage when the mixing speed was increased from 60 rpm till it reached the optimum point at 100 rpm. After the optimum point (i.e.120, 140 and 160 rpm) the flocs breakage rate might have increased gradually to surpass the rate of floc formation due to high mixing intensity. It was noticed that the flocs were broken slowly because flocs had a compact structure as shown in SEM images in the next section. When the mixing speed was increased to 200 rpm, there is an immediate and rapid increase in floc breakage more than 50%. More floc breakage occurred with further increases in the mixing speed to 300 and 400 rpm.

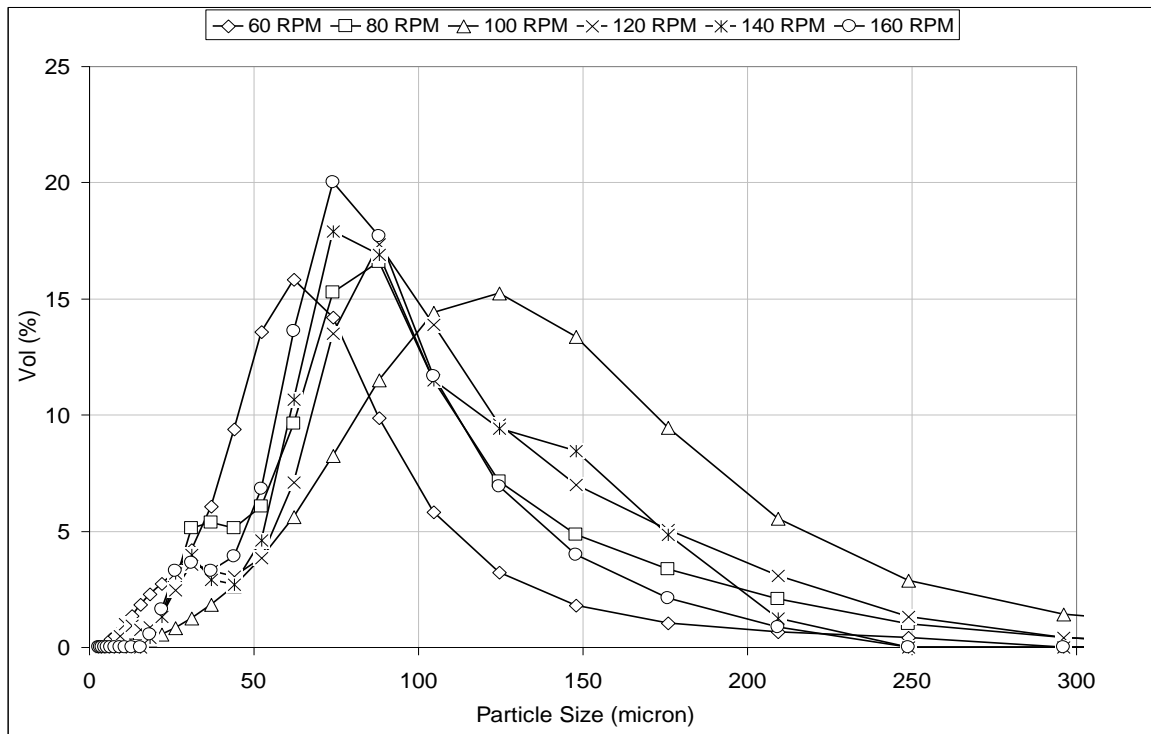


Figure 5.29- Zinc particle size distributions for 60 s rapid mixing time. (initial [Zn]= 50 ppm, pH 8.7, 30 mg/l ferric chloride, rapid mixing for 60 s @ 60, 80, 100, 120, 140 and 160 rpm).

Similarly, nickel particle size distributions are presented in Figures 5.30, 5.31, 5.32 and 5.33 for 30, 60, 90 and 120 s, respectively, at different mixing speeds. At 100 rpm mixing speed, as it can be seen in Figure 5.30, 55.2% of particles were in the range of 13-37 μm , the range where most of the particle size presence, while it was 23.2%, 26.3% and 10.5% for 150, 200, and 250 rpm respectively. The results again show that the formation of flocs during rapid mixing phase is greatly influenced by the duration and intensity of mixing. On increasing the mixing speed to 150 rpm, there is an immediate and rapid increase in nickel flocs breakage more than 50%. More flocs breakage occurs with further increases in the mixing speed to 200 and 250 rpm. Therefore mixing speed of 100 rpm was considered as mixing speed limit.

The results presented in Figure 5.31 for mixing time of 60s. In comparison with results in figure 4.32, for higher mixing time of 60 s, the flocs might start to break for extended mixing time producing more microflocs. The particle size distribution decreased to 48.9% over the same range of particle sizes of 13-37 μm at 100 rpm mixing speed. The flocs gradually break where the flocs interior structure could be less compacted. At other mixing speeds of 150, 200 and 250 rpm, the particle size distributions were 25.1%, 25.6% and 18.5%, respectively. This means higher mixing intensity increase the flocs breakage even with same mixing duration as previously observed with zinc flocs.

The results for 90 s rapid mixing are shown in figure 5.32. At 100 rpm the particle size distribution was 34.1% in the range of 13-37 μm . This indicates that rapid mixing up to 90 s might break more flocs into microflocs. For mixing time of 120 s the particle size distribution was 39.7% in the same range as shown in Figure 5.33, indicating that large flocs breaks under prolonged mixing. However, there seems to be a slight improvement in the percentage of particles in the range of 13-37 μm . This might be due to some agglomeration of small flocs during the last 30 seconds from 90 to 120s.

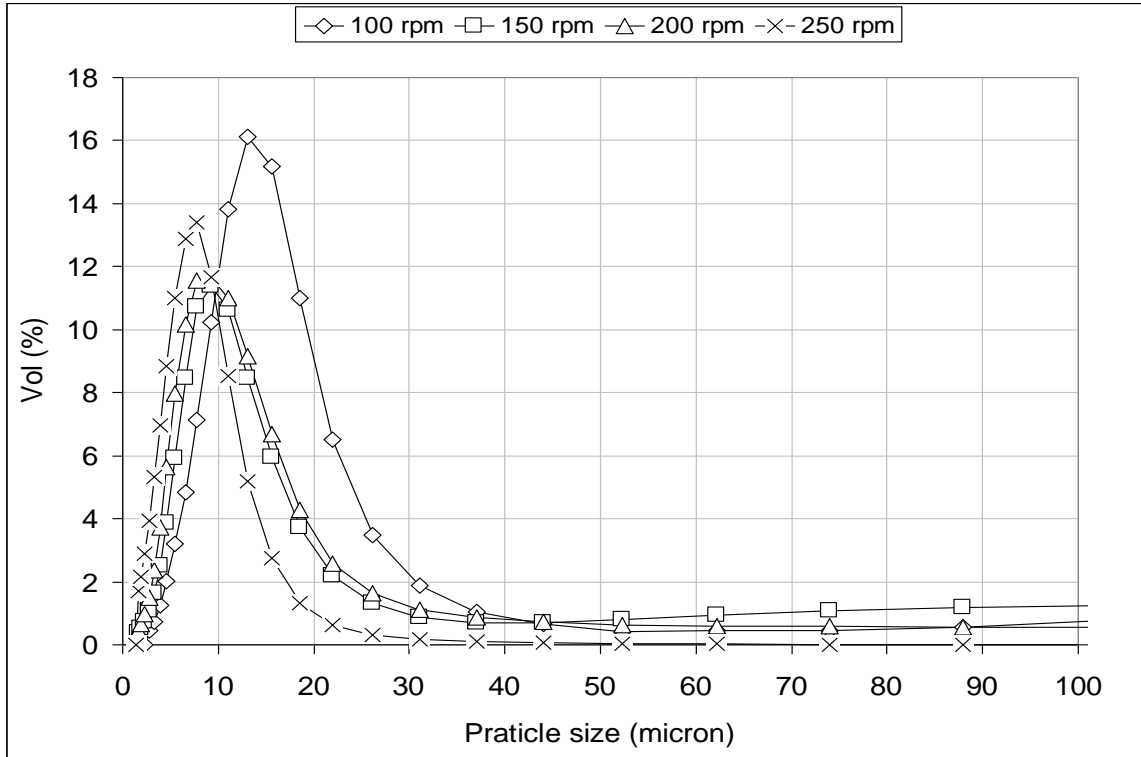


Figure 5.30- Nickel particle size distribution for 30s mixing time. (initial [Ni]= 50 ppm, pH 10.2, 30 mg/l ferric chloride coagulant rapid mixing for 30s @ 100,150, 200, 250 rpm)

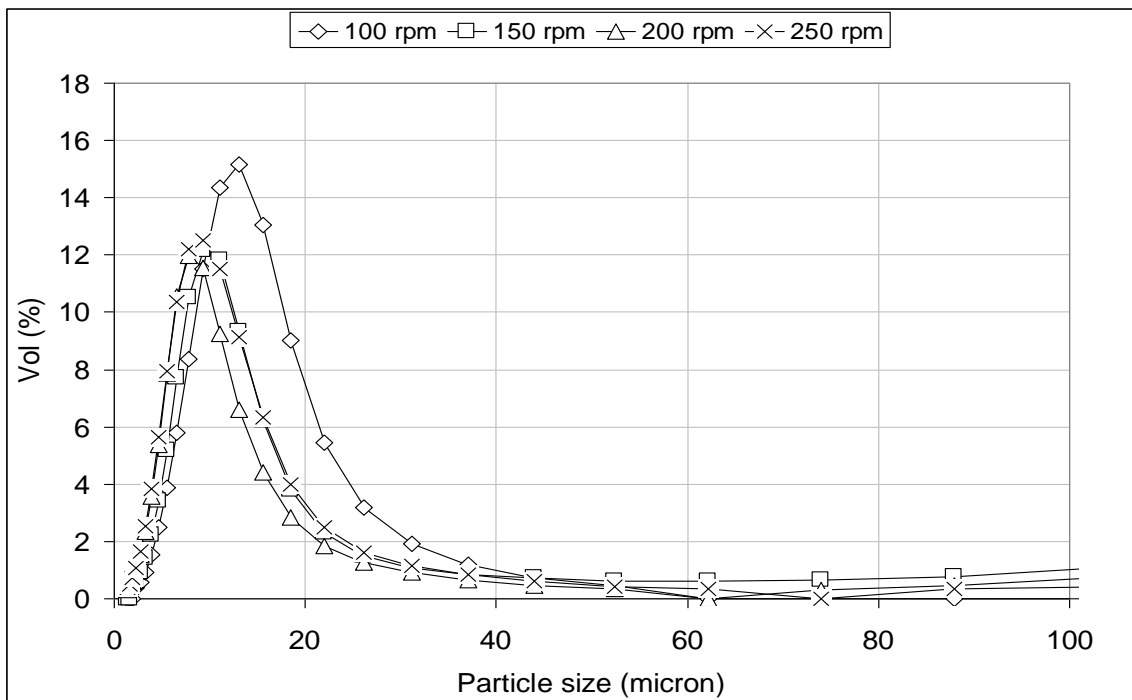


Figure 5.31- Nickel particle size distribution for 60s mixing time. (initial [Ni]= 50 ppm, pH 10.2, 30 mg/l ferric chloride coagulant rapid mixing for 60s @ 100,150, 200, 250 rpm)

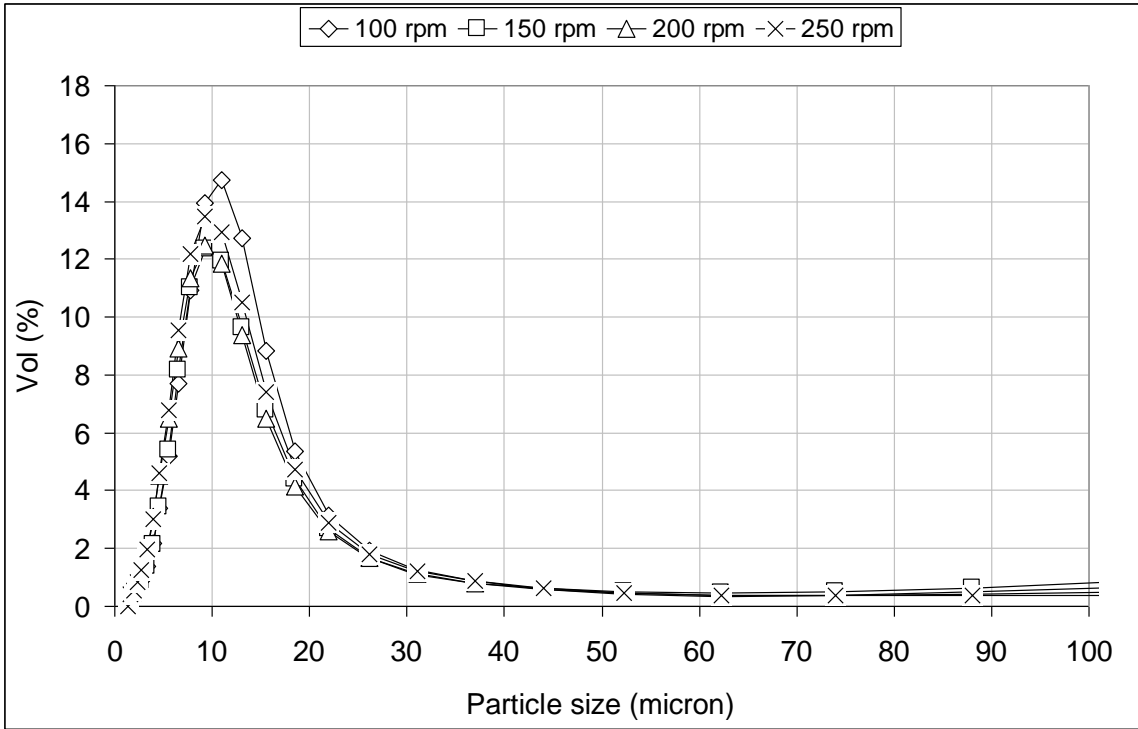


Figure 5.32- Nickel particle size distribution for 90s mixing time. (initial [Ni]= 50 ppm, pH 10.2, 30 mg/l ferric chloride coagulant rapid mixing for 90s @ 100,150, 200, 250 rpm)

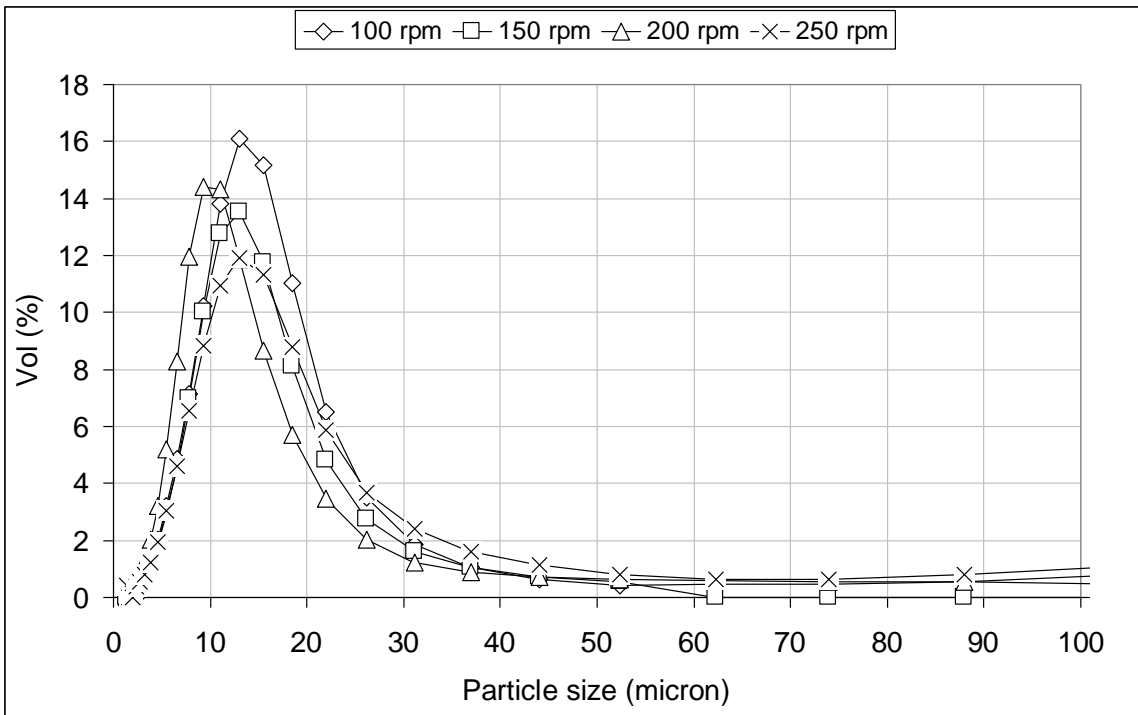


Figure 5.33- Nickel particle size distribution for 120s mixing time. (initial [Ni]= 50 ppm, pH 10.2, 30 mg/l ferric chloride coagulant rapid mixing for 120s @ 100, 150, 200 and 250 rpm)

Similarly, nickel particle size distribution was presented in Figure 5.34. At mixing time of 30 s and 80 rpm mixing speed, the total particle size distribution was 53.9% for particle size in the range of 13-37 μm . While it was 23.5%, 45.5%, 29.7% and 18.9% for mixing speeds of 60, 100, 120 and 140 rpm, respectively. This indicates that 80 rpm is the optimum mixing speed for nickel removal at optimum mixing time of 30 s.

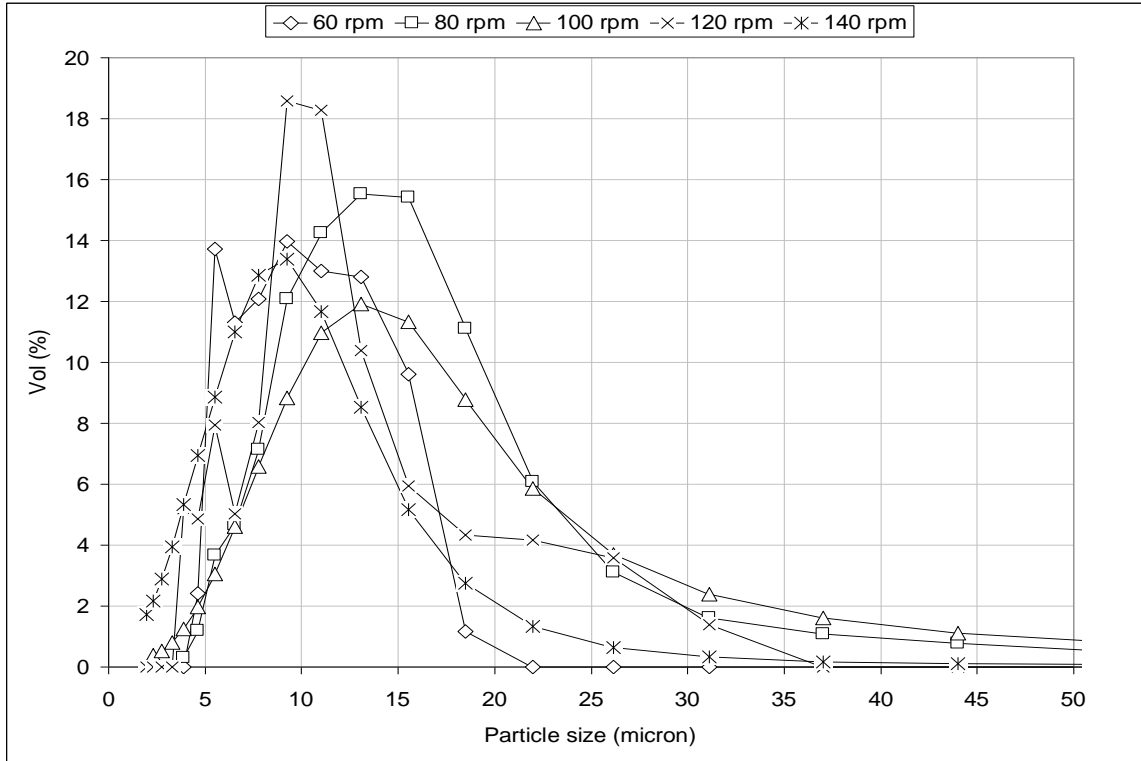


Figure 5.34 - Nickel particle size distribution for 30s rapid mixing time. (initial [Ni]= 50 ppm, pH 10.2, 30 mg/l ferric chloride, rapid mixing for 60s @ 60, 80, 100, 120, and 140 rpm).

In the present study, the measuring techniques for optimal metal removal were more representative than those used by previous researchers. Since most of them were using turbidity index and total suspended solid analysis which can contribute in a significant amount of error in the results. The optimal mixing parameter values (mixing rpm and time) obtained was lower than what was recommended in the reported literature. In the present study, the measurement technique and procedure as well as data analysis gave more systematic findings than conflicting recommendations in the reported literature for the same metals. From optimal data obtained, it can be concluded that the levels of the

rapid mixing parameters vary dependent on the type of heavy metal present in wastewater as well as the type of coagulant used.

For combined metal in solution, containing 50 ppm zinc and 50 ppm nickel, two pH values of 9.0 and 9.5 were investigated. The pH selection based on the optimum pH of each metal obtained in this study (zinc pH 8.7 and nickel pH 10.2). Ferric chloride at a dose of 60 mg/l was used as a coagulant. For rapid mixing parameters, a speed of 100 rpm which was optimum in zinc and nickel coagulation was used. A time of 30 s of mixing duration which was optimum for nickel coagulation and close to optimum for zinc removal. From data obtained, 30 s mixing was critical for nickel flocs formation because beyond this mixing time nickel flocs breakage is more than flocs formation, while it was close to optimum of 60 s for zinc flocs formation. The results obtained are shown in Figure 5.35 for combined zinc-nickel solution at pH 9 and 9.5.

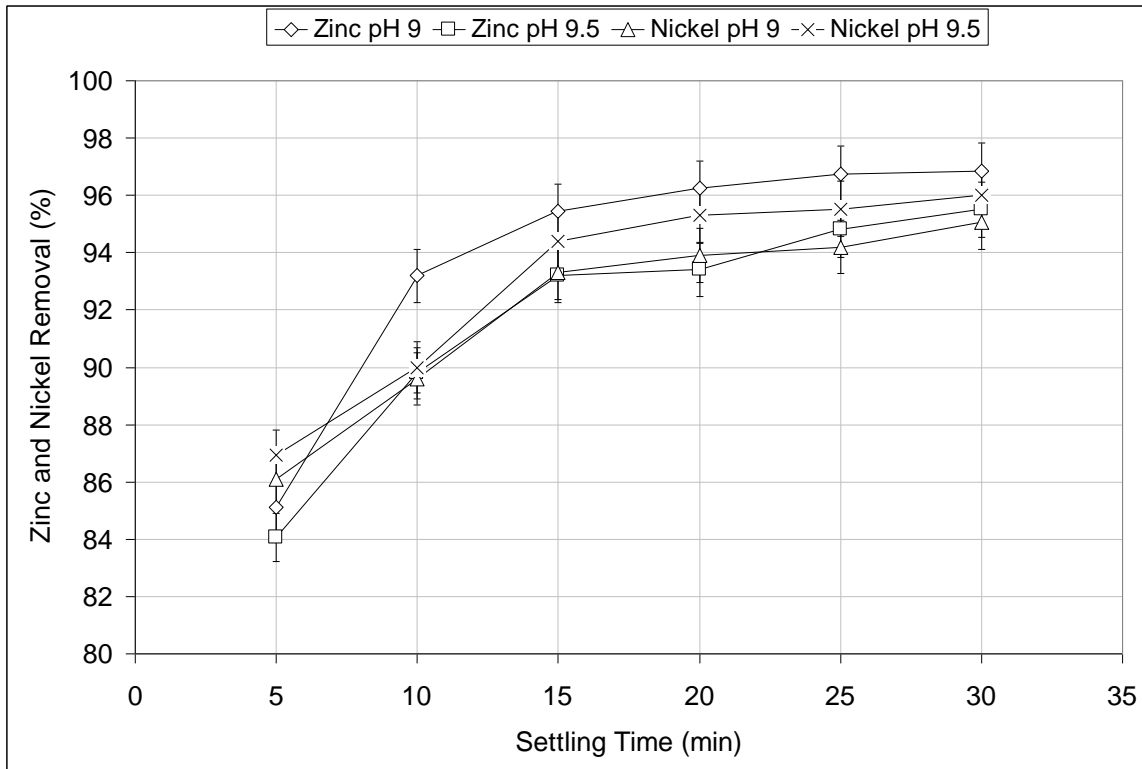


Figure 5.35- Zinc and nickel removal in combined solution vs. settling time at pH 9 and 9.5. ([Zn]= 50 ppm, [Ni]= 50 ppm, ferric chloride 60 mg/l, rapid mixing 30 s @ 100 rpm, flocculant 0.5 ml/l, slow mixing 15 min @ 50 rpm)

For comparison, the data of sole zinc removal percentage at pH 8.7 and zinc removal percentage in combined solution with nickel at pH 9-9.5 were plotted in Figure 5.36. Also, the data of sole nickel removal percentage at pH 10.2 and nickel removal percentage in combined with zinc at pH 9-9.5 were plotted in Figure 5.37. As can be seen in Figures 5.36 and 5.37 that the zinc and nickel combined solution removal was slightly lower of about 2-3% than individual metal solution. The optimal operating parameters for precipitation and coagulation of combined solution of zinc and nickel can be considered as: pH value of 9-9.5, ferric chloride coagulant at dose of 60 mg/l, rapid mixing of 30 s at 100 rpm.

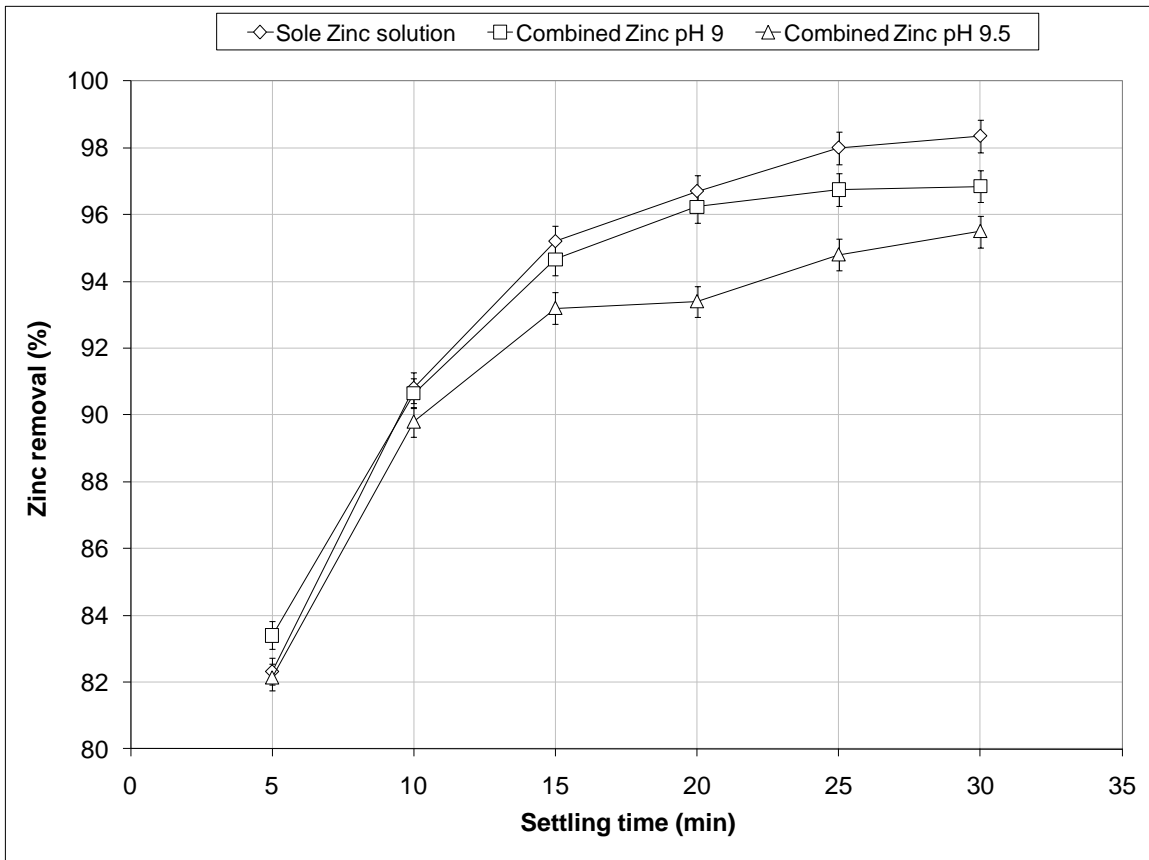


Figure 5.36- Zinc removal percentage vs. settling time for sole (pH 8.7) and combined zinc solution with nickel at pH 9-9.5. ([Zn]= 50 ppm, [Ni]= 50 ppm, ferric chloride 60 mg/l, rapid mixing 30 s @ 100 rpm, flocculant 0.5 ml/l, slow mixing 15 min @ 50 rpm)

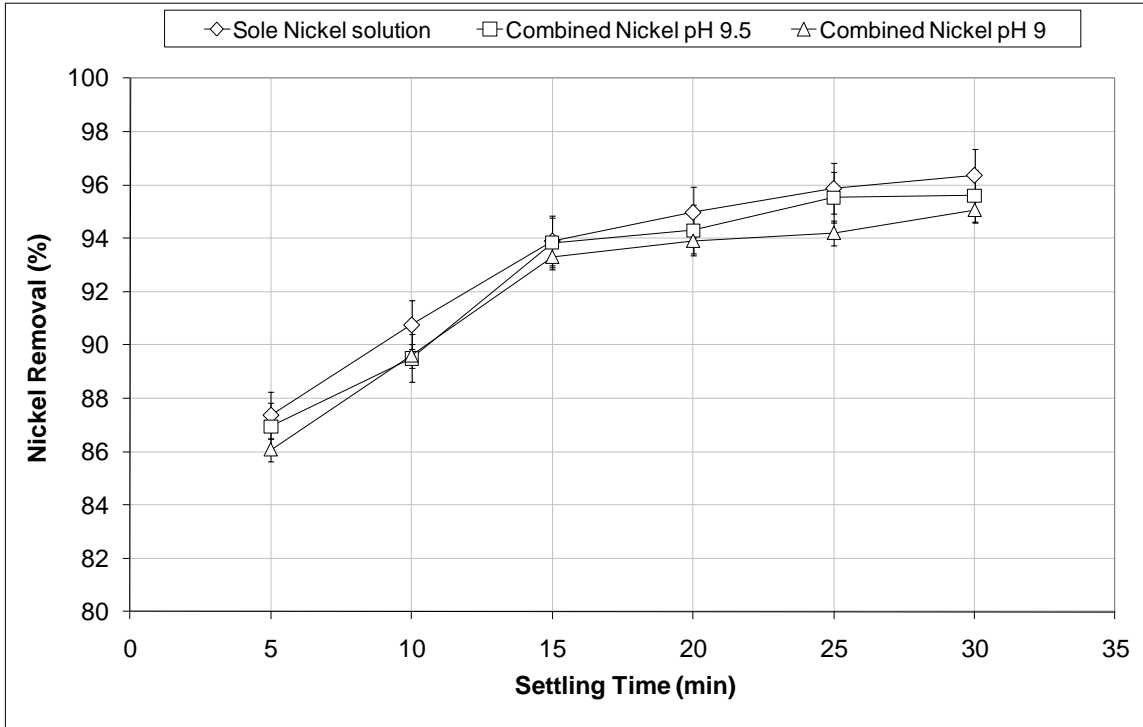


Figure 5.37- Nickel removal percentage vs. settling time for sole (pH 10.2) and combined nickel solution with zinc at pH 9-9.5. ([Zn]= 50 ppm, [Ni]= 50 ppm, ferric chloride 60 mg/l, rapid mixing 30 s @ 100 rpm, flocculant 0.5 ml/l, slow mixing 15 min @ 50 rpm)

5.5 Metal Coagulated Particles Imaging

Scanning electron microscope (SEM) was used to study structural surface of the zinc precipitate particles. The images were taken for zinc flocs after coagulation with 30 mg/l of ferric chloride at different mixing speeds (60, 100 and 150 rpm) and times (30, 60 and 90 s), and without coagulant addition as a reference. Visual observation of the images presented in Figure 5.38 for the case without coagulant show that zinc flocs have a fine surface texture.

The image of floc with the mixing speed of 60rpm and the mixing time of 30s is presented in Figure 5.39a. After adding the coagulant, the flocs formed rapidly with rough surface. The flocs appeared more lumpy and compact when the mixing speed increased to 100 rpm as shown in Figure 5.39b. At mixing speed of 150 rpm as shown in Figure 5.39c, the flocs were deteriorated under a high shearing; hence it looked more flaky and flimsy.

It was observed during experiments that flocs formed rapidly after increasing mixing speed to an optimum of 100 rpm. They looked denser and larger after formed even when increasing the mixing speed to 150 rpm. The flocs start to break slowly on increasing the speed to certain level. When comparing the images in Figures 5.39, 5.40 and 5.41, it was noticed that the mixing time has affected the structure of the flocs more than mixing speed. Rapid mixing for 30 s was not enough to disperse the coagulant thoroughly into fluid bulk, and thus the charge on the particles was not neutralized. Consequently, high repelling force was still present and hence the agglomeration was prevented even though optimum mixing speed was used.

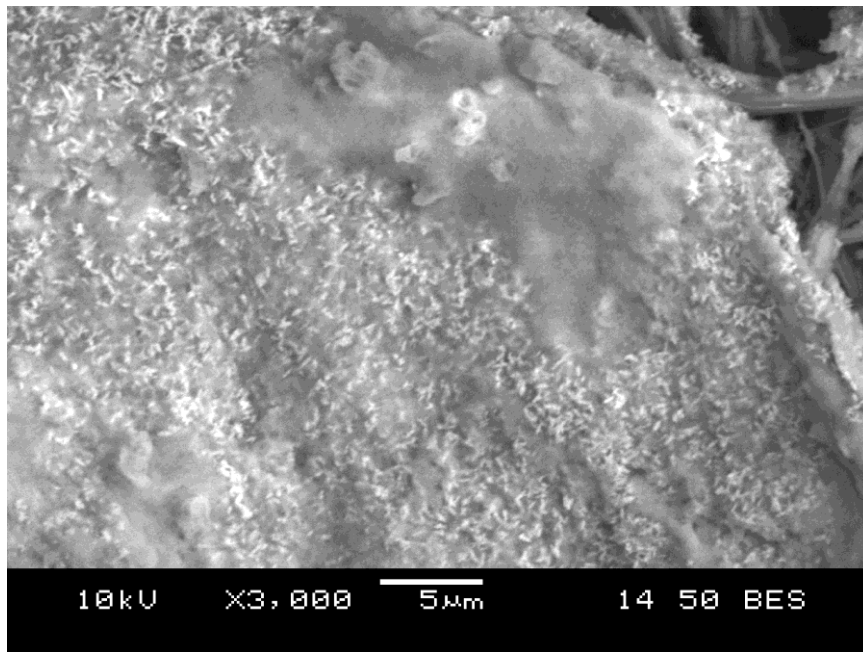
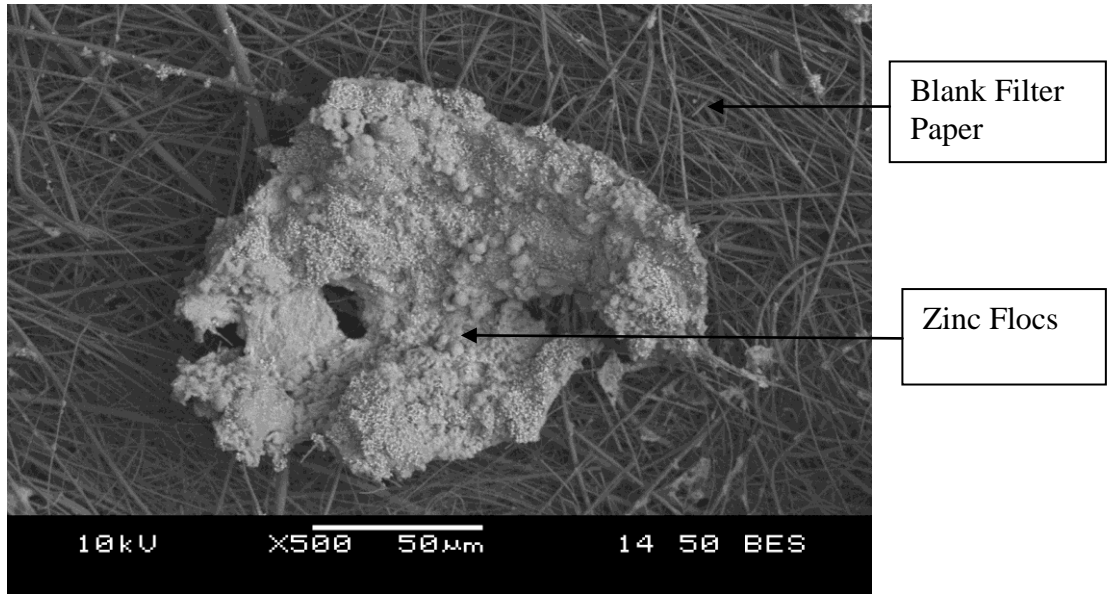
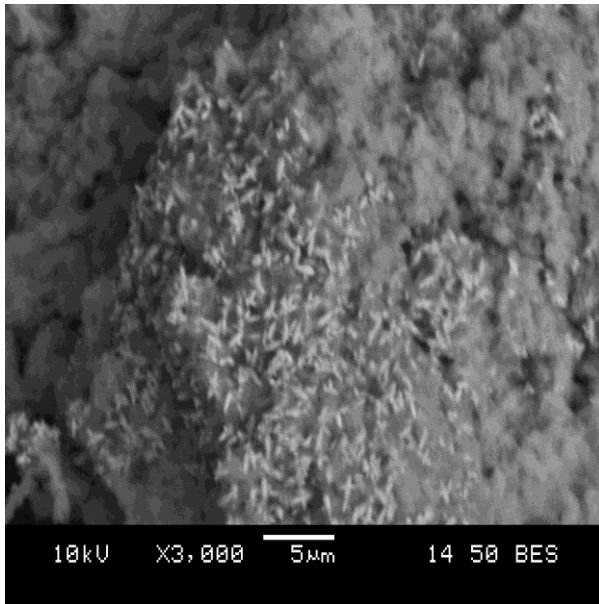
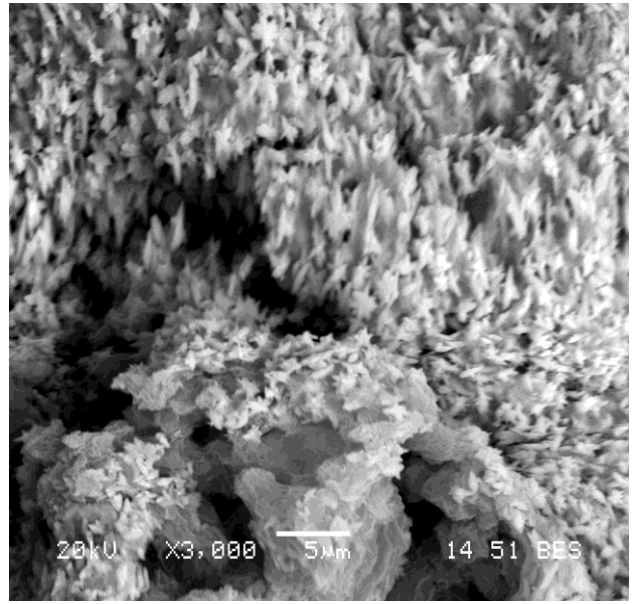


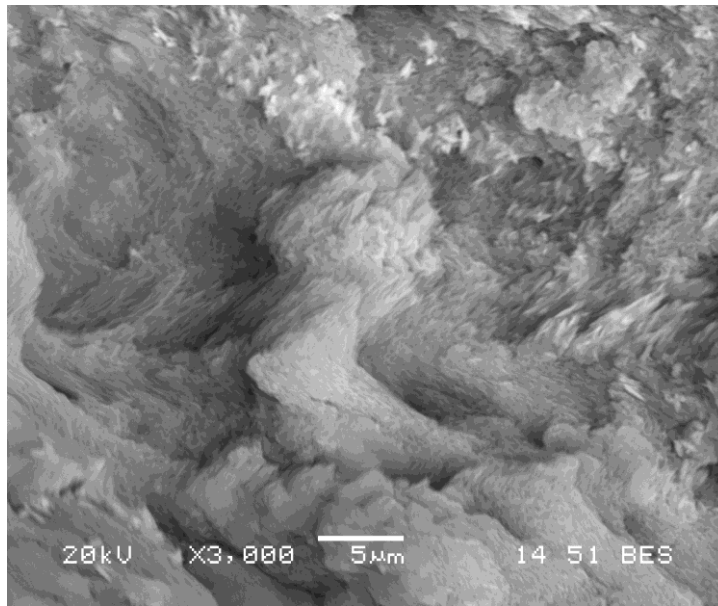
Figure 5.38 SEM images for zinc flocs, no coagulant used.
([Zn]=50ppm, pH 8.7, slow mixing 10 min@ 50rpm)



(a)



(b)



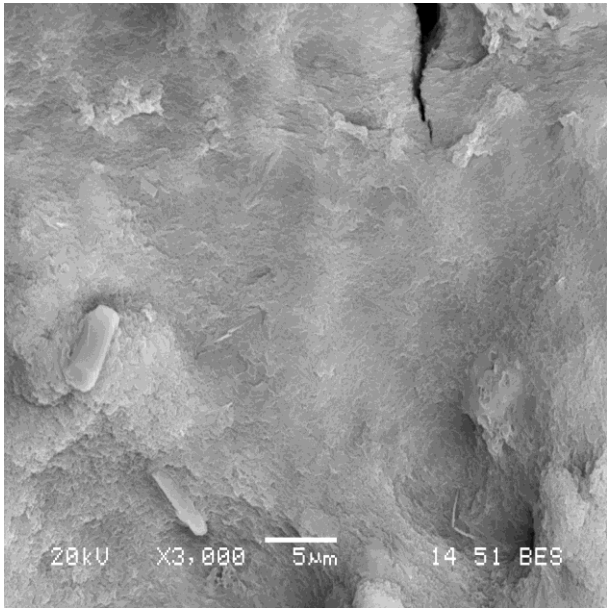
(c)

Figure 5.39- SEM images for Zinc flocs, 30mg/l ferric chloride, 30 s rapid mixing time and different rapid mixing speeds, (a) 60 rpm, (b) 100 rpm, (c) 150 rpm

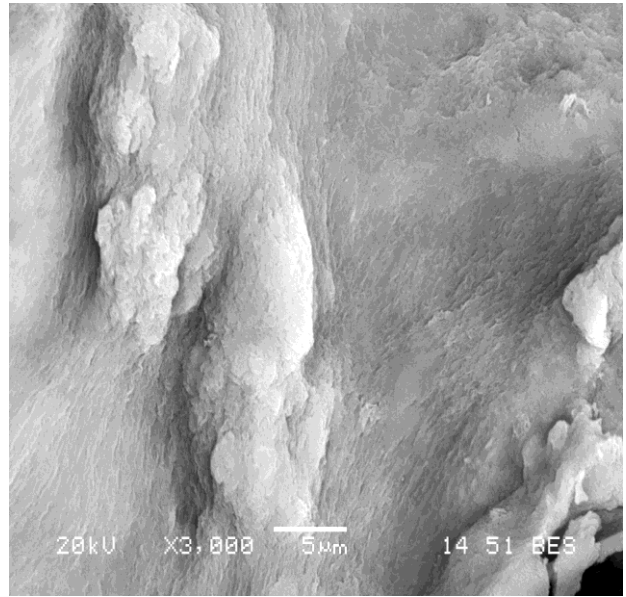
The images presented in Figure 5.40 for 60 s rapid mixing time at different mixing speed show that increasing the mixing time to 60 s enhanced the flocs structure significantly. The images of the zinc flocs in figure 5.40a show that the flocs appear to have stronger and solid surface than that of 30 s shown in Figure 5.39a. Flocs became denser and more solid when increasing the mixing speed to 100 rpm as shown in Figure 5.40b. Also, floc surface is smoother which would help flocs settling faster. When the mixing speed was increased to 150 rpm, limited flocs breakage occurred as can be seen in Figure 5.40c.

Rapid mixing time seemed to have a stronger effect on the floc surface structure than the rapid mixing speed. At 90s mixing time, the surface structure didn't change significantly with the mixing speed from 60 to 150 rpm. Larger flocs formed with an extended mixing time at the same mixing speed. Increasing mixing time to 90s, as shown in Figure 5.41, has limited effect on the surface structure of the flocs compared to 60s due to strong bridging bonds between the particles after coagulation.

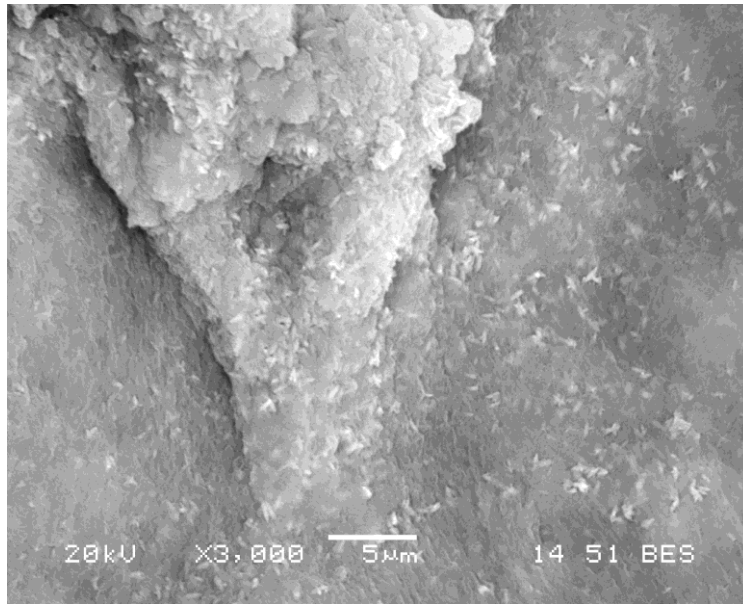
The image of the floc surface in Figure 5.40b shows that the flocs formed after 60s rapid mixing at 100 rpm appeared to have a denser and compact structure with smooth surface and more regular shape than others in Figures 5.39, 5.40 and 5.41. The flocs would thus settle faster, resulting in a better metal removal. This agrees with the measured metal removal previously presented.



(a)

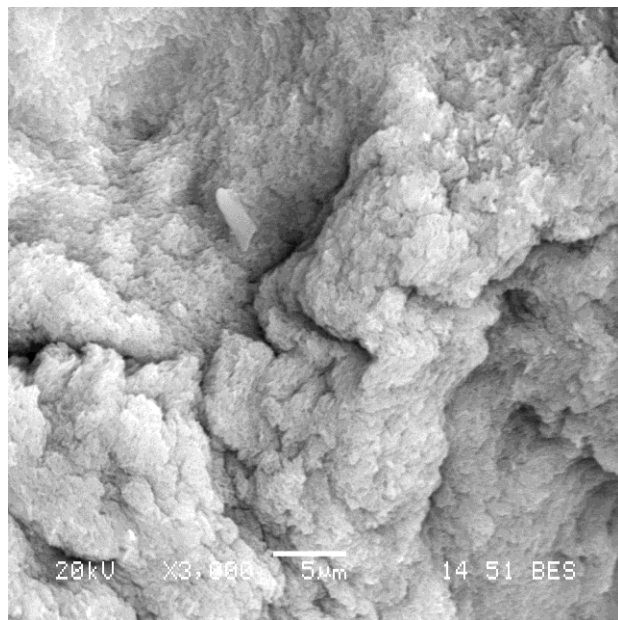


(b)

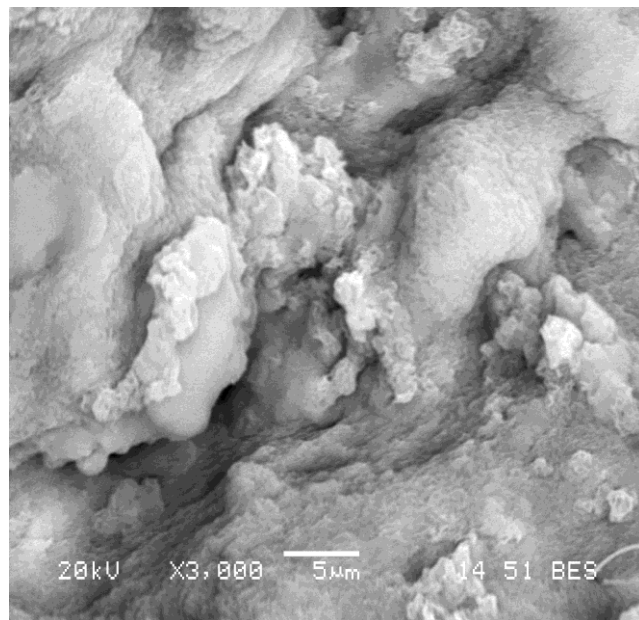


(c)

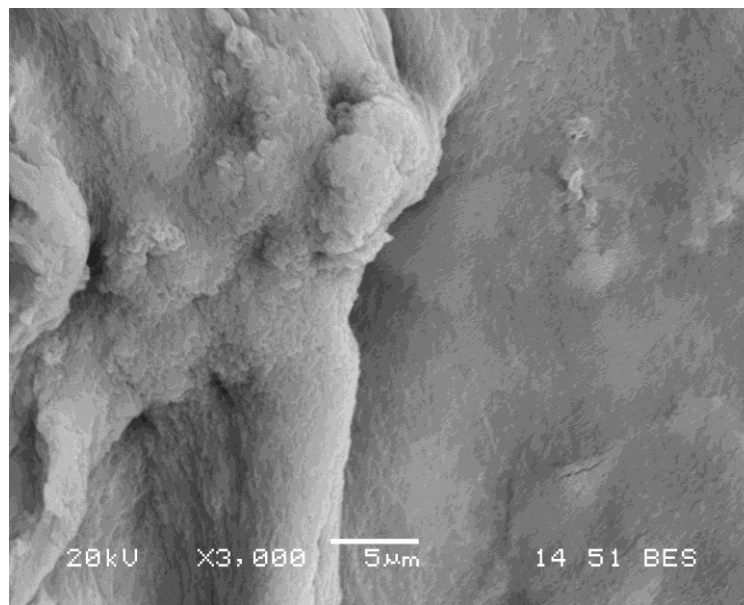
Figure 5.40 SEM images for zinc flocs, 30mg/l ferric chloride, 60 s rapid mixing time at different rapid mixing speeds, (a) 60 rpm, (b) 100 rpm, (c) 150 rpm



(a)



(b)



(c)

Figure 5.41- SEM images for zinc flocs, 30 mg/l ferric chloride, 90 s rapid mixing time at different rapid mixing speed, (a) 60 rpm, (b) 100 rpm, (c) 150 rpm

Similarly, the images presented in Figure 5.42 for nickel floes show that without coagulant, the floes seemed to have a fine surface structure. The nickel particles formed a thin layer of nickel salt precipitates with small floes.

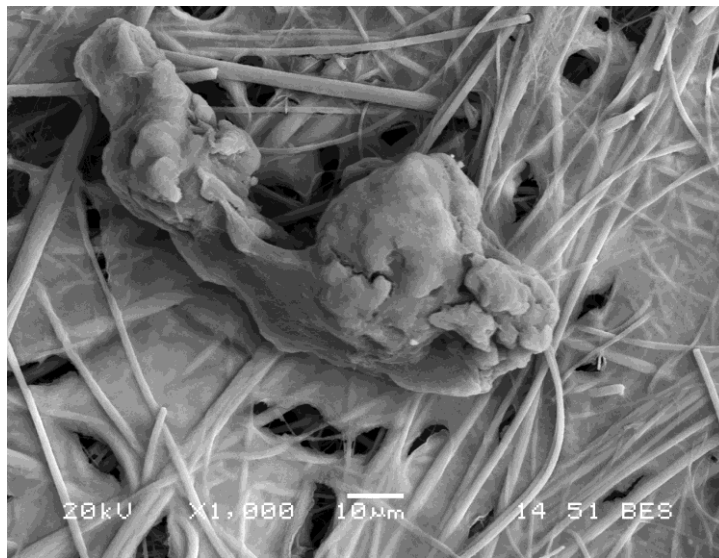
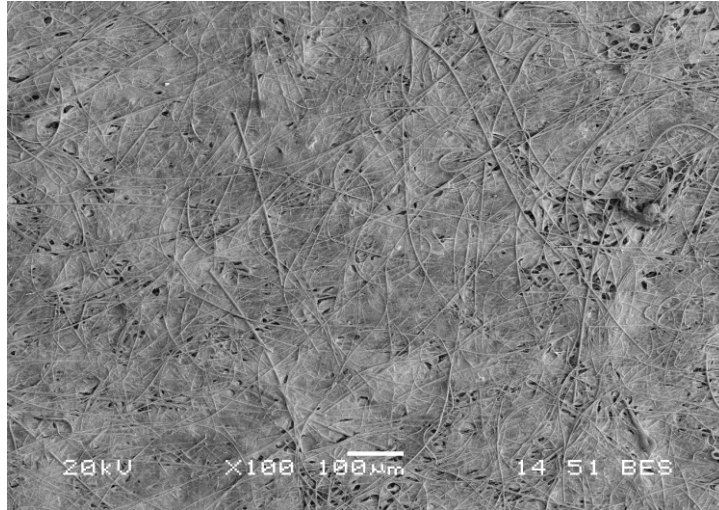
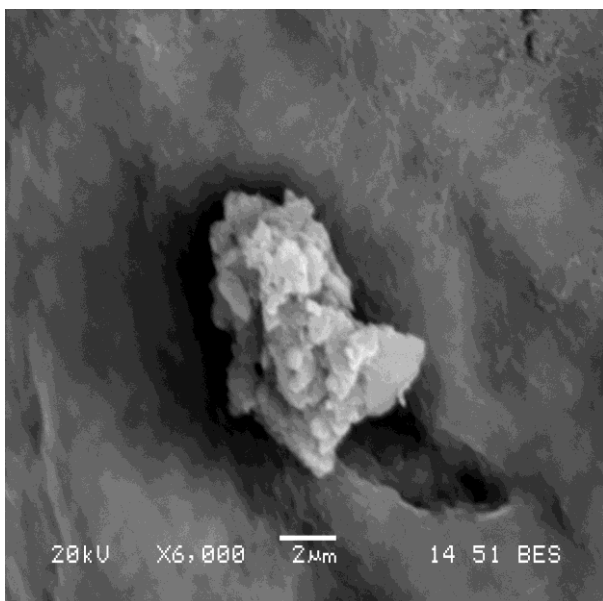


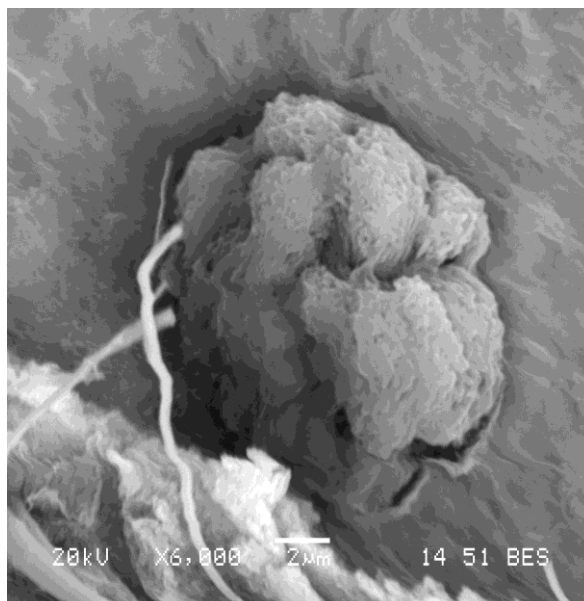
Figure 5.42 – SEM image of nickel floes, with no coagulant addition.

After adding the coagulant at the optimum dose, mixing speed 60 rpm and time 30 s, nickel flocs formed gradually with a compact structure but not enough mixing to form larger flocs as shown in Figure 5.43a. The flocs were larger and appeared to be more structure compacted when mixing speed was increased to 80 rpm as shown in Figure 5.43b. When the mixing speed increased to 120 rpm, as shown in Figure 5.43c, flocs were deteriorated under higher shearing.

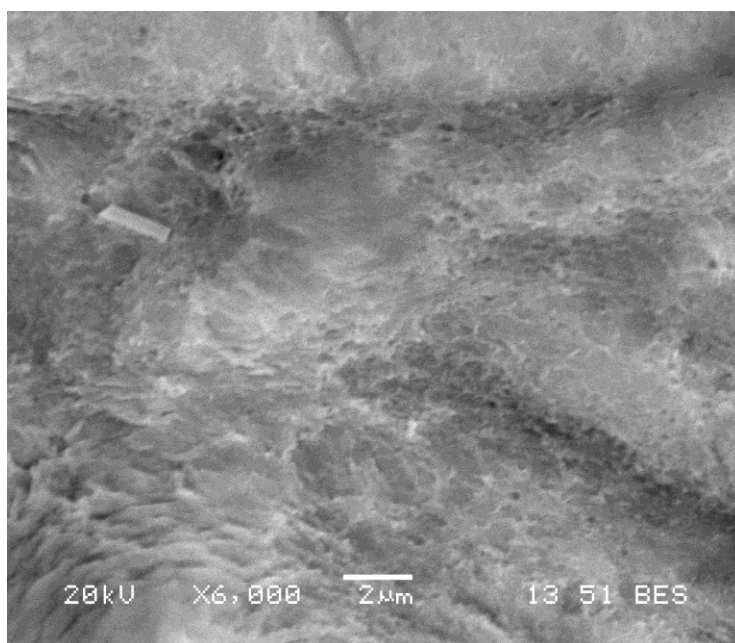
It was observed that flocs formed rapidly after increasing mixing speed to an optimum of 80rpm. The flocs started to break gradually and then rapidly on further increases in the mixing speed and time. As can be seen in Figures 5.43, 5.44 and 5.45, the mixing time affected the flocs structure more than the mixing speed. Rapid mixing at 80 rpm for 30 s was enough to disperse the coagulant thoroughly into the fluid bulk, resulting in larger floc size and limited floc breakage. This in agreement with a higher nickel removal previously presented.



(a)

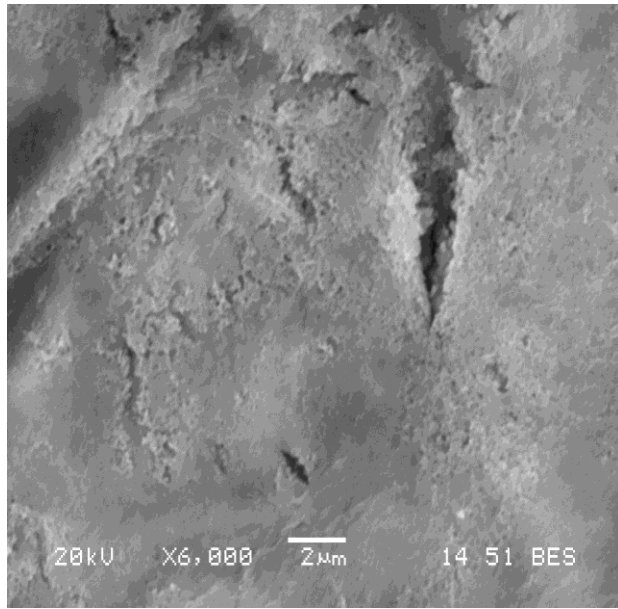


(b)

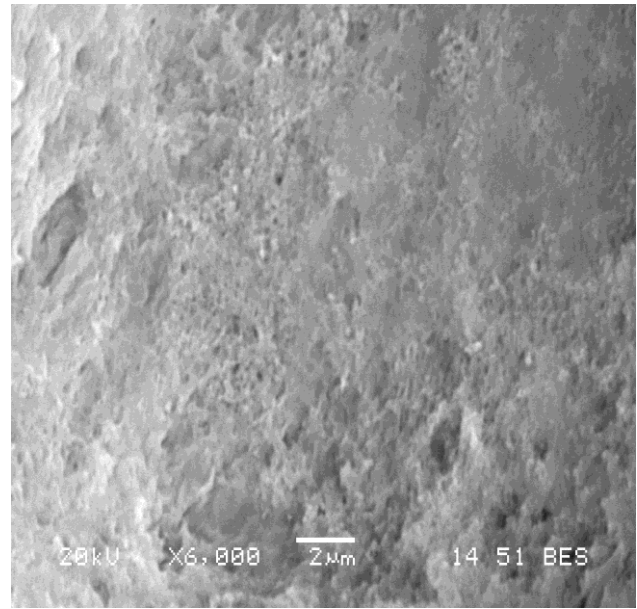


(c)

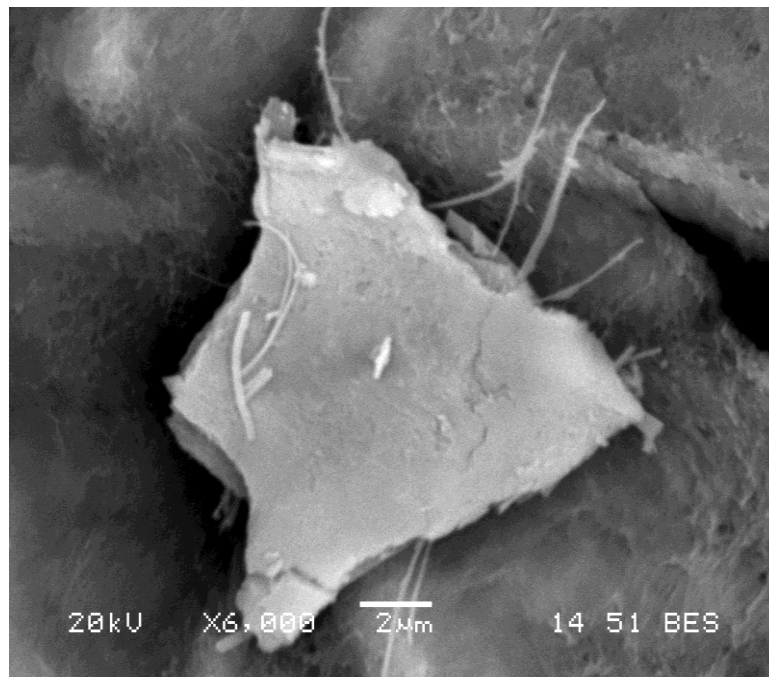
Figure 5.43- SEM images for nickel flocs, 30mg/l ferric chloride, 30 s rapid mixing time at different rapid mixing speeds, (a) 60 rpm, (b) 80 rpm, (c) 120 rpm



(a)

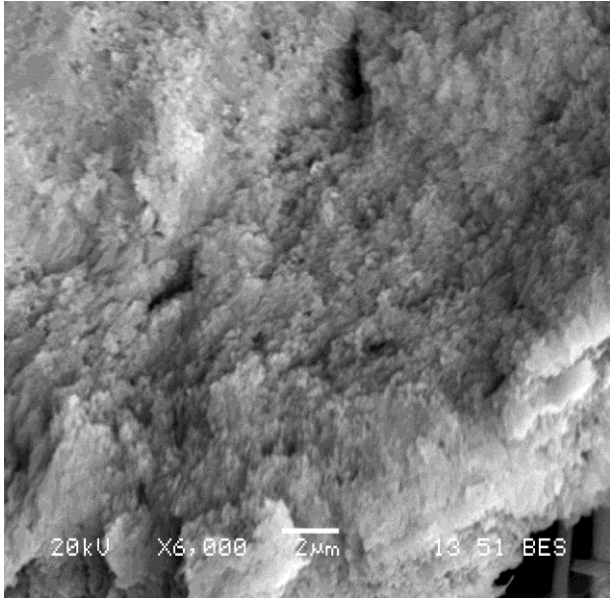


(b)

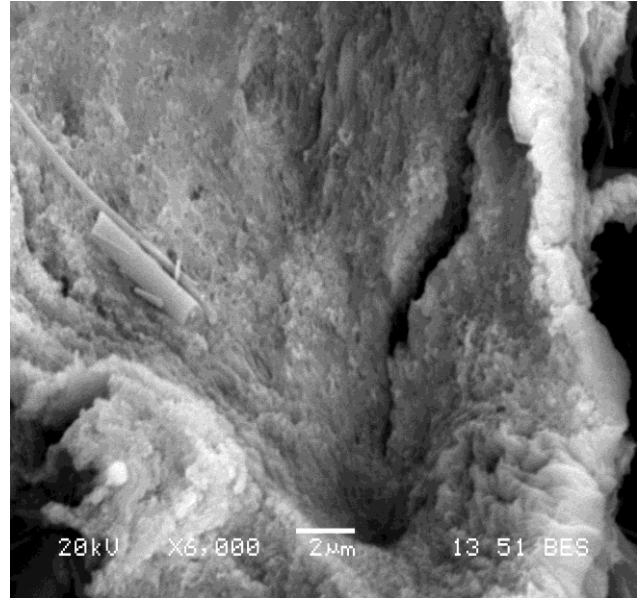


(c)

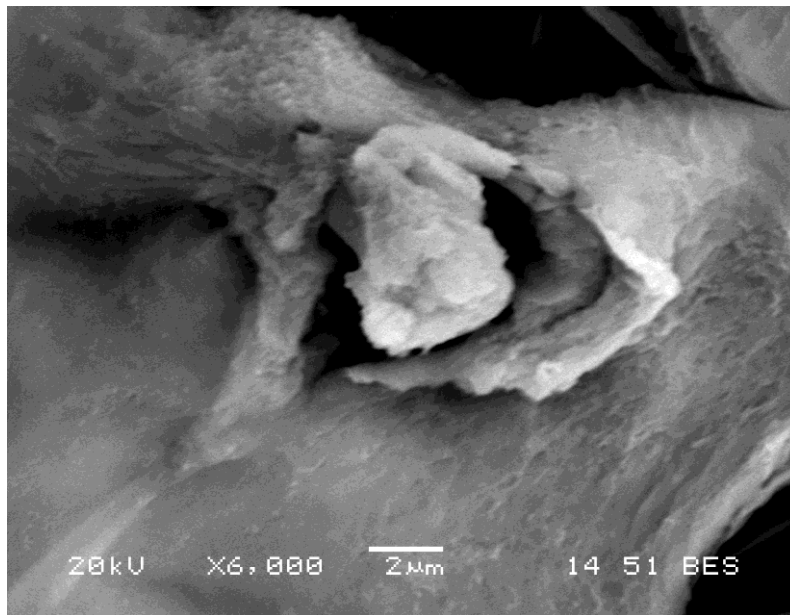
Figure 5.44- SEM images for nickel flocs, 30mg/l ferric chloride, 60 s rapid mixing time at different rapid mixing speeds, (a) 60 rpm, (b) 80 rpm, (c) 120 rpm



(a)



(b)



(c)

Figure 5.45- SEM images for nickel flocs, 30mg/l ferric chloride, 90 s rapid mixing time at different rapid mixing speeds, (a) 60 rpm, (b) 80 rpm, (c) 120 rpm

6 Conclusions and Recommendations

6.1 Conclusions

The bench-scale studies were performed to determine the suitable coagulant and the optimum rapid mixing time and speed for zinc and nickel precipitation. For simulated solutions of 50 ppm of zinc ions and nickel ions individually, the optimum pH values were found to be 8.7 and 10.2 for zinc and nickel precipitation, respectively. For combined solution the optimal pH ranging from 9 to 9.5. Ferric chloride was found to be superior over ferrous sulfate and aluminum sulfate in zinc and nickel removal. An optimum removal was obtained at pH = 8.7 with 30 mg/l of ferric chloride for zinc and pH = 10.2 with 30mg/l ferric chloride for nickel. For varying rapid mixing time and impeller speed, improvements ranging from a minimum of 70-80% to a maximum of 98.9% for zinc and 97.6% for nickel were observed.

In the reported literature, there are rather contradictory recommendations for rapid mixing parameters. American Water Works Association stated that there were no exact values to establish the mixing speed and the residence time required to disperse a coagulant in water. However, in the present study, it was found that there were distinct optimum mixing times and speeds for zinc and nickel coagulation. The optimum mixing time was 60 s for zinc and 30 s for nickel with the optimum mixing impeller speed of 100 rpm for zinc and 80 rpm for nickel. The reported literature did not examine the wide range of mixing times and speeds with a systematic procedure. In the present study, the wide range of mixing times and speeds were studied, and this enabled clarification of the reasons of conflicting recommendations in literature.

Effects of mixing speed and time on the coagulation process in the rapid mixing step were investigated by monitoring particle size distribution. Several jar tests were performed at various combinations of mixing times and speeds. The particle size distribution for zinc after 60 s of rapid mixing at 100 rpm showed that more than 72% of the particles were in the range of 52- 148 μm . For nickel, 54% of the particles were in the range of 13-37 μm with 30 s of rapid mixing at 80 rpm. These optimum conditions for

microflocs formation in rapid mixing step could affect the sequential process, such as flocculation and sedimentation. Optimum rapid mixing conditions for maximum growth of microflocs facilitated the high removal of zinc and nickel from the simulated wastewaters.

Scanning Electron Microscopy (SEM) images were also taken for zinc and nickel flocs' surface after rapid mixing step. The visual examination of the SEM images showed that ferric chloride addition at the optimum conditions facilitated the formation of denser flocs of zinc and nickel. The flocs formation and breakage are different for zinc and nickel. Zinc ions formed larger and stronger flocs in coagulation step at optimum condition than those with nickel ions.

6.2 Recommendations

The following recommendations are made for further studies:

- Using different types of coagulant and investigating their affects on mixing conditions.
- More studies could be focused on interior structure of the flocs formed during rapid mixing step, since zinc formed larger and stronger flocs than nickel.
- Flocculation step play important part of heavy metal precipitation, further studies on flocculant types used and optimum process conditions on slow mixing should be investigated.
- More studies could be focused on the precipitation process scale up using the optimum parameters obtained in this study.

References

Abdul Aziz, H., Alias, S., Assari, F., and Adlan, M.N., (2007), The use of Alum, Ferric Chloride and Ferrous Sulfate as Coagulants in Removing Suspended Solids, Color and COD from Semi-aerobic Landfill Leachate at Controlled pH, *Waste Management Research*, 2007:25: pp 556-565

American Water Works Association (AWWA) and American Society of Chemical Engineers (ASCE), (1997), *Water Treatment Plant Design*, 3rd edition; McGraw Hill: New York.

Amirtharajah, A. and Mills, K.M., (1982), Rapid-Mixing Design for Mechanisms of Alum Coagulation, *J AWWA* 4:210–216.

Amirtharajah, A. and O'Melia, C.R., (1990), Coagulation Processes: Destabilization, Mixing and Flocculation, in *Water Quality and Treatment*, American Water Works Association, ed by Pontius FW, McGraw-Hill, New York, pp 269–365

Blanco, AB., Sanz, B., Liama, M.J., and Serra, JL., (1999), Biosorption of Heavy Metals to Immobilized *Phormidium Laminosum* Biomass, *J. Biotechnol.* 69:227-240

Blaser, S., (2000), Break-Up of Flocs in Contraction and Swirling Flows. *Colloids and Surfaces, A* 166:215–223.

Bradl, H., (2005). *Heavy Metals in the Environment: Origin, Interaction and Remediation*, Chapter 3, pp 282 Academic Press, 2005.

Brakalov, L.B., (1987), A Connection between Orthokinetic Coagulation Capture Efficiency of Aggregates and their Maximum Size. *Chem. Eng. Sci.* 42:2373–2383

Bratty, J., (2006), *Coagulation and Flocculation in Water and Wastewater*, 2nd edition, WA Publishing, Alliance House, P 42-43, 116-119.

Camp, T. R. (1968), Floc Volume Concentration, *Journal of American Water Works Association* 60, 656 and 673.

Chapter 681, *Sewers, Article 1, Sewage and Land Drainage, By-Law No. 457-2000*, Toronto Municipal Code Sewers, City of Toronto, Ontario, Canada, 2000.

Clark, M.M. and Flora, J.R., (1991), Floc Restructuring in Varied Turbulent Mixing. *Journal of Colloid and Interface Science* 147:407–421

Dharmappa H.B., Verink, J., Fujiwara, O. and Vigneswaran S., (1993), Optimal Design of a Flocculator, *Water Research* 27(3), 513-519

Dundar, M., Nuhoglu, C., and Nuhoglu, Y., (2008), Biosorption of Cu (II) Ions onto the Litter of Natural Trembling Poplar Forest, *Journal of Hazardous Materials*, 151, 86–95

Ebeling, M., Sibrell, P.L., Ogden, S.R., and Summerfelt, S.T., (2003), Evaluation of Chemical Coagulation/ Flocculation Aids for the Removal of Suspended Solids and Phosphorus from Intensive Recirculation Aquaculture Effluent Discharge, *Aquacultural Engineering* 29 (2003) 23- 42

Eckenfelder, W.W., (2000), *Industrial Water Pollution Control* 3rd Edition, McGraw Hill, New York.

Francois, R.J. and Van Haute, A.A., (1984), Floc Strength Measurements Giving Experimental Support for a Four Level Hydroxide Floc Structure, *Studies in Environmental Science* 23:221–234

Gardea, J.L., Tiemann, K.J., Gonzalez, J.H., Henning J.A., and Townsend M.S., (1996), Ability of Silica-Immobilized Medicago Sativa (Alfalfa) to Remove Copper Ions from Solution, *J. Hazard Mater.* 57:29-39.

Gloaguen, V., and Morvan H., (1997), Removal of Heavy Metal Ions from Aqueous Solution by Modified Barks, *J. Environ. Sci. Health* A32:90.

Hereit, F., Mutl, S. and Vagner, A., (1983) The Formation of Separable Suspensions and the Methods of its Assessment. *Proc. Int. Conf. IWA. Paris, France.* 0095-0099

Hudson, H.E., Jr. and Wolfner, J. P. (1967), Design of Mixing and Sedimentation Basin, *Journal of American Water Works Association* 59, 1257-1268.

Jeon C., Park JY., and Yoo, YJ., (2001), Removal of Heavy Metals in Plating Wastewater using Carboxylated Alginic Acid, *Korean J. Chem. Eng.* 18:955.

Johnson, P.D., Girinathannair, P., Ohlinger, K.N. and Ritch, S., (2008), Enhanced Removal of Heavy Metals in Primary Treatment using Coagulation and Flocculation, *Water Environment Research*; May 2008; 80, 5; ProQuest Science Journals pg. 472

Kan, C., Huang, C. and Pan, J.R., (2002), Coagulation of High Turbidity Water: the Effect of Rapid Mixing, *Journal of water supply: Research and Technology*, 2002. 51.2, pp 77-85

Kan, C., and Huang, C.,(1998), Coagulation Monitoring in Surface Water Treatment Facilities, *Water Science and Technology*, Vol 38 No. 3, pp 237-244

Kawamura, S., (1976), Consideration in Improving Flocculation, *Journal of American Water Works Association* 68, 328-336

Kim, S.J., Jeung, S.Y., and Moon, H., (1998), Removal and Recovery of Heavy Metal Ions in Fixed and Semi-fluidized Beds, *Korean J. Chem. Eng.* 15:37.

Koohestanian, A., Hosseini, M. and Abbasian, Z., (2008), The Separation Method for Removing of Colloidal Particles from Raw Water, *American-Eurasian J. Agric. & Environ. Sci.*, 4 (2): 266-273, 2008

Lee, S. I., Seo, I. S. and Koopman, B., (1994), Effect of Mean Velocity Gradient and Mixing Time on Particle Removal, Seawater Induced Flocculation, *Water, Air and Soil Pollution* 78: 179- 188, 1994

Lee, S.H., Jung, C.H., Chung, H., Lee, M.Y., and Yang, J.W., (1998), Removal of Heavy Metals from Aqueous Solution by Apple Residues, *Proces Biochem*, 33: 205.

Lettermann, R. D., Quon, J. K. and Gemmel, R. S. (1973) Influence of Rapid Mixing Parameters on Flocculation. *Journal of American Water Works Association* 65, 716-725.

Lujan, JR., Damall, DW., Stark, PC., Rayson, GD., and Gardea, JL., (1994), Metal Ion Binding by Algae and Higher Plant Tissues: A Phenomenological Study of Solution pH Dependence, 12:803-816.

Malkoc, E., (2006), Ni (II) Removal from Aqueous Solutions using Cone Biomass of *Thuja Orientalis*, *Journal of Hazardous Materials*, B137, 899–908

Mhaisalkar V.A., Paramasivam, R. and Bhole, A.G., (1991), Optimizing Physical Parameters of Rapid Mixing for Coagulation / Flocculation of Turbid Waters, *Water Research* 25(1), 43-52.

Mofa, AS., (1995), Plants Proving Their Worth in Toxic Metal Cleanup, *Science* 269:302-305

Mooyoung, H. and Lawler D.F., (1992) The Relative Insignificance of G in Flocculation. *Journal of American Water Works Association* October, 79-91.

Muhle, K., (1993), Floc Stability in Laminar and Turbulent Flow, in *Coagulation and Flocculation*, ed by Dobias B. Marcel Dekker, New York, pp 355–390

Noyes, R., (1994). *Unit Operation in Environmental Engineering*, 2nd edition 1994, p.118-123

Park, S. M., Jun, H.B., Jung, M.S. and Koo, H.M., (2006), Effect of Velocity Gradient and Mixing Time on Particle Growth in a Rapid Mixing Tank, *Water science & technology*, Vol 53 No7 pp 95-102, 2006

Patoczka, J., Johnson, R.K. and Scheri, J.J., (1998), Trace Heavy Metals Removal with Ferric Chloride , Presented at Water Environment Federation Industrial Wastes Technical Conference, Nashville, TN, 1998

Patterson, J.W, and Minear, R.A., (1975), Physical-Chemical Methods of Heavy Metals Removal, In Heavy Metals in the Aquatic Environment (P.A. Krenkel, ed.), pp. 261–276. Oxford, England: Pergamon Press.

Peters, R.W., Y.Ku, and Bhattacharyya, D., (1985), Evaluation of Recent Treatment Techniques for Removal of Heavy Metals from Industrial Wastewaters, AIChE Symposium Series, Separation of Heavy Metals and Other Contaminants, 81(243): 165–203

Reichle, R., McCurdy, K., and Hepler L., (1975) Zinc Hydroxide: Solubility Product and Hydroxy-Complex Stability Constants from 12.5-75°C. Can. J. Chem. 53, 3841.

Rossini, M., Garrido, J.G. and Galluzzo, M., (1998), Optimization of the Coagulation and Flocculation Treatment: Influence of Rapid Mixing Parameters, Wat. Res. Vol. 33, No. 8, pp. 1817-1826, 1999

Serra, T., Colomer, J. and Casamitjana, X., (1997), Aggregation and Breakup of Particles in a Shear Flow. Journal of Colloid and Interface Science 187:466–473

Sheng W.Y., Peng, X.F., Lee, D. J. and Su, A., (2006), Coagulation of Particles through Rapid Rixing, Drying Technology, 24: 1271- 1276, 2006

Strnadova, N. and Schejbal, P., (1997), The Removal of Metals by Improved Chemical Precipitation, Volume 7, number 6 p.29-32.

Suleyman, M.A. and Evison, L.M., (1995), Optimizing Physical Parameters Affecting Coagulation of Turbid Water with Moringa Oleifera Seeds, Water Research, 29(12), 2689-2695

Summary Report: Control and Treatment Technology for the Metal Finishing Industry; Sulfide Precipitation, Technology Transfer Division, Washington, D.C., 1980. US EPA, 625/8-80-003

Technical Resource Document (1987).Treatment Technologies for Metal/Cyanide-Containing Wastes, Hazardous Waste Engineering Research Laboratory, NTIS Order Number PB 38-143896, US EPA (1987)

United State Environmental Protection Agency, Development Document for the Final Effluent Limitations: Guidelines and Standards for the Metal Products and Machinery Point Source Category, US EPA Washington D.C., 2003

U.S. Army Corps of Engineers (2001), Engineering and Design, Precipitation /Coagulation /Flocculation, Chapter 2-10.

Volesky, B., (1990), Biosorption and biosorbents, Volesky B., (Ed.) Biosorption of Heavy Metals, CRC press, Florida. pp. 3-5

Vrale, L. and Jorden, R. M. (1971), Rapid Mixing in Water Treatment, Journal of American Water Works Association 63, 52-58

Wang, J., and Chen, C., (2006), Biosorption of Heavy Metals by *Saccharomyces Cerevisiae*: A review, Biotechnology Advances, 24, 427–451

World Health Organization (1984), Geneva, Guidelines for Drinking Water Quality

Water Specialists Technologies LLC,
www.waterspecialists.biz/html/precipitation_by_ph_.html, Date accessed (April, 2010).

www.afonline.com/articales/00sum04.html, Date accessed: (April, 2010).

www.phippsbird.com/fig2.html, Date accessed (April, 2010).

Young, S., Stanley S.J. and Smith, D.W., (2000), Effect of Mixing on the Kinetics of Polymer-Aided Flocculation, Journal of water supply: Research and Technology, 2000

Appendixes

Appendix A

Velocity gradient verses agitator paddle for standard Jar Test.

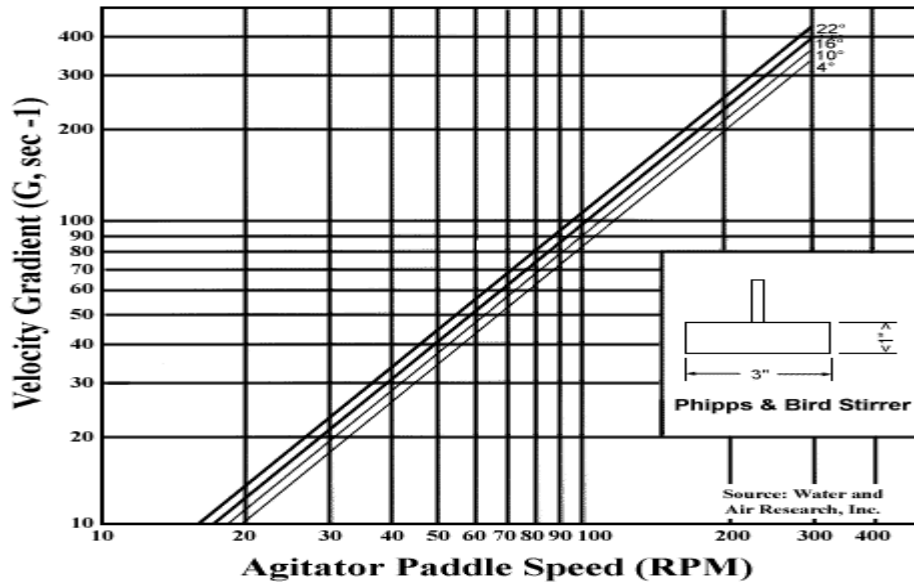


Figure A.1- Velocity gradient vs. rpm for a 2-liter square beaker (11.5x11.5x25cm), using a Phipps & Bird stirrer (2.5x7.6 cm) (Ebeling et al., 2003; www.phippsbird.com).

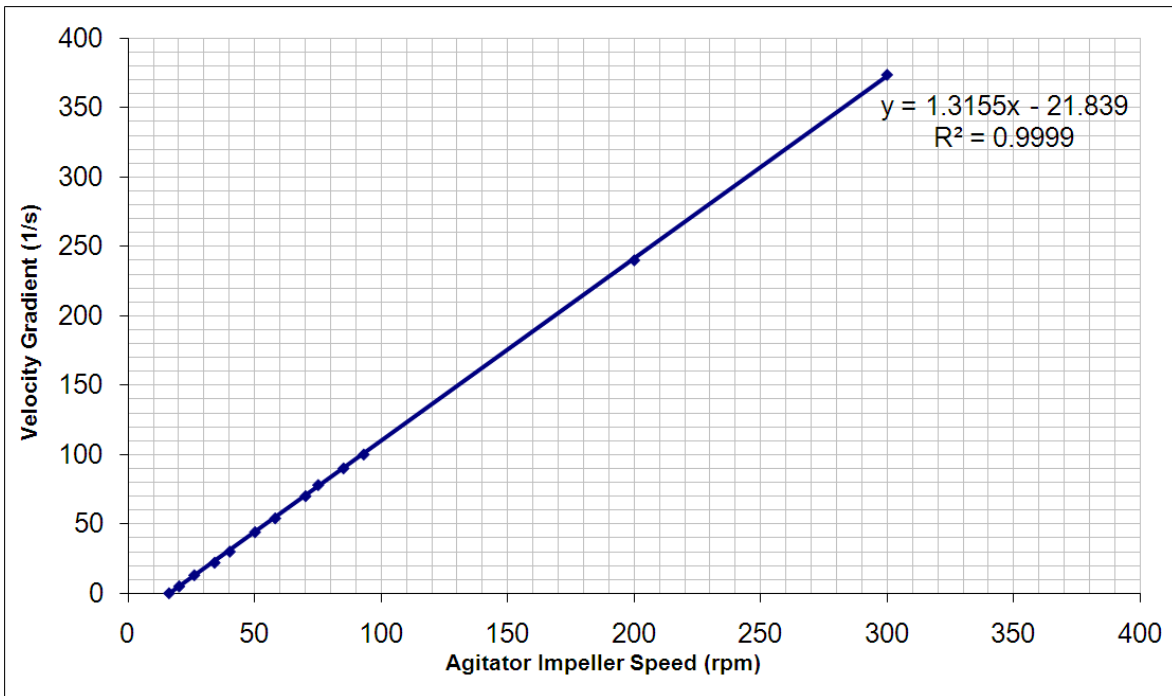


Figure A.2- Velocity Gradient vs. rpm for a 2-liter Square Beaker (11.5x11.5x25cm), Using a Phipps & Bird Stirrer (2.5x7.6 cm) at 22°C (Ebeling et al., 2003; www.phippsbird.com).

Reynold's number verses agitator paddle speed (rpm) for standard Jar Test

$$Re = \frac{D^2 N \rho}{\mu}$$

Where

Re = Reynold's number

D = stirrer diameter, 0.076 m

N = Rotational speed (revolution / second)

P = Water density, 1000 kg/m³

μ = Water viscosity, 10⁻³ N-s/m²

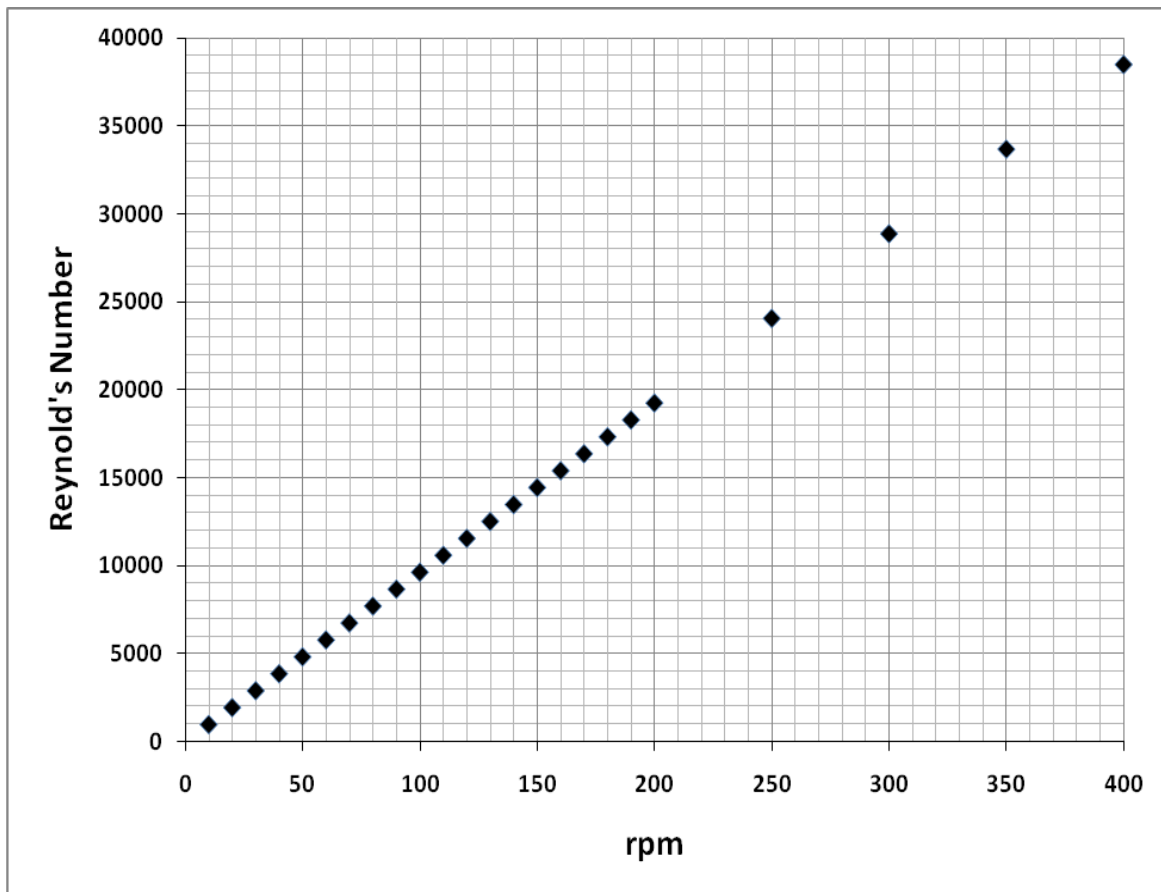


Figure A.3- Reynold's number verses agitator paddle speed (rpm) for standard Jar Test.

Appendix B

Experimental Errors

The error was calculated by average deviation from the following equation

$$\text{Average Deviation} = \frac{1}{N} \sqrt{\sum_1^N (\bar{X} - X_i)^2}$$

Where

N = number of experimental data points

X_i = value of the individual data point

\bar{X} = average of the data points

- Metal concentration measurement in the supernatant.

Sample #1 $X_1 = 49.1$

Sample #1 $X_2 = 48.5$

Sample #1 $X_3 = 48.2$

Sample #2 $X_4 = 50.4$

Sample #2 $X_5 = 48.8$

Sample #2 $X_6 = 49.4$

Sample #3 $X_7 = 48.7$

Sample #3 $X_8 = 50.0$

Sample #3 $X_9 = 49.1$

Total number of samples $N = 9$

$\bar{X} = 49.2$

Average deviation = $\pm 2.23\%$

- Dilution of samples

Pipette withdraw wastewater samples volume error

Error = $\pm 0.005\%$

- Balance weight error

Error = $\pm 0.005\%$

- Manual Reading error

Error = $\pm 0.050\%$

Total Errors = $\pm 2.29\%$

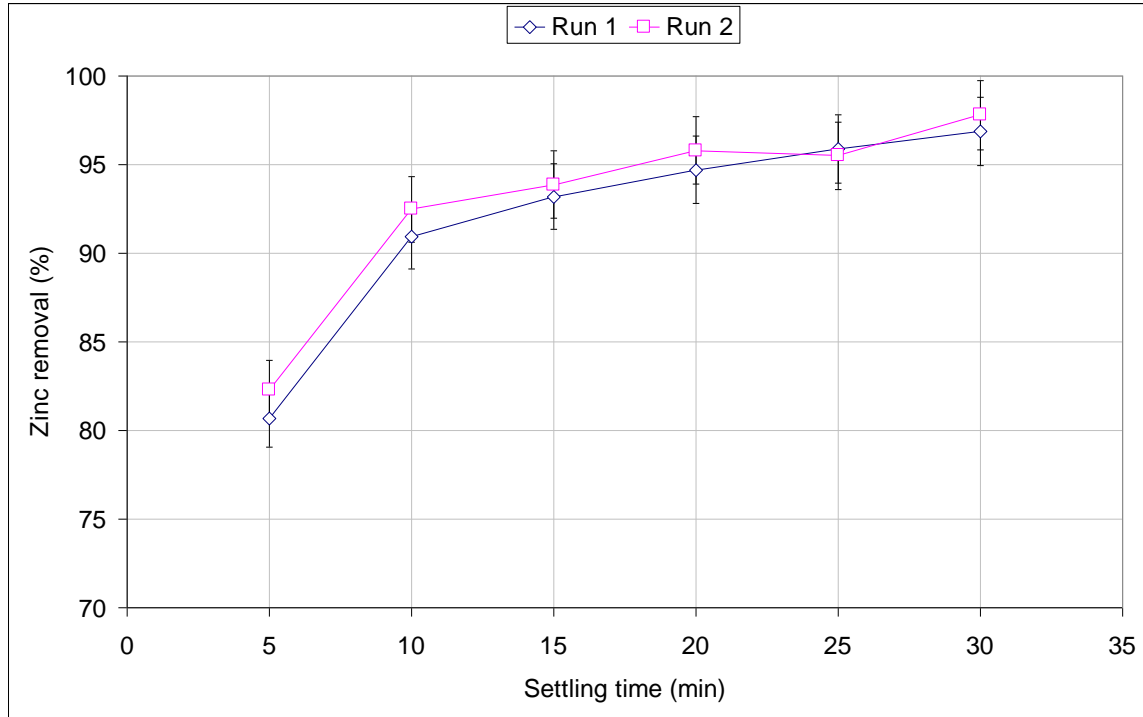


Figure B.1- Zinc removal % vs. settling time. (initial [Zn]= 50 ppm, pH 8.7, 30 mg/l ferric chloride, rapid mixing for 60 s @ 100 rpm, 0.5ml/l flocculant, slow mixing 15 min @ 50 rpm, settling time 30 min).

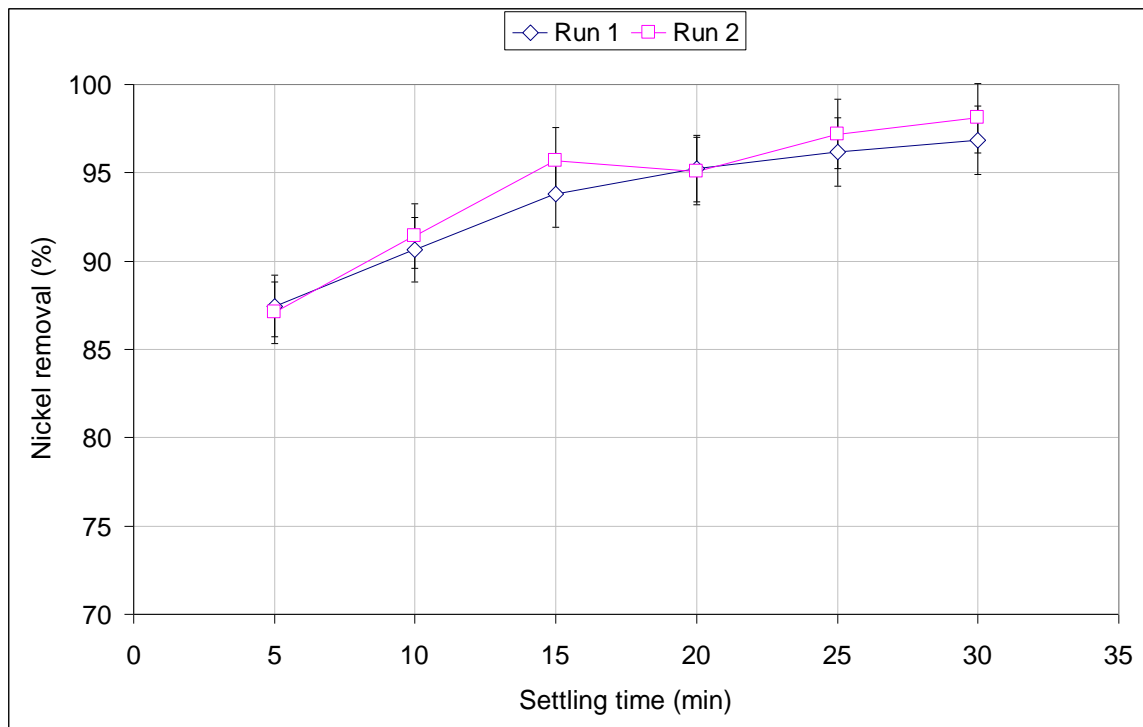


Figure B.2- Nickel removal % vs. settling time. (initial [Ni]= 50 ppm, pH 10.2, 30 mg/l ferric chloride, rapid mixing for 30 s @ 80 rpm, 0.5ml/l flocculant, slow mixing 15 min @ 50 rpm, settling time 30 min).

Appendix C

Particle Size Distribution

Table C.1- Particle size distribution for zinc using ferric chloride, ferrous sulfate, and aluminum sulfate at 30mg/l dosage and no coagulant. (initial [Zn]= 50ppm, pH 8.7, rapid mixing for 120 s @ 180 rpm, 0.5ml/l flocculant slow mixing 15 min @ 50 rpm). Figure 5.8

Particle size µm	Ferric Chloride vol%	Ferrous sulfate vol%	Alum vol%	No coagulant vol%
2.75	0	0	0	0
3.27	0	0	0	0
3.89	0	0	0	0
4.62	0	0	0	0
5.50	0	0	0	0
6.54	0	0.55	0	0
7.78	0	1.28	0	0
9.25	0	2.72	0.71	0.42
11.00	0	2.46	1.78	0.99
Sum	0	7.01	2.49	1.41
13.08	0.47	0.91	3.11	2.01
15.56	1.17	0.41	2.96	4.22
18.50	2.89	0.7	2.36	7.2
22.00	5.17	2.68	2.6	11.13
26.16	5.85	7.59	4.73	16.25
31.11	4.88	7.92	11.04	18.75
37.00	5.16	4.26	20.01	17.18
44.00	8.16	3.66	20.21	11.27
52.33	14.99	7.44	13.85	5.65
62.23	20.87	18.06	7.89	2.63
74.00	16.92	20.66	4.38	1.27
88.00	7.99	9.75	2.52	0.65
Sum	60.77	55.91	28.64	10.2
104.70	3.16	3.16	1.29	0.38
124.50	1.33	1.59	0.56	0
148.00	0.63	1.43	0	0
176.00	0.36	1.42	0	0
209.30	0	0.98	0	0
248.90	0	0.37	0	0
296.00	0	0	0	0

Table C.2 - Particle size distribution for nickel using ferric chloride, ferrous sulfate, and aluminum sulfate at 30mg/l dosage and no coagulant. (initial [Ni]= 50ppm, pH 10.2, rapid mixing for 120 s @ 180 rpm, 0.5ml/l flocculant, slow mixing 15 min @ 50 rpm). Figure 5.12

Particle Size (μm)	Ferric chloride vol%	Ferrous sulfate vol%	Alum vol%	No coagulant vol%
2.312	0	1.07	0	0
2.75	0	2.53	0	0
3.27	0	4.39	0	0
3.89	0	3.87	0	0.69
4.62	0	7.09	0	6.55
5.5	1.6	8.57	1.46	21.89
6.54	3.02	6.15	2.69	13.95
7.78	3.62	5.2	5.13	18.79
9.25	9.01	6.17	10.23	17.08
11	15.1	11.25	13.23	9.71
13.08	11.76	13.34	15.36	7.62
15.56	11.45	9.9	16.02	3.72
18.5	12.74	4.3	12.37	0
22	9.72	1.42	7.37	0
26.16	8.72	1.04	3.96	0
31.11	5.44	0.96	2.03	0
37	2.79	1.31	1.23	0
Sum	62.62	32.27	58.34	11.34
44	1.54	1.9	0.89	0
52.33	0.96	2.12	0.74	0
62.23	0.63	1.93	0.77	0
74	0.51	1.9	0.9	0
88	0.44	0.58	1.15	0
104.7	0.35	0.92	1.44	0
124.5	0	0.1	1.45	0
148	0	0.84	1.03	0
176	0	0.61	0.55	0
209.3	0	0.54	0	0
248.9	0	0	0	0

Table C.3- Zinc particle size distributions for 30 and 60 s mixing time. (Initial [Zn]= 50ppm, pH 8.7, 30 mg/l ferric chloride coagulant, rapid mixing for 30 and 60 s @ 100,200,300,400 rpm). Figures 5.25, 5.26

30 s Rapid mixing					60 s rapid mixing				
particle size	100 rpm	200 rpm	300 rpm	400 rpm	particle size	100 rpm	200 rpm	300 rpm	400 rpm
(μm)	vol%	vol%	vol%	vol%	(μm)	vol%	vol%	vol%	vol%
2.75	0	0	0	0	2.75	0	0	0	0.78
3.27	0	0	0	0	3.27	0	0	0	1.05
3.89	0	0	0	0	3.89	0	0	0.41	1.42
4.62	0	0	0	0	4.62	0	0	0.55	1.92
5.5	0	0	0	0.43	5.5	0	0	0.77	2.51
6.54	0	0	0	0.77	6.54	0	0.35	1.08	3.12
7.78	0	0.33	0.34	1.28	7.78	0	0.49	1.51	3.59
9.25	0.32	0.49	0.54	1.97	9.25	0	0.69	2.07	3.8
11	0.49	0.75	0.88	2.91	11	0	0.98	2.72	3.8
13.08	0.77	1.14	1.39	4.32	13.08	0	1.36	3.32	3.76
15.56	1.2	1.65	2.13	6.54	15.56	0	1.82	3.81	3.9
18.5	1.77	2.26	3.13	9.85	18.5	0.36	2.28	4.36	4.44
22	2.43	3.02	4.58	13.68	22	0.54	2.72	5.36	5.6
26.16	3.17	4.16	6.84	16.07	26.16	0.82	3.24	7.33	7.5
31.11	4.23	6.23	10.27	15.3	31.11	1.23	4.18	10.56	9.73
37	6.16	9.84	14.38	11.52	37	1.82	6.07	14.06	10.85
44	9.6	14.56	16.73	7.17	44	2.63	9.4	14.95	10.11
52.33	14.21	17.23	15.1	3.96	52.33	3.83	13.59	12.08	7.42
62.23	16.98	15.08	10.21	2.09	62.23	5.62	15.83	7.34	4.53
74	15.27	9.8	5.61	1.12	74	8.24	14.21	3.71	2.48
88	10.39	5.37	2.87	0.63	88	11.49	9.86	1.78	1.35
104.7	5.96	2.91	1.56	0.39	104.7	14.39	5.81	0.92	0.8
124.5	3.22	1.73	0.98	0	124.5	15.22	3.21	0.56	0.56
148	1.77	1.16	0.71	0	148	13.35	1.79	0.41	0.45
176	1.02	0.84	0.56	0	176	9.45	1.04	0.34	0.4
Sum	22.36	12.01	6.68	1.02	Sum	63.9	21.71	4.01	3.56
209.3	0.63	0.63	0.46	0	209.3	5.54	0.65	0	0.35
248.9	0.41	0.47	0.39	0	248.9	2.86	0.43	0	0
296	0	0.35	0.34	0	296	1.42	0	0	0
352	0	0	0	0	352	0.75	0	0	0
418.6	0	0	0	0	418.6	0.44	0	0	0

Table C.4- Zinc particle size distributions for 90 and 120 s mixing time. (Initial [Zn]= 50ppm, pH 8.7, 30 mg/l ferric chloride coagulant, rapid mixing for 90 and 120 s @ 100,200,300,400 rpm). Figures 5.27, 5.28

90 s Rapid mixing					120 s Rapid mixing				
particle size	100 rpm	200 rpm	300 rpm	400 rpm	particle size	100 rpm	200 rpm	300 rpm	400 rpm
(μm)	vol%	vol%	vol%	vol%	(μm)	vol%	vol%	vol%	vol%
2.75	0	0	0	0	2.75	0	0.63	0	0
3.27	0	0	0	0	3.27	0	0.89	0	0
3.89	0	0	0	0	3.89	0	1.26	0	0
4.62	0	0	0	0.31	4.62	0	1.74	0	0
5.5	0	0	0.38	0.52	5.5	0	2.29	0.43	0.47
6.54	0	0	0.62	0.86	6.54	0	2.78	0.59	0.77
7.78	0	0	0.99	1.36	7.78	0	3.12	0.8	1.21
9.25	0	0	1.51	2.08	9.25	0.49	3.23	1.09	1.8
11	0.34	0.44	2.13	3.11	11	0.85	3.17	1.49	2.58
13.08	0.47	0.66	2.79	4.73	13.08	1.41	3.06	2.02	3.76
15.56	0.65	0.98	3.56	7.3	15.56	2.17	3.05	2.69	5.72
18.5	0.9	1.4	4.74	10.96	18.5	3.14	3.29	3.48	8.84
22	1.22	1.86	6.9	14.77	22	4.47	3.86	4.52	12.77
26.16	1.63	2.35	10.56	16.38	26.16	6.51	4.81	6.05	15.62
31.11	2.09	3.03	15.1	14.54	31.11	9.64	6.17	8.4	15.54
37	2.6	4.33	17.37	10.22	37	13.61	7.96	11.55	12.3
44	3.21	6.94	14.96	6.04	44	16.48	9.93	14.31	8.14
52.33	4.05	11.32	9.46	3.23	52.33	15.92	11	14.35	4.77
62.23	5.28	15.88	4.8	1.7	62.23	11.61	10.22	11.26	2.62
74	7.06	16.87	2.21	0.94	74	6.64	7.22	7.03	1.43
88	9.53	13.63	1.04	0.57	88	3.29	4.09	3.92	0.81
104.7	12.65	8.89	0.55	0.38	104.7	1.6	2.11	2.23	0.5
124.5	15.31	5.18	0.33	0	124.5	0.87	1.16	1.4	0.35
148	15.22	2.87	0	0	148	0.55	0.76	0.95	0
176	10.63	1.58	0	0	176	0.41	0.57	0.67	0
Sum	63.34	32.15	1.92	0.95	Sum	6.72	8.69	9.17	1.66
209.3	4.96	0.89	0	0	209.3	0.34	0.47	0.46	0
248.9	1.68	0.54	0	0	248.9	0	0.38	0.31	0
296	0.52	0.36	0	0	296	0	0	0	0
352	0	0	0	0	352	0	0	0	0
418.6	0	0	0	0	418.6	0	0	0	0

Table C.5 - Nickel particle size distribution for 30 and 60 s mixing time. (initial [Ni]= 50ppm, pH 10.2, 30 mg/l ferric chloride coagulant rapid mixing for 30, 60 s @ 100,150,200,250 rpm). Figures 5.30, 5.31

30 s Rapid mixing					60 s rapid mixing				
Particle size	100 rpm	150 rpm	200 rpm	250 rpm	Particle size	100 rpm	150 rpm	200 rpm	250 rpm
(μm)	vol%	vol%	vol%	vol%	(μm)	vol%	vol%	vol%	vol%
1.38	0	0	0.36	0	1.38	0	0	0.32	0.38
1.64	0	0.38	0.47	1.71	1.64	0	0	0.43	0.51
1.95	0	0.51	0.66	2.16	1.95	0	0.4	0.63	0.73
2.31	0	0.73	0.97	2.9	2.31	0.38	0.59	0.97	1.08
2.75	0.44	1.07	1.5	3.94	2.75	0.59	0.91	1.52	1.65
3.27	0.73	1.62	2.36	5.32	3.27	0.94	1.42	2.35	2.53
3.89	1.24	2.49	3.71	6.95	3.89	1.55	2.21	3.58	3.83
4.62	2.03	3.86	5.64	8.86	4.62	2.49	3.4	5.38	5.65
5.50	3.21	5.92	7.98	11.01	5.50	3.87	5.2	7.86	7.96
6.54	4.85	8.47	10.17	12.87	6.54	5.8	7.72	10.56	10.38
7.78	7.13	10.72	11.55	13.39	7.78	8.37	10.52	11.98	12.2
9.25	10.23	11.39	11.67	11.67	9.25	11.5	12.17	11.54	12.52
11.00	13.82	10.62	11.01	8.52	11.00	14.37	11.83	9.26	11.5
13.08	16.11	8.46	9.16	5.18	13.08	15.17	9.31	6.61	9.12
15.56	15.17	5.94	6.67	2.75	15.56	13.03	6.23	4.41	6.34
18.50	11.01	3.74	4.29	1.34	18.50	9.02	3.79	2.84	4.01
22.00	6.52	2.2	2.59	0.64	22.00	5.46	2.29	1.85	2.48
26.16	3.49	1.31	1.62	0.33	26.16	3.19	1.49	1.26	1.63
31.11	1.88	0.88	1.12	0.18	31.11	1.92	1.08	0.91	1.16
37.00	1.06	0.71	0.86	0.11	37.00	1.18	0.86	0.66	0.85
Sum	55.24	23.24	26.31	10.53	sum	48.97	25.05	18.54	25.59
44.00	0.65	0.7	0.72	0.08	44.00	0.72	0.73	0.47	0.61
52.33	0.43	0.79	0.64	0.05	52.33	0.45	0.63	0.34	0.43
62.23	0.45	0.95	0.6	0.04	62.23	0	0.6	0	0.33
74.00	0.46	1.09	0.58	0	74.00	0	0.64	0.32	0
88.00	0.57	1.18	0.57	0	88.00	0	0.78	0.47	0.36
104.70	0.8	1.27	0.56	0	104.70	0	1.1	0.76	0.44
124.50	1.17	1.49	0.56	0	124.50	0	1.66	1.24	0.48
148.00	1.64	1.93	0.54	0	148.00	0	2.45	1.86	0.46
176.00	2.05	2.48	0.48	0	176.00	0	3.09	2.45	0.38
209.30	2.11	2.66	0.39	0	209.30	0	2.91	2.6	0
248.90	1.7	2.1	0	0	248.90	0	1.99	2.09	0
296.00	1.1	1.27	0	0	296.00	0	1.09	1.31	0
352.00	0.65	0.68	0	0	352.00	0	0.57	0.74	0
418.60	0.4	0.39	0	0	418.60	0	0.34	0.43	0

Table C.6 - Nickel particle size distribution for 30 and 60 s mixing time. (initial [Ni]= 50ppm, pH 10.2, 30 mg/l ferric chloride coagulant rapid mixing for 90, 120 s @ 100,150,200,250 rpm). Figures 5.32, 5.33

90 s Rapid mixing					120 s Rapid Mixing				
Particle size	100 rpm	150 rpm	200 rpm	250 rpm	Particle size	100 rpm	150 rpm	200 rpm	250 rpm
(μm)	vol%	vol%	vol%	vol%	(μm)	vol%	vol%	vol%	vol%
1.38	0	0	0	0	1.38	0	0	0	0
1.64	0	0	0.36	0.4	1.64	0	0	0.32	0
1.95	0.38	0.41	0.53	0.56	1.95	0	0.35	0.5	0.39
2.31	0.57	0.59	0.82	0.83	2.31	0.44	0.51	0.8	0.54
2.75	0.88	0.89	1.3	1.27	2.75	0.73	0.77	1.27	0.8
3.27	1.39	1.37	2.03	1.97	3.27	1.24	1.2	2.02	1.24
3.89	2.19	2.15	3.08	3.03	3.89	2.03	1.88	3.22	1.96
4.62	3.4	3.43	4.52	4.59	4.62	3.21	2.95	5.21	3.06
5.50	5.17	5.42	6.47	6.8	5.50	4.85	4.59	8.28	4.6
6.54	7.71	8.17	8.92	9.55	6.54	7.13	6.98	11.96	6.57
7.78	10.94	10.99	11.35	12.2	7.78	10.23	10.01	14.4	8.82
9.25	13.94	12.36	12.48	13.46	9.25	13.82	12.78	14.34	10.96
11.00	14.74	11.93	11.84	12.94	11.00	16.11	13.52	11.88	11.93
13.08	12.72	9.62	9.36	10.5	13.08	15.17	11.76	8.66	11.33
15.56	8.85	6.8	6.47	7.41	15.56	11.01	8.13	5.72	8.77
18.50	5.37	4.38	4.15	4.73	18.50	6.52	4.82	3.46	5.86
22.00	3.13	2.68	2.61	2.89	22.00	3.49	2.73	2.01	3.69
26.16	1.91	1.66	1.68	1.82	26.16	1.88	1.62	1.24	2.39
31.11	1.26	1.09	1.13	1.22	31.11	1.06	1.04	0.87	1.61
37.00	0.86	0.78	0.79	0.87	37.00	0.65	0.72	0.71	1.12
sum	34.1	27.01	26.19	29.44	sum	39.78	30.82	22.67	34.77
44.00	0.59	0.61	0.57	0.63	44.00	0.43	0.54	0.63	0.81
52.33	0.42	0.5	0.44	0.47	52.33	0.45	0	0.59	0.65
62.23	0.35	0.46	0.38	0.38	62.23	0.46	0	0.55	0.65
74.00	0.39	0.49	0.37	0.36	74.00	0.57	0	0.53	0.79
88.00	0.52	0.62	0.4	0.38	88.00	0.8	0	0.47	1.1
104.70	0.69	0.87	0.49	0.39	104.70	1.17	0	0.36	1.53
124.50	0.72	1.26	0.64	0.35	124.50	1.64	0	0	1.93
148.00	0.55	1.76	0.88	0	148.00	2.05	0	0	2.09
176.00	0.36	2.22	1.19	0	176.00	2.11	0	0	1.85
209.30	0	2.3	1.41	0	209.30	1.7	0	0	1.33
248.90	0	1.86	1.33	0	248.90	1.1	0	0	0.82
296.00	0	1.21	0.98	0	296.00	0.65	0	0	0.49
352.00	0	0.7	0.63	0	352.00	0.4	0	0	0.32
418.60	0	0.42	0.4	0	418.60	0	0	0	0

Table C.7 - Zinc particle size distributions for 60 s mixing time. (initial [Zn]= 50ppm, pH 8.7, 30 mg/l ferric chloride, rapid mixing for 60 s @ 60, 80, 100, 120, 140 and 160 rpm). Figure 5.29

Particle size (μm)	60 rpm vol%	80 rpm vol%	100 rpm vol%	120 rpm vol%	140 rpm vol%	160 rpm vol%
2.75	0	0	0	0	0	0
3.27	0	0	0	0	0	0
3.89	0	0	0	0	0	0
4.62	0	0	0	0	0	0
5.5	0	0	0	0	0	0
6.54	0.35	0	0	0	0	0
7.78	0.49	0	0	0	0	0
9.25	0.69	0	0	0.49	0	0
11	0.98	0.51	0	1.01	0	0
13.08	1.36	0.6	0	0.95	0	0
15.56	1.82	0.55	0	0.77	0	0
18.5	2.28	0.69	0.36	0.87	0.4	0.54
22	2.72	1.25	0.54	1.36	1.32	1.62
26.16	3.24	2.82	0.82	2.45	3.18	3.3
31.11	4.18	5.11	1.23	3.58	3.99	3.62
37	6.07	5.38	1.82	3.29	2.9	3.28
44	9.4	5.13	2.63	3.04	2.69	3.9
52.33	13.59	6.06	3.83	3.85	4.6	6.83
62.23	15.83	9.64	5.62	7.11	10.65	13.6
74	14.21	15.28	8.24	13.52	17.9	20.03
88	9.86	16.6	11.49	17.35	16.89	17.71
104.7	5.81	11.51	14.39	13.87	11.51	11.68
124.5	3.21	7.14	15.22	9.58	9.43	6.94
148	1.79	4.84	13.35	7.01	8.44	3.97
176	1.04	3.37	9.45	5.07	4.85	2.12
sum	21.71	43.46	63.9	52.88	51.12	42.42
209.3	0.65	2.09	5.54	3.09	1.25	0.86
248.9	0.43	1.01	2.86	1.33	0	0
296	0	0.42	1.42	0.41	0	0
352	0	0	0.75	0	0	0
418.6	0	0	0.44	0	0	0

Table C.8 - Nickel particle size distribution for 30 s. (initial [Ni]= 50ppm, pH 10.2, 30 mg/l ferric chloride, rapid mixing for 30 s @ 60, 80, 100, 120, and 140 rpm). Figure 5.34

Particle size(μm)	60 rpm vol%	80 rpm vol%	100 rpm vol%	120 rpm vol%	140 rpm vol%
1.945	0	0	0	0	1.71
2.312	0	0	0.39	0	2.16
2.75	0	0	0.54	0	2.9
3.27	0	0	0.8	0	3.94
3.89	0	0.31	1.24	5.2	5.32
4.62	2.43	1.19	1.96	4.85	6.95
5.5	13.73	3.67	3.06	7.94	8.86
6.54	11.31	4.67	4.6	5.03	11.01
7.78	12.07	7.14	6.57	8.04	12.87
9.25	13.97	12.07	8.82	18.58	13.39
11	13	14.25	10.96	18.27	11.67
13.08	12.8	15.52	11.93	10.38	8.52
15.56	9.61	15.41	11.33	5.94	5.18
18.5	1.18	11.11	8.77	4.32	2.75
22	0	6.09	5.86	4.17	1.34
26.16	0	3.12	3.69	3.57	0.64
31.11	0	1.6	2.39	1.4	0.33
37	0	1.07	1.61	0	0.18
Sum	23.59	53.92	45.58	29.78	18.94
44	0	0.78	1.12	0	0.11
52.33	0	0.51	0.81	0	0.08
62.23	0	0.33	0.65	0	0.05
74	0	0	0.65	0	0.04
88	0	0	0.79	1.3	0
104.7	0	0	1.1	1.51	0
124.5	0	0.39	1.53	0.5	0
148	0	0.42	1.93	0	0
176	0	0.35	2.09	0	0
209.3	0	0	1.85	0	0
248.9	0	0	1.33	0	0
296	0	0	1.63	0	0

Appendix D

Optimum pH Calculation

- Optimization of the function in Figure 4.1 for optimum pH for Zinc

$$y = 0.9689x^4 - 33.717x^3 + 421.32x^2 - 2223.8x + 4199$$

$$\frac{dy}{dx} = 3.8756x^3 - 101.151x^2 + 842.64x - 2223.8 = 0 \quad \text{To find the optimum point}$$

Solve for

$$x = 8.7$$

$$\therefore pH = 8.7$$

- Optimization of the function in Figure 4.2 for optimum pH for Nickel

$$y = 0.385x^4 - 17.778x^3 + 286.09x^2 - 1916.7x + 4572.6$$

$$\frac{dy}{dx} = 1.54x^3 - 53.334x^2 + 572.18x - 1916.7 = 0$$

Solve for

$$x = 10.2$$

$$\therefore pH = 10.2$$